Research Square

Preprints are preliminary reports that have not undergone peer review.
They should not be considered conclusive, used to inform clinical practice,
or referenced by the media as validated information.

# Antimicrobial and Anticancer Activities of Graphene Oxide: Mechanistic Insights into Structure–Activity Relationships, Nano–Bio Interactions, and Translational Biomedical Applications

**Zankhana Patel**
Gandhinagar University
**Vaishali Pandya**
Gandhinagar University
**Bhavana Jodha**
Central University of Gujarat
**Sunita Patel**
Central University of Gujarat
**Nakul Kumar**
nakul.kumar07@yahoo.com

Gandhinagar University

**Research Article**

**Keywords:** Graphene Oxide, Carbon Nanomaterials, Antimicrobial Activity, Anticancer Activity, Reactive Oxygen Species, A549 Cells, MDA-MB-231 Cells, MCF-7 Cells

**Posted Date:** September 25th, 2026

**DOI:** https://doi.org/10.21203/rs.3.rs-10861149/v1

**License:** This work is licensed under a Creative Commons Attribution 4.0 International License.
Read Full License

**Additional Declarations:** No competing interests reported.

# Antimicrobial and Anticancer Activities of Graphene Oxide: Mechanistic Insights into Structure–Activity Relationships, Nano–Bio Interactions, and Translational Biomedical Applications

Zankhana Patel[1], Vaishali Pandya[2] and Bhavana Jodha[3], Sunita Patel[4], Nakul Kumar[1*]

Gandhinagar Institute of Science, Gandhinagar University, Kalol, Gandhinagar, Gujarat, India, 382721[1-2]

School of Life Sciences, Central University of Gujarat, Kundhela, Vadodara, India[3-4]

Email: zpatel43@gmail.com[1], research.vaishali24@gmail.com[2], jodhabhavana@gmail.com[3] sunitap@cug.ac.in[4] nakul.kumar07@yahoo.com[1*]

## Abstract

Graphene oxide (GO) has emerged as one of the most extensively investigated two-dimensional carbon nanomaterials owing to its exceptional physicochemical properties, structural versatility, and remarkable biological activity. Unlike pristine graphene, graphene oxide possesses abundant oxygen-containing functional groups distributed across a heterogeneous $sp^2$-hybridized carbon framework, conferring excellent aqueous dispersibility, tunable surface chemistry, and enhanced interaction with biological systems. These unique characteristics have positioned GO as a promising multifunctional nanoplatform for numerous biomedical applications, particularly in antimicrobial therapy and cancer nanomedicine. The increasing prevalence of antimicrobial resistance together with the limited efficacy and systemic toxicity associated with conventional chemotherapeutics has intensified the search for alternative therapeutic strategies capable of overcoming biological resistance through mechanisms fundamentally different from those of traditional drugs. In this context, graphene oxide represents an attractive candidate because its biological activity arises primarily from its intrinsic physicochemical properties rather than from conventional pharmacological receptor-mediated interactions.

**Keywords:** Graphene Oxide; Carbon Nanomaterials; Antimicrobial Activity; Anticancer Activity; Reactive Oxygen Species; A549 Cells; MDA-MB-231 Cells; MCF-7 Cells

## 1. Introduction

### 1.1 Emergence of Carbon Nanomaterials in Modern Biomedicine

The remarkable progress achieved in nanoscience over the past three decades has fundamentally transformed the landscape of biomedical research by enabling the development of materials possessing physicochemical characteristics unattainable in conventional bulk systems. As material dimensions decrease to the nanometre scale, quantum confinement

effects, increased surface-to-volume ratios, enhanced surface reactivity, and tunable electronic properties collectively give rise to unique biological behaviours that cannot be predicted from their macroscopic counterparts. Consequently, nanotechnology has become one of the most rapidly expanding interdisciplinary fields, integrating principles from materials science, chemistry, molecular biology [Adéla Jiříčková et. al. 2022; David López-Díaz et. al. 2020], medicine, and engineering to create innovative platforms for disease diagnosis, targeted drug delivery, tissue regeneration, antimicrobial therapy, and cancer treatment. [Tais Monteiro Magne et. al. 2021]

Among the diverse classes of engineered nanomaterials investigated to date, carbon-based nanomaterials have attracted exceptional scientific attention because of their extraordinary mechanical strength, electrical conductivity, thermal stability, chemical versatility, and compatibility with molecular functionalization. The carbon atom possesses remarkable hybridization flexibility, enabling the formation of one-dimensional, two-dimensional, and three-dimensional nanostructures exhibiting distinct physicochemical characteristics. This versatility has led to the development of an extensive family of carbon nanomaterials, including fullerenes (0D), carbon nanotubes (1D), graphene (2D), graphene oxide, reduced graphene oxide, graphene quantum dots, carbon nano horns, carbon nanofibers, and hybrid graphene-based composites. Each member of this family offers unique structural features that influence interactions with biological systems and determine their suitability for specific biomedical applications. [Zare, Pariya et al. 2021]

The isolation of graphene in 2004 represented a transformative milestone in materials science, demonstrating for the first time that stable, free-standing, atomically thin two-dimensional crystals could exist under ambient conditions. Graphene consists of a single atomic layer of carbon atoms arranged in a hexagonal honeycomb lattice through $sp^2$ hybridization, producing exceptional electron mobility, tensile strength, thermal conductivity, and optical transparency. [Adéla Jiříčková et. al. 2022] These unprecedented properties stimulated enormous scientific interest across numerous disciplines, ultimately leading to the awarding of the 2010 Nobel Prize in Physics to Andre Geim and Konstantin Novoselov for their pioneering work on graphene. [Geim, A. K. et. al. 2007] Despite these exceptional characteristics, pristine graphene exhibits several limitations that restrict its direct biomedical application. Its highly hydrophobic nature promotes irreversible aggregation in aqueous media, significantly reducing colloidal stability under physiological conditions. Furthermore, the absence of surface functional groups limits opportunities for chemical conjugation with biomolecules, therapeutic agents, or targeting ligands. These constraints motivated the development of chemically modified

graphene derivatives, among which graphene oxide has emerged as the most extensively investigated platform owing to its superior aqueous dispersibility, abundant surface functionality, and remarkable adaptability for biomedical engineering.

Graphene oxide is generated through the controlled oxidation of graphite, resulting in the incorporation of oxygen-containing functional groups throughout the basal planes and sheet edges. This oxidation process converts an electronically homogeneous graphene lattice into a chemically heterogeneous nanostructure containing both graphitic $sp^2$ domains and oxidized $sp^3$ regions. The coexistence of these domains creates a multifunctional material that simultaneously retains many desirable characteristics of graphene while acquiring enhanced hydrophilicity, colloidal stability, and chemical reactivity. Consequently, graphene oxide serves not merely as an oxidized derivative of graphene but as a distinct nanomaterial with unique physicochemical properties and biological behaviour. [Hummers, W. S. et. al. 1958]

The biomedical significance of graphene oxide extends beyond its structural characteristics. The material's high specific surface area provides abundant interaction sites for proteins, nucleic acids, lipids, and small-molecule therapeutics, while its oxygen-containing functional groups enable extensive covalent and non-covalent functionalization. [Gostaviceanu, Andreea et al. 2024] These properties have facilitated the development of advanced nanoplatforms for controlled drug delivery, biosensing, molecular imaging, gene therapy, regenerative medicine, antimicrobial coatings, and cancer therapeutics. [Oliveira, Alexandra M. L. et al. 2022] Importantly, unlike conventional pharmaceuticals whose activity often depends on highly specific molecular targets, graphene oxide exerts biological effects through multifactorial physicochemical interactions at the nano–bio interface. [Grilli et al. 2022] This unique mode of action substantially reduces the probability of acquired resistance and broadens its therapeutic applicability.

As research in nanomedicine continues to evolve, graphene oxide has increasingly been recognized as a bridge between materials science and translational biomedicine. Its biological performance is intrinsically governed by the interplay between structural morphology, surface chemistry, electronic properties, and dispersion behaviour. Understanding these relationships is therefore essential for the rational design of safe and effective graphene oxide-based biomedical systems. [Loh, K. P., et al. 2010] Rather than viewing graphene oxide solely as a nanomaterial, it should be regarded as a dynamic bio interactive platform whose physicochemical attributes directly dictate its interactions with cells, tissues, and microorganisms.

### 1.2 Evolution from Pristine Graphene to Functionalized Graphene Oxide

The discovery of graphene fundamentally transformed materials science by demonstrating that atomically thin two-dimensional crystals could exist as thermodynamically stable materials with unprecedented physicochemical properties. Since its isolation from graphite through mechanical exfoliation in 2004, graphene has become one of the most extensively investigated nanomaterials because of its exceptional electrical conductivity, thermal conductivity, mechanical strength, flexibility, optical transparency, and chemical stability. Structurally, pristine graphene consists of a single atomic layer of carbon atoms arranged in a perfect hexagonal honeycomb lattice, where each carbon atom is covalently bonded to three neighbouring carbon atoms through $sp^2$ hybridization. The remaining unhybridized p orbital forms an extended delocalized π-electron cloud over the entire lattice, imparting graphene with remarkable electronic mobility and mechanical robustness. [Armano, A et al. 2019]

The perfect crystalline architecture of pristine graphene is simultaneously its greatest strength and its principal limitation for biomedical applications. The highly conjugated π-electron network produces an extremely hydrophobic surface with minimal chemical functionality. Consequently, graphene exhibits strong π–π stacking interactions that promote irreversible aggregation in aqueous media, reducing its effective surface area and limiting its interaction with biological environments. Furthermore, the chemically inert basal plane provides relatively few reactive sites for conjugation with biomolecules, therapeutic agents, targeting ligands, or imaging probes. These inherent limitations significantly restrict the direct utilization of pristine graphene in physiological systems, where dispersion stability, biocompatibility, and controllable surface chemistry are essential prerequisites. [Zare, Pariya et al. 2021]

To overcome these limitations, controlled oxidation of graphite was developed as a versatile chemical strategy to introduce oxygen-containing functional groups into the graphene lattice. This oxidation process converts pristine graphene into graphene oxide (GO), a chemically heterogeneous derivative possessing dramatically different physicochemical characteristics. Unlike pristine graphene, GO is no longer a perfectly crystalline carbon sheet. Instead, oxidation disrupts portions of the continuous $sp^2$ carbon network through the incorporation of hydroxyl (-OH), epoxy (-C-O-C-), carbonyl (C=O), and carboxyl (-COOH) groups distributed across both basal planes and sheet edges. [Adéla Jiříčková et. al. 2022]The resulting material contains discrete graphitic domains interspersed with oxidized amorphous regions, producing a structurally heterogeneous carbon framework.

The transformation from graphene-to-graphene oxide represents considerably more than a simple increase in oxygen content. It fundamentally alters every aspect of material behaviour, including electronic properties, mechanical flexibility, colloidal stability, surface charge

distribution, interfacial chemistry, and biological interactions. The disruption of the continuous π-electron network decreases electrical conductivity but simultaneously generates numerous chemically active sites capable of interacting with proteins, phospholipids, nucleic acids, polysaccharides, and cellular membranes. These structural modifications convert GO from an electronically optimized material into a biologically interactive nanoplatform suitable for diverse biomedical applications.

The oxidation process also increases the interlayer spacing between adjacent graphene sheets. In graphite, neighbouring layers are separated by approximately 0.34 nm owing to strong van der Waals attractions. During oxidation, insertion of oxygen-containing functional groups together with intercalated water molecules expands the interlayer distance to approximately 0.8–1.0 nm, depending on oxidation degree and hydration state. This expanded interlayer spacing weakens inter sheet attractions, facilitating efficient exfoliation into single- or few-layer GO nanosheets with high colloidal stability in aqueous environments. The resulting dispersibility represents one of the defining characteristics distinguishing graphene oxide from pristine graphene and underpins its extensive use in biological investigations. [Marcano, D. C., et al. 2010] Importantly, graphene oxide should not be regarded as a single chemically uniform material. Instead, it represents an entire family of oxidized graphene derivatives whose physicochemical properties vary according to synthesis methodology, oxidation intensity, purification procedures, lateral sheet dimensions, defect density, and oxygen-to-carbon ratio. [Sali, S. et al. 2019] Consequently, graphene oxide synthesized through different protocols may exhibit substantial variation in biological behaviour despite sharing the same general chemical identity. Establishing robust structure–activity relationships therefore require comprehensive physicochemical characterization before biological evaluation, ensuring that observed cellular responses can be interpreted in the context of defined material properties rather than generic assumptions regarding graphene oxide.

The transition from pristine graphene to graphene oxide therefore illustrates one of the central concepts in nanobiotechnology: deliberate modification of atomic-scale structure can profoundly alter interactions at cellular and molecular interfaces. Rather than diminishing graphene's scientific value, oxidation broadens its biomedical utility by introducing chemical complexity that enables controlled interaction with living systems.

### 1.3 Structural Hallmarks of Graphene Oxide: Defect Engineering, Morphology, and Interlayer Architecture

The biological behaviour of graphene oxide is fundamentally governed by its structural organization at multiple hierarchical levels. [Tadyszak, K. et al. 2018] Unlike conventional

nanomaterials whose functionality often depends primarily on chemical composition, GO derives its biological activity from a combination of atomic arrangement, lattice defects, sheet morphology, edge architecture, and surface topology. Each of these structural characteristics influences how graphene oxide approaches, adheres to, penetrates, and ultimately modulates biological membranes.

At the atomic level, graphene oxide comprises alternating $sp^2$-hybridized graphitic islands and $sp^3$-hybridized oxidized domains. [Vejpravová, J., 2021] The graphitic regions preserve localized electronic conductivity, whereas oxidized regions disrupt π-electron delocalization and introduce structural strain into the lattice. This heterogeneous arrangement creates nanoscale electronic discontinuities that facilitate localized electron transfer processes and contribute significantly to reactive oxygen species generation during biological interactions. Rather than representing imperfections, these defect-rich regions constitute active sites that determine much of GO's biological functionality.

One of the defining structural characteristics of graphene oxide is its exceptionally large lateral dimension relative to its atomic thickness. Individual GO sheets may extend from several hundred nanometres to tens of micrometres while remaining only a single or few atomic layers thick. [Mohammad Rezaei D. et al. 2018] Such geometry produces an extraordinarily high aspect ratio and enormous specific surface area available for molecular adsorption and cellular interaction. From a biological perspective, this geometry enables simultaneous interaction with multiple membrane receptors, extracellular proteins, and phospholipid domains, creating interface dynamics fundamentally different from those observed with spherical nanoparticles.

Scanning electron microscopy and high-resolution transmission electron microscopy consistently demonstrate that graphene oxide possesses highly flexible nanosheets characterized by pronounced wrinkling, folding, corrugation, and irregular edge morphology. [Paredes, J. I., et al. 2008 & 2009] These features are not merely artifacts arising during sample preparation; rather, they originate from intrinsic lattice strain generated by oxidation-induced disruption of carbon–carbon bonding. The coexistence of rigid graphitic domains and flexible oxidized regions generates local mechanical heterogeneity, allowing GO sheets to undergo dynamic conformational changes during interaction with biological structures. Similar large-area wrinkled sheets with pronounced edge irregularities were observed in the physicochemical characterization supporting this study, providing the structural basis for subsequent biological evaluation.

Wrinkling substantially increases effective surface area by exposing otherwise inaccessible basal regions and creating nanoscale valleys capable of adsorbing proteins, lipids, extracellular

matrix molecules, and soluble biomacromolecules. Increased surface roughness also enhances mechanical interlocking with bacterial envelopes and mammalian plasma membranes, prolonging contact duration and facilitating physicochemical interactions. These topographical features are particularly important during antimicrobial activity, where intimate membrane contact precedes membrane disruption and oxidative injury. [San, H. et al. 2022] The edges of graphene oxide sheets represent another structurally unique region of exceptional biological significance. Compared with the relatively inert basal plane, sheet edges exhibit higher defect density, increased chemical reactivity, and greater exposure of oxygen-containing functional groups. These edge regions frequently possess atomically sharp geometries capable of exerting localized mechanical stress upon contact with lipid bilayers. Numerous experimental and computational investigations have demonstrated that these sharp edges may penetrate bacterial membranes, disrupt phospholipid organization, and initiate membrane rupture. This "nano-knife" effect has emerged as one of the hallmark mechanisms underlying GO-mediated antibacterial activity.

Defect engineering also profoundly influences graphene oxide's physicochemical performance. Structural defects arise from vacancies, Stone–Wales rearrangements, oxidation-induced lattice distortion, edge discontinuities, and incomplete restoration of graphitic order following synthesis. Although traditionally regarded as crystallographic imperfections, defects serve as chemically active centres that facilitate adsorption, catalytic reactions, electron transfer, and reactive oxygen species production. [Stankovich, S., et al. 2007] Higher defect density generally increases chemical reactivity but may simultaneously reduce mechanical integrity and electronic conductivity, illustrating the delicate balance required to optimize graphene oxide for biomedical applications.

Interlayer architecture constitutes another critical determinant of GO functionality. Oxidation-induced expansion of interlayer spacing reduces van der Waals attraction between adjacent sheets, promoting efficient exfoliation into individual nanosheets upon ultrasonication or mechanical agitation. [Lerf, A., et al. 1998] Expanded spacing also facilitates penetration of solvent molecules and biomacromolecules into the layered structure, increasing hydration, dispersion stability, and accessibility of reactive functional groups. These characteristics are particularly advantageous in biological fluids, where homogeneous dispersion ensures reproducible cellular exposure and minimizes aggregation-associated variability.

The structural flexibility of graphene oxide further distinguishes it from many rigid inorganic nanomaterials. Thin GO sheets readily bend, fold, curl, and wrap around microorganisms or mammalian cells under physiological conditions. Such dynamic behaviour enables graphene

oxide to maximize contact area while adapting to complex biological surfaces. [D'Amora, U. 2023] In bacterial systems, flexible sheets may envelop entire microbial cells, physically isolating them from nutrients and disrupting essential physiological processes. In mammalian systems, conformational flexibility facilitates extensive membrane contact, influencing receptor clustering, membrane curvature, cytoskeletal organization, and intracellular uptake pathways.

Collectively, these structural hallmarks establish graphene oxide as a highly dynamic two-dimensional nanomaterial whose biological activity cannot be attributed to a single physicochemical parameter. Instead, biological performance emerges from the synergistic interaction of atomic structure, defect distribution, nanosheet morphology, edge architecture, and interlayer organization. Understanding these structural features provides the essential framework for interpreting subsequent discussions regarding surface chemistry, antimicrobial mechanisms, and anticancer activity.

**1.4 Physicochemical Determinants Governing Nano–Bio Interactions**

The interface between engineered nanomaterials and living systems is governed by a complex interplay of physicochemical parameters that determine how nanoparticles are recognized, transported, internalized, and processed by biological structures. In the case of graphene oxide, biological responses arise not from conventional ligand–receptor interactions alone but from the integrated influence of size, morphology, surface chemistry, charge distribution, oxidation state, colloidal stability, and electronic structure. These determinants collectively define the "biological identity" of graphene oxide after exposure to physiological environments. [Anastasiadis, S.H. 2022]

One of the most influential physicochemical properties of graphene oxide is its exceptionally high specific surface area. Unlike spherical nanoparticles, whose interaction with cells is restricted by limited contact geometry, GO provides an expansive two-dimensional interface capable of simultaneous adsorption of proteins, lipids, carbohydrates, and nucleic acids. This high surface area substantially increases the probability of intermolecular interactions and facilitates formation of a dynamic protein corona upon exposure to biological fluids. The composition of this adsorbed biomolecular layer subsequently influences cellular recognition, immune activation, intracellular trafficking, and biodistribution.

Surface charge represents another major determinant of biological behaviour. Oxygen-containing functional groups, particularly carboxyl and hydroxyl moieties, impart an overall negative surface potential under physiological pH conditions. This electrostatic character influences colloidal stability by generating repulsive forces between adjacent GO sheets,

thereby reducing aggregation. [Gorohovs, M. et al. 2025] Simultaneously, surface charge regulates interactions with positively charged membrane proteins, extracellular matrix components, and microbial cell walls. Electrostatic attraction often serves as the initial step preceding stronger hydrophobic, hydrogen-bonding, or van der Waals interactions.

Colloidal stability is especially critical for reproducible biological evaluation. Aggregated graphene oxide exhibits reduced effective surface area, altered sedimentation behaviour, and non-uniform cellular exposure, leading to inconsistent experimental outcomes. Stable dispersions maintain individual nanosheets in suspension, maximizing accessible surface area and ensuring homogeneous interaction with target cells. Consequently, optimization of dispersion conditions represents an essential prerequisite for accurate interpretation of antimicrobial and anticancer studies, as emphasized in the biological evaluation framework developed for this work.

Another defining characteristic of graphene oxide is its electronic heterogeneity. Residual graphitic domains embedded within oxidized regions generate localized electron-rich and electron-deficient areas capable of participating in redox reactions. These nanoscale electronic gradients facilitate electron transfer between graphene oxide and cellular components, contributing to oxidative stress generation and disruption of intracellular redox homeostasis. Because oxidative stress represents a common pathway underlying both antibacterial and anticancer activity, electronic structure serves as a critical bridge linking physicochemical properties with biological outcomes.

The importance of these physicochemical determinants extends beyond in vitro observations. In physiological systems, they collectively influence protein adsorption, membrane adhesion, cellular uptake, intracellular trafficking, immune recognition, and therapeutic efficacy. Consequently, understanding nano–bio interactions require simultaneous consideration of multiple interdependent material properties rather than isolated physicochemical variables. This integrated perspective forms the conceptual basis for the subsequent discussion of graphene oxide surface chemistry and its role in mediating antimicrobial and anticancer responses.

### 1.5 Chemical Heterogeneity and Surface Functionalization of Graphene Oxide: The Foundation of Nano–Bio Interactions

Among all graphene-derived nanomaterials, graphene oxide (GO) occupies a unique position because of its remarkable chemical heterogeneity. Unlike pristine graphene, which consists almost entirely of a continuous network of $sp^2$-hybridized carbon atoms, GO exhibits a structurally heterogeneous lattice containing both graphitic and oxidized domains. [Adéla

Jiříčková et. al. 2022] The introduction of oxygen-containing functional groups during oxidation fundamentally transforms GO from a chemically inert two-dimensional carbon sheet into a highly reactive, hydrophilic, and biologically interactive nanoplatform. This heterogeneous surface chemistry governs virtually every aspect of GO's interaction with biological systems, including its colloidal stability, protein adsorption, cellular uptake, antimicrobial efficacy, and anticancer activity.

The biological behaviour of graphene oxide cannot be understood solely in terms of its elemental composition. Rather, it arises from the spatial distribution, chemical identity, density, and accessibility of its oxygen-containing functional groups. These groups are not uniformly distributed throughout the carbon lattice but instead occur in distinct chemical environments that collectively generate a dynamic and multifunctional surface capable of interacting with a diverse range of biomolecules.

According to the widely accepted Lerf–Klinowski structural model, hydroxyl and epoxy groups are predominantly located on the basal plane of graphene oxide, whereas carbonyl and carboxyl groups are concentrated near sheet edges and defect sites. This heterogeneous distribution results in localized differences in polarity, charge density, hydrogen-bonding capability, and electron distribution across the nanosheet surface. Consequently, different regions of a single graphene oxide sheet may participate simultaneously in electrostatic attraction, hydrogen bonding, hydrophobic interactions, π–π stacking, and electron-transfer reactions. [Lerf, A., et al. 1998]

This chemical complexity distinguishes graphene oxide from conventional nanomaterials whose surfaces often exhibit relatively homogeneous chemistry. Instead of possessing one dominant reactive functionality, GO behaves as a multifunctional molecular interface capable of adapting dynamically to the surrounding biological environment. [Shabnam S. et al. 2021]

### 1.5.1 Hydroxyl Functional Groups and Hydrophilic Surface Behaviour

Hydroxyl (-OH) groups constitute one of the principal oxygen-containing functionalities introduced during graphite oxidation. Distributed primarily across the basal plane, these groups significantly enhance the hydrophilicity of graphene oxide by increasing its ability to form hydrogen bonds with surrounding water molecules.

Hydroxyl-mediated hydration has profound implications for biomedical applications. The extensive hydration shell surrounding graphene oxide prevents irreversible aggregation through steric stabilization and electrostatic repulsion, thereby maintaining individual nanosheets in suspension under physiological conditions. Stable aqueous dispersions maximize

the effective surface area available for interaction with microorganisms and mammalian cells, ensuring uniform biological exposure during in vitro experiments.

Furthermore, hydroxyl groups serve as important anchoring sites for proteins, polysaccharides, nucleic acids, peptides, and pharmaceutical compounds. Their hydrogen-bonding capability facilitates reversible adsorption of biological macromolecules while preserving overall structural integrity. Upon exposure to biological fluids, these interactions contribute to the formation of a protein corona, which subsequently influences cellular recognition, membrane adhesion, receptor engagement, intracellular trafficking, and immune responses. [Kim, C. et al. 2020] From a therapeutic perspective, hydroxyl groups also permit extensive chemical modification through esterification, etherification, and polymer conjugation reactions. Functionalization strategies exploiting these groups have enabled the development of targeted drug-delivery systems, tissue engineering scaffolds, biosensors, and stimuli-responsive nanocarriers. Thus, hydroxyl groups not only enhance colloidal stability but also expand the versatility of graphene oxide as a biomedical platform. [Luceño-Sánchez, J.A. et al. 2018, Ximena Jaramillo-Fierro et al. 2024]

### 1.5.2 Epoxy Functional Groups: Structural Distortion and Mechanical Flexibility

Epoxy (-C–O–C-) groups are another abundant oxygen-containing functionality distributed throughout the basal plane of graphene oxide. Their incorporation disrupts the planar geometry of the graphene lattice by converting localized $sp^2$-hybridized carbon atoms into $sp^3$-hybridized configurations. This transition introduces lattice strain, atomic-scale distortion, and increased mechanical flexibility.

The presence of epoxy groups is therefore directly responsible for the characteristic wrinkled and corrugated morphology observed in scanning electron microscopy and transmission electron microscopy studies of graphene oxide. Rather than forming perfectly planar sheets, GO develops undulating topographical features that substantially increase effective surface area and promote intimate contact with biological membranes. Such morphological flexibility allows graphene oxide to conform dynamically to the irregular surfaces of bacterial envelopes and mammalian cells, maximizing interfacial interactions.

Epoxy groups also influence the electronic properties of graphene oxide by interrupting the delocalized π-electron system. Localized disruption of electron delocalization generates regions with differing electron densities, thereby contributing to the electronic heterogeneity that facilitates redox reactions and reactive oxygen species (ROS) generation. Consequently, epoxy groups indirectly participate in oxidative mechanisms that underlie both antimicrobial and anticancer activity. [D'Amora, U., et al. 2023]

### 1.5.3 Carbonyl Functional Groups: Electron Transfer and Redox Activity

Carbonyl (C=O) groups are typically concentrated near structural defects and sheet edges, where oxidation is thermodynamically favoured. These functionalities contribute substantially to the redox behaviour of graphene oxide owing to their ability to participate in electron transfer reactions. Electron transfer between graphene oxide and biological molecules represents one of the central mechanisms governing oxidative stress. During interaction with cellular membranes or intracellular organelles, localized electron exchange may disrupt redox homeostasis, resulting in excessive production of reactive oxygen species such as superoxide anions, hydrogen peroxide, and hydroxyl radicals. These highly reactive intermediates initiate oxidative damage to membrane lipids, cytoplasmic proteins, mitochondrial enzymes, and nucleic acids.

In mammalian cancer cells, oxidative stress frequently exceeds the antioxidant buffering capacity, leading to mitochondrial dysfunction, ATP depletion, DNA damage, activation of stress-responsive kinases, and induction of intrinsic apoptotic pathways. Similarly, bacterial antioxidant defence systems become overwhelmed under sustained ROS exposure, resulting in irreversible oxidation of essential biomolecules and progressive cellular dysfunction. [Gurunathan, S. et al. 2019] Thus, carbonyl groups contribute significantly to the oxidative component of graphene oxide-mediated cytotoxicity by facilitating electron transfer and amplifying intracellular redox imbalance.

### 1.5.4 Carboxyl Functional Groups: Surface Charge and Electrostatic Interactions

Carboxyl (-COOH) groups are predominantly located along sheet edges, where they impart a strongly negative surface charge under physiological pH conditions through ionization to carboxylate ($-COO^-$) species.

The negative surface potential generated by these groups performs several biologically important functions. First, electrostatic repulsion between neighbouring GO sheets prevents aggregation, preserving colloidal stability in aqueous environments. Second, negatively charged surfaces influence interactions with positively charged membrane proteins, extracellular matrix components, and bacterial cell wall constituents. [Shiva Shahriari et al. 2021]

In Gram-positive bacteria, positively charged teichoic acids embedded within the thick peptidoglycan layer promote electrostatic attraction with graphene oxide, facilitating close membrane contact and enhancing antibacterial activity. In mammalian cells, electrostatic interactions influence membrane adsorption, receptor clustering, and subsequent internalization through endocytic pathways. [Gorohovs, M. et al. 2025] Carboxyl groups also

serve as the principal sites for covalent bioconjugation. Carbodiimide-mediated coupling reactions readily attach antibodies, peptides, nucleic acids, polymers, growth factors, and therapeutic molecules to graphene oxide through amide bond formation. Such functionalization strategies have greatly expanded the application of GO in targeted drug delivery, biosensing, tissue engineering, and precision oncology.

**1.6 Electronic Heterogeneity: Linking Physicochemical Structure to Biological Function**

One of the defining characteristics distinguishing graphene oxide from many other nanomaterials is its electronic heterogeneity. Unlike pristine graphene, whose electrons are delocalized across an uninterrupted $sp^2$ carbon lattice, GO contains alternating graphitic and oxidized domains that generate localized differences in electronic density.

Residual graphitic islands retain relatively high electron mobility, whereas oxidized $sp^3$ regions exhibit reduced conductivity. The resulting coexistence of electron-rich and electron-deficient domains establishes numerous localized redox-active centres distributed throughout the nanosheet.

This electronic heterogeneity is not merely a structural consequence of oxidation; it constitutes the mechanistic foundation of graphene oxide's biological activity. Electron transfer occurring at these localized interfaces facilitates ROS generation, oxidative stress, and disruption of cellular metabolic homeostasis. The physicochemical characterization supporting this work—including UV–Visible spectroscopy, FTIR, NMR, ESI-MS, TGA, and PXRD—demonstrated that the synthesized GO possessed abundant oxygen-containing functional groups while retaining residual $sp^2$ domains, providing the structural basis for these redox-mediated biological interactions. [Choi, Y.-J. et al. 2018]

Within bacterial cells, oxidative damage compromises membrane integrity, inactivates respiratory enzymes, and damages genomic DNA. In cancer cells, ROS accumulation disrupts mitochondrial membrane potential, impairs oxidative phosphorylation, activates p53-dependent and p53-independent stress pathways, promotes cytochrome c release, and initiates caspase-mediated apoptosis. Importantly, because cancer cells often maintain intrinsically elevated basal ROS levels due to metabolic reprogramming, even modest additional oxidative stress generated by graphene oxide may exceed the cellular antioxidant threshold, resulting in selective cytotoxicity. The coexistence of graphitic and oxidized regions therefore enables graphene oxide to function simultaneously as a mechanically active nanosheet and a chemically reactive redox mediator. This dual functionality distinguishes GO from conventional antimicrobial agents and chemotherapeutics, whose biological effects typically depend upon single molecular targets. [Liu, S., et al. 2011]

### 1.7 Surface Chemistry as the Central Determinant of Biological Performance

Collectively, the oxygen-containing functional groups distributed across graphene oxide establish a multifunctional physicochemical interface capable of integrating structural mechanics, colloidal stability, surface charge regulation, molecular adsorption, electron transfer, and chemical functionalization. Rather than acting independently, hydroxyl, epoxy, carbonyl, and carboxyl groups function synergistically to produce a highly adaptive surface whose biological behaviour emerges from the combined effects of its heterogeneous chemistry. [Ng, I.M.J. et al. 2022] The antimicrobial and anticancer activities of graphene oxide should not be viewed simply as intrinsic properties of a carbon nanomaterial. Instead, they represent the biological manifestation of carefully balanced physicochemical characteristics that originate during synthesis and are subsequently expressed through interactions at the nano–bio interface. This concept of structure–property–function relationships underpin modern nanomedicine and provides the conceptual framework for interpreting the biological findings presented in the subsequent sections of this monograph. [Tadyszak, K., et al 2018]

### 1.8 The Global Antimicrobial Resistance Crisis: Emergence of Graphene Oxide as a Non-Antibiotic Antimicrobial Nanoplatform

The remarkable success of antibiotics during the twentieth century transformed modern medicine by dramatically reducing mortality associated with infectious diseases and enabling advances in surgery, transplantation, oncology, neonatal medicine, and intensive care. Since the introduction of penicillin into clinical practice, antimicrobial agents have become indispensable therapeutic tools for the prevention and treatment of bacterial infections. However, the widespread and frequently inappropriate use of antibiotics in human medicine, veterinary practice, agriculture, and aquaculture has imposed an unprecedented selective pressure on microbial populations, accelerating the evolution and dissemination of antimicrobial resistance (AMR). Consequently, bacterial pathogens that were once readily susceptible to conventional antibiotics have progressively acquired sophisticated genetic and physiological mechanisms that enable survival under antimicrobial exposure, thereby compromising the effectiveness of many first-line therapeutic agents.

Antimicrobial resistance is now recognized as one of the most significant global public health threats of the twenty-first century. Unlike many emerging infectious diseases that arise from novel pathogens, AMR represents the gradual erosion of therapeutic efficacy against organisms that have coexisted with humans for centuries. The consequences extend far beyond individual treatment failure. Resistant infections are associated with prolonged hospitalization, increased healthcare expenditure, greater morbidity, higher mortality rates, and substantial

socioeconomic burden. Furthermore, the diminishing effectiveness of antibiotics threatens the safety of numerous medical procedures—including organ transplantation, prosthetic implantation, chemotherapy, and major surgical interventions—that rely upon effective infection control.

The biological basis of antimicrobial resistance is remarkably complex and multifactorial. Bacteria employ diverse adaptive strategies that collectively reduce intracellular antibiotic concentrations, modify molecular targets, enzymatically inactivate antimicrobial compounds, or establish protected physiological states that permit survival during antibiotic exposure. Horizontal gene transfer through conjugation, transformation, and transduction further accelerates dissemination of resistance determinants across bacterial populations, allowing resistance genes to spread rapidly between taxonomically unrelated species. The remarkable genetic plasticity of microorganisms therefore enables continual adaptation to newly introduced antimicrobial agents, frequently outpacing the development of novel antibiotics.

Among clinically important pathogens, multidrug-resistant Gram-positive organisms such as methicillin-resistant *Staphylococcus aureus* (MRSA) and vancomycin-resistant *Enterococcus* species have become major causes of hospital-acquired infections. Simultaneously, Gram-negative bacteria—including *Escherichia coli*, *Klebsiella pneumoniae*, *Acinetobacter baumannii*, and particularly *Pseudomonas aeruginosa*—have evolved formidable resistance mechanisms that severely restrict available therapeutic options. The intrinsic impermeability of the Gram-negative outer membrane, together with multidrug efflux pumps, enzymatic degradation systems, and biofilm formation, collectively renders these pathogens among the most difficult bacterial infections to eradicate.

The limited pace of antibiotic discovery has further intensified this crisis. Most currently available antibiotics belong to a relatively small number of chemical classes discovered during the so-called "golden era" of antibiotic development between the 1940s and 1960s. Since then, relatively few fundamentally new antibacterial scaffolds have entered clinical practice. Consequently, many recently approved agents represent incremental chemical modifications of existing antibiotics rather than truly novel therapeutic mechanisms. Because resistance mechanisms directed against one member of an antibiotic class frequently confer cross-resistance to structurally related compounds, the long-term effectiveness of these agents remains uncertain.

These challenges have stimulated intense investigation into alternative antimicrobial strategies that operate independently of conventional biochemical targets. Rather than inhibiting specific enzymes or metabolic pathways, emerging non-antibiotic antimicrobial materials aim to disrupt

fundamental structural and physicochemical processes essential for microbial survival. Nanotechnology has become particularly attractive in this regard because nanomaterials frequently exert biological effects through multiple simultaneous mechanisms, thereby reducing the likelihood of resistance development.

Among the diverse nanomaterials investigated for antimicrobial applications, graphene oxide occupies a particularly distinctive position. Unlike traditional antibiotics that typically target a single molecular pathway, GO possesses no specific biochemical target. Instead, its antimicrobial activity originates from the intrinsic physicochemical characteristics of its two-dimensional nanosheet architecture, heterogeneous surface chemistry, high specific surface area, and redox-active carbon framework. These properties collectively enable GO to interact directly with bacterial membranes, proteins, extracellular polymers, and intracellular macromolecules through multiple complementary mechanisms.

The antimicrobial efficacy of graphene oxide therefore arises from multifactorial physicochemical interactions rather than conventional pharmacological inhibition. This distinction has profound therapeutic implications. Because bacterial adaptation would require simultaneous resistance against several independent mechanisms—including mechanical disruption, oxidative injury, membrane extraction, and physical isolation—the probability of rapidly developing complete resistance is theoretically much lower than that associated with conventional antibiotics. Although bacterial adaptation to nanomaterials remains an active area of investigation, current evidence suggests that the multifaceted mode of action of graphene oxide represents a promising strategy for overcoming limitations associated with single-target antimicrobial agents. [Ng, I.M.J. et al. 2022]

### 1.8.1 Structural Basis of Graphene Oxide-Mediated Antibacterial Activity

The antibacterial properties of graphene oxide originate directly from the structural and chemical features established during synthesis and physicochemical characterization. The large lateral dimensions of GO nanosheets provide extensive contact surfaces capable of interacting simultaneously with multiple bacterial cells, while atomically thin sheet edges concentrate mechanical stress at the nano–bio interface. Oxygen-containing functional groups—including hydroxyl, epoxy, carbonyl, and carboxyl moieties—enhance aqueous dispersibility and promote close association with microbial surfaces through hydrogen bonding, electrostatic attraction, and van der Waals interactions. [Perreault, F., et al. 2015] As highlighted in the biological rationale for this work, these physicochemical attributes provide the mechanistic foundation for antimicrobial evaluation and enable GO to interact with bacterial cell envelopes through multiple complementary pathways.

Unlike conventional antibiotics that must penetrate bacterial cells to inhibit intracellular targets, graphene oxide initiates antimicrobial activity at the cell surface. Upon contact with bacterial envelopes, flexible nanosheets conform to membrane topography, maximizing contact area and facilitating localized mechanical interactions. [Vi, T.T.T. et al. 2020] High aspect-ratio sheets may partially envelop bacterial cells, increase the duration of membrane contact and create favourable conditions for subsequent oxidative and physicochemical damage. This contact-dependent behaviour distinguishes GO from diffusible antimicrobial agents and emphasizes the importance of nanosheet morphology in determining biological performance.

The chemical heterogeneity of graphene oxide further amplifies its antimicrobial potential. Negatively charged oxygen-containing functional groups regulate electrostatic interactions with bacterial cell walls, while residual graphitic domains facilitate electron transfer processes that contribute to reactive oxygen species generation. The simultaneous presence of hydrophilic oxidized regions and hydrophobic graphitic domains also enables GO to interact with diverse membrane components possessing varying physicochemical characteristics. Consequently, graphene oxide behaves not simply as a passive surface but as a dynamic interface capable of continuously adapting to the complex architecture of bacterial envelopes.

### 1.8.2 Differential Susceptibility of Gram-Positive and Gram-Negative Bacteria

Although graphene oxide exhibits broad-spectrum antibacterial activity, the magnitude of bacterial susceptibility varies substantially according to cell envelope architecture. [Mauricio D., et al. (2017] These differences provide important insight into the relationship between nanosheet physico chemistry and microbial ultrastructure. Gram-positive bacteria possess a relatively simple envelope organization consisting of a cytoplasmic membrane surrounded by a thick peptidoglycan meshwork enriched with teichoic and lipoteichoic acids. Although the peptidoglycan layer may exceed 20–40 nm in thickness, it remains highly porous and permits relatively unrestricted diffusion of nanoscale materials. Consequently, graphene oxide can readily establish direct contact with the underlying membrane, facilitating mechanical disruption and oxidative injury. The abundance of positively charged teichoic acids further promotes electrostatic interactions with negatively charged GO surfaces, increasing membrane adhesion and enhancing antibacterial efficacy.

Representative Gram-positive organisms evaluated in this study *Staphylococcus aureus* and *Enterococcus faecalis* therefore provide appropriate models for investigating GO-mediated membrane interactions. Previous experimental observations consistently demonstrate larger zones of inhibition against these organisms compared with Gram-negative bacteria, supporting

the concept that the absence of an outer membrane facilitates direct physicochemical interactions between GO nanosheets and bacterial membranes. This trend is also reflected in the antimicrobial framework developed for the present work.

In contrast, Gram-negative bacteria possess a considerably more complex cell envelope comprising an inner cytoplasmic membrane, a thin peptidoglycan layer, and an additional outer membrane enriched with lipopolysaccharide (LPS). This outer membrane functions as an effective permeability barrier that limits penetration of many antimicrobial agents and reduces direct contact between graphene oxide and the cytoplasmic membrane. The densely packed LPS layer also contributes to membrane rigidity and restricts nanosheet insertion, thereby diminishing the efficiency of mechanical disruption. [Umar, M.F. et al. 2020]

Among Gram-negative pathogens, *Pseudomonas aeruginosa* is widely regarded as one of the most intrinsically resistant bacterial species. Its remarkable resilience results from the combined action of low outer membrane permeability, highly efficient multidrug efflux systems, extensive metabolic adaptability, and an exceptional capacity for biofilm formation. Biofilms further impede nanomaterial penetration by embedding bacterial communities within a dense extracellular polymeric matrix that acts as a physical and chemical diffusion barrier. Consequently, *P. aeruginosa* often exhibits the smallest inhibition zones following GO treatment, not because graphene oxide lacks antibacterial activity, but because the bacterium possesses multiple overlapping defence mechanisms that collectively reduce nanosheet access to vulnerable cellular targets.

These structural differences underscore an important principle in nanobiology: the biological activity of graphene oxide is determined not only by the intrinsic properties of the nanomaterial but also by the physicochemical characteristics of the target organism. Antimicrobial performance therefore emerges from reciprocal interactions between nanosheet structure and microbial cell envelope architecture rather than from material properties alone.

### 1.9 Graphene Oxide as a Multi-Mechanistic Non-Antibiotic Antimicrobial Agent

One of the most compelling attributes of graphene oxide is that it does not rely upon a single dominant mechanism to inhibit bacterial growth. Instead, its antibacterial activity arises through the convergence of multiple complementary processes that occur simultaneously at the nano–bio interface. This multi-mechanistic behaviour differentiates GO from conventional antibiotics and provides a strong rationale for its investigation as a next-generation antimicrobial material. [Yaragalla, S. et al. 2021]

Current evidence indicates that four principal mechanisms collectively contribute to graphene oxide-mediated bacterial killing:

1. **Physical membrane disruption** resulting from direct interaction of atomically sharp nanosheet edges with bacterial envelopes, producing localized membrane deformation, pore formation, and eventual loss of structural integrity.
2. **Oxidative stress induction**, whereby residual $sp^2$ domains and oxygen-rich defect sites facilitate electron transfer reactions leading to generation of reactive oxygen species that damage lipids, proteins, and nucleic acids.
3. **Extraction of membrane phospholipids**, in which strong hydrophobic and van der Waals interactions destabilize lipid bilayers by removing phospholipid molecules from bacterial membranes, thereby compromising membrane function.
4. **Cellular entrapment and isolation**, where flexible GO sheets wrap around bacterial cells or microcolonies, restricting nutrient diffusion, interfering with gas exchange, and preventing normal cellular proliferation.

Importantly, these mechanisms are not mutually exclusive. Rather, they reinforce one another, resulting in progressive bacterial injury that culminates in irreversible loss of viability. This synergistic mode of action substantially reduces dependence upon any single molecular target and thereby offers a promising strategy for combating multidrug-resistant bacterial pathogens.

### 1.10 The Global Burden of Cancer and the Need for Next-Generation Therapeutic Strategies

Cancer remains one of the leading causes of morbidity and mortality worldwide, representing a major public health challenge that continues to impose profound medical, social, and economic burdens. Despite substantial advances in molecular biology, precision medicine, immunotherapy, and targeted therapeutics, the incidence of many malignancies continues to increase due to population ageing, environmental exposures, lifestyle changes, and improved diagnostic capabilities. The biological complexity of malignant disease, together with remarkable tumour heterogeneity and adaptive resistance mechanisms, has prevented the development of universally effective therapeutic strategies. Consequently, there is growing interest in innovative treatment platforms capable of targeting cancer cells through mechanisms fundamentally distinct from those employed by conventional chemotherapeutic agents.

Cancer is not a single disease but rather a heterogeneous group of disorders characterized by uncontrolled cellular proliferation, evasion of programmed cell death, sustained angiogenesis, metabolic reprogramming, immune escape, genomic instability, and metastatic dissemination. These hallmarks arise through the progressive accumulation of genetic mutations, epigenetic alterations, and dysregulated intracellular signalling pathways that collectively transform normal cells into malignant phenotypes. Importantly, considerable heterogeneity exists not

only between different tumour types but also among patients with the same diagnosis and even among individual cells within a single tumour mass. Such heterogeneity profoundly influences therapeutic response and remains one of the principal obstacles to durable clinical remission.

Traditional cancer therapies—including surgery, radiotherapy, and systemic chemotherapy—have substantially improved survival for many malignancies. However, these modalities possess significant limitations. Surgical intervention is generally effective only for localized disease and is frequently incapable of eradicating disseminated micro metastases. Radiotherapy, while highly effective for local tumour control, inevitably exposes adjacent healthy tissues to ionizing radiation, thereby increasing the risk of treatment-associated toxicity. Systemic chemotherapy remains a cornerstone of cancer management; however, most cytotoxic agents exhibit limited selectivity between rapidly proliferating malignant cells and normal tissues with high proliferative capacity, including bone marrow, gastrointestinal epithelium, and hair follicles. [Krasteva Natalia et al. 2019] Chemotherapy is frequently associated with myelosuppression, gastrointestinal toxicity, alopecia, infertility, and cumulative organ damage, all of which restrict treatment intensity and compromise patient quality of life.

Another major limitation of conventional chemotherapy is the progressive development of drug resistance. Cancer cells possess extraordinary adaptive capacity, enabling them to evade cytotoxic injury through multiple mechanisms including increased drug efflux, enhanced DNA repair, altered apoptotic signalling, metabolic adaptation, epithelial–mesenchymal transition, and acquisition of cancer stem cell phenotypes. These resistance mechanisms frequently emerge during treatment, resulting in tumour recurrence and therapeutic failure. The multifactorial nature of chemoresistance underscores the need for alternative therapeutic platforms capable of inducing cancer cell death through complementary physicochemical mechanisms rather than single molecular targets.

Nanotechnology has emerged as one of the most promising approaches for addressing these limitations. Nanomaterials possess dimensions comparable to those of biological macromolecules and subcellular organelles, allowing intimate interaction with cellular membranes, intracellular compartments, and molecular signalling pathways. Their high surface-area-to-volume ratio, tunable physicochemical properties, and capacity for multifunctional surface modification enable simultaneous integration of therapeutic delivery, diagnostic imaging, molecular targeting, and controlled drug release within a single platform. Unlike conventional small-molecule therapeutics, many nanomaterials exert biological effects

through direct physicochemical interactions at the nano–bio interface, thereby offering opportunities to circumvent traditional mechanisms of drug resistance.

Among the wide variety of nanomaterials currently under investigation, graphene oxide has attracted particular attention because of its unique two-dimensional architecture, chemically active surface, and remarkable capacity to interact with cellular membranes and intracellular organelles. Rather than functioning solely as a passive drug carrier, GO possesses intrinsic biological activity that may contribute directly to tumour suppression through oxidative stress induction, membrane perturbation, mitochondrial dysfunction, and activation of programmed cell death pathways. This multifunctional behaviour distinguishes graphene oxide from many conventional nanocarriers and positions it as a promising candidate for the development of next-generation anticancer nanomedicines.

**1.11 Breast and Lung Cancer: Clinical Significance and Molecular Heterogeneity**

Among all human malignancies, breast cancer and lung cancer remain the two most extensively studied owing to their high global incidence, substantial mortality, and remarkable biological diversity. Although both diseases arise from epithelial tissues, they differ considerably in their molecular pathogenesis, genetic alterations, therapeutic responsiveness, and clinical outcomes. Investigation of graphene oxide across representative models of these cancers therefore provides valuable insight into the influence of tumour phenotype on nanomaterial-mediated cytotoxicity. [Jarosz Anna et al. 2016]

Lung cancer continues to represent the leading cause of cancer-related mortality worldwide. Approximately 85% of lung cancers are classified as non-small-cell lung carcinoma (NSCLC), a heterogeneous group that includes adenocarcinoma, squamous cell carcinoma, and large-cell carcinoma. Lung adenocarcinoma, from which the A549 cell line is derived, is the most common histological subtype and is characterized by complex molecular alterations involving KRAS, EGFR, ALK, TP53, and PI3K signalling pathways. Despite major advances in targeted therapies and immune checkpoint inhibitors, many patients eventually develop therapeutic resistance, highlighting the need for complementary treatment strategies capable of bypassing conventional signalling pathways.

Breast cancer similarly exhibits extraordinary biological heterogeneity. Modern molecular classification categorizes breast tumours into distinct intrinsic subtypes based upon gene-expression profiles and receptor status, including luminal A, luminal B, HER2-enriched, basal-like, and triple-negative breast cancer (TNBC). Each subtype possesses unique biological characteristics, prognostic implications, and therapeutic vulnerabilities.

Luminal A breast cancers generally express estrogen receptors (ER), progesterone receptors (PR), low proliferative indices, and relatively intact cell-cycle regulatory mechanisms. These tumours typically respond well to endocrine therapy and generally exhibit favourable clinical outcomes. The MCF-7 cell line represents one of the most widely utilized in vitro models of luminal A breast carcinoma and retains many of these molecular characteristics, making it particularly suitable for evaluating differential responses to graphene oxide.

In contrast, triple-negative breast cancer lacks expression of estrogen receptors, progesterone receptors, and human epidermal growth factor receptor 2 (HER2). Because these tumours lack the molecular targets exploited by endocrine therapies and HER2-directed agents, systemic chemotherapy remains the principal treatment option. TNBC is generally associated with aggressive clinical behaviour, early metastasis, high recurrence rates, and poor long-term prognosis. The MDA-MB-231 cell line represents an established model of triple-negative breast cancer characterized by high invasiveness, mesenchymal features, enhanced migratory capacity, and pronounced genomic instability. [Krętowski, R. et al. 2022]

The inclusion of A549, MCF-7, and MDA-MB-231 cells in the present investigation therefore enables systematic comparison of graphene oxide-mediated cytotoxicity across three clinically relevant tumour phenotypes that differ substantially in molecular biology, proliferative behaviour, metabolic characteristics, and therapeutic responsiveness. Such comparative evaluation is essential for determining whether the biological activity of graphene oxide is broadly cytotoxic or selectively influenced by tumour phenotype.

**1.12 Molecular Basis for Differential Sensitivity to Graphene Oxide**

One of the central hypotheses underlying graphene oxide-mediated cancer therapy is that malignant cells are inherently more susceptible than normal cells to disturbances in oxidative homeostasis. Unlike healthy tissues, cancer cells maintain chronically elevated levels of reactive oxygen species owing to accelerated metabolism, mitochondrial dysfunction, oncogene activation, chronic inflammation, and rapid proliferation. Although tumour cells simultaneously upregulate antioxidant defence systems to maintain viability, they often exist near the threshold of oxidative tolerance. Consequently, even modest additional oxidative stress generated by external agents may overwhelm endogenous antioxidant capacity, resulting in irreversible cellular injury.

Graphene oxide is uniquely positioned to exploit this vulnerability. Its heterogeneous carbon lattice, abundant oxygen-containing functional groups, and residual $sp^2$ domains facilitate electron transfer reactions that promote intracellular ROS generation. [Amedea B. S., et al. 2014, Jing Wu et. al. 2015] Excessive ROS accumulation induces lipid peroxidation, oxidation

of structural and enzymatic proteins, DNA strand breaks, and disruption of mitochondrial membrane potential. [Tanveer A Tabish *et al* 2017, Ruomin Liao et al. 2024, Anna J. et. al. 2015, Khan, M. et. al. 2016, Shih-Ming T. et al. 2017, Mittal S, et. al. 2016, Neha A, et. al. 2013, Feng Xia C. et. al. 2019] These events collectively impair ATP production, activate stress-responsive kinases, and trigger intrinsic apoptotic signalling through cytochrome c release and caspase activation. Similar mechanistic pathways have been proposed in studies of GO-induced cytotoxicity and align with the biological rationale underlying the present investigation.

Cellular sensitivity is strongly influenced by molecular determinants including p53 status, antioxidant enzyme expression, metabolic phenotype, membrane composition, and DNA repair capacity. [Aggarwal V. et al. 2019, Hany E. M., 2021, Haolan W. et. al. 2023] MCF-7 cells possess functional wild-type TP53, enabling activation of p21-mediated cell-cycle arrest following DNA damage or oxidative stress. Temporary cell-cycle arrest provides these cells with an opportunity to repair molecular damage before re-entering the proliferative cycle. Consequently, MCF-7 cells frequently demonstrate greater resistance to oxidative injury and cytotoxic agents than more genetically unstable breast cancer models. [Weiyu F. et. al., 2022] By contrast, MDA-MB-231 cells harbour mutant TP53, resulting in defective checkpoint regulation and impaired coordination of DNA damage responses. [Yi, L., Zhang et. al. 2019, Liu CC. et. al. 2017] Loss of normal p53 function reduces the ability of these cells to arrest the cell cycle and initiate effective repair following oxidative injury. Instead, accumulated molecular damage rapidly progresses toward apoptosis or necrotic cell death. This mechanistic distinction provides a compelling biological explanation for the markedly greater sensitivity of MDA-MB-231 cells observed following graphene oxide exposure in the present work, [Alfredo Cruz-Gregorio 2026] where $IC_{50}$ values decreased from 219.44 μg/mL at 24 hours to 105.40 μg/mL at 48 hours, compared with the substantially higher $IC_{50}$ values observed for MCF-7 cells (1578.34 μg/mL at 24 hours and 306.70 μg/mL at 48 hours). [Sohaebuddin, S.K., et. al. 2010]

A549 lung adenocarcinoma cells display an intermediate phenotype. Exposure to graphene oxide produces progressive reductions in cell viability accompanied by characteristic morphological alterations including cell rounding, shrinkage, decreased adherence, membrane irregularity, and reduced cell density, consistent with cumulative oxidative stress and mitochondrial dysfunction. These findings suggest that graphene oxide exerts concentration- and time-dependent antiproliferative effects across multiple tumour types while the magnitude

of response remains strongly influenced by tumour-specific molecular characteristics. [Singh, S. et. al. 2021]

### 1.13 Rationale and Objectives of the Present Investigation

The physicochemical characterization presented in the preceding chapter established that the synthesized graphene oxide possessed large-area flexible nanosheets with pronounced wrinkling, abundant oxygen-containing functional groups, residual graphitic domains, expanded interlayer spacing, and controlled structural integrity. These characteristics collectively provide the mechanistic basis for biological interaction by enhancing aqueous dispersibility, membrane contact, electrostatic attraction, and redox activity. As emphasized in the rationale for biological evaluation, these material attributes justify systematic investigation of both antimicrobial and anticancer properties through well-defined in vitro models. [Seabra, A. B., et al., 2014] The present study was designed to evaluate the biological performance of graphene oxide across two major biomedical domains. Antimicrobial activity was assessed against representative Gram-positive (*Staphylococcus aureus* and *Enterococcus faecalis*) and Gram-negative (*Escherichia coli* and *Pseudomonas aeruginosa*) bacterial pathogens to investigate the influence of cell-envelope architecture on susceptibility. Anticancer activity was examined using A549 lung adenocarcinoma cells together with two molecularly distinct breast cancer models, MCF-7 (luminal A) and MDA-MB-231 (triple-negative), enabling comparative evaluation of tumour phenotype-dependent responses.

The overarching hypothesis of this investigation is that the biological activities of graphene oxide are intrinsic consequences of its structural and chemical properties. Specifically, the study proposes that the combination of two-dimensional morphology, defect-rich carbon lattice, oxygen-containing functional groups, and electronic heterogeneity enables GO to interact with microorganisms and cancer cells through multiple complementary mechanisms—including membrane perturbation, oxidative stress, metabolic disruption, and induction of programmed cell death. [Yang, K., et al. 2010] Establishing these structure–activity relationships will not only improve our understanding of graphene oxide biology but also contribute to the rational development of safer and more effective graphene-based antimicrobial coatings, infection-resistant biomaterials, targeted nanomedicines, and multifunctional therapeutic platforms.

### 1.14 Objectives

The present study comprehensively investigates the antimicrobial and anticancer activities of synthesized graphene oxide by establishing direct relationships between its physicochemical characteristics and biological performance. Particular emphasis is placed on elucidating the

mechanistic pathways responsible for bacterial growth inhibition and selective cytotoxicity against representative human cancer cell lines. Antimicrobial investigations were performed against clinically significant Gram-positive bacteria (*Staphylococcus aureus* and *Enterococcus faecalis*) and Gram-negative bacteria (*Escherichia coli* and *Pseudomonas aeruginosa*). The anticancer potential of graphene oxide was evaluated using three human cancer models representing distinct molecular phenotypes: A549 human lung adenocarcinoma cells, MCF-7 luminal A breast carcinoma cells, and MDA-MB-231 triple-negative breast carcinoma cells. Through integrated physicochemical characterization and biological evaluation, the study seeks to define structure–activity relationships that may facilitate the rational design of graphene oxide-based biomedical materials.

## 2. Materials and Methods

### 2.1 Biological Evaluation of Graphene Oxide

The biological performance of graphene oxide (GO) was systematically investigated through complementary antimicrobial and anticancer studies designed to evaluate its efficacy against clinically relevant bacterial pathogens and representative human cancer cell lines. The experimental workflow was developed to establish direct correlations between the physicochemical characteristics of graphene oxide and its biological activity, thereby enabling interpretation of antimicrobial and cytotoxic responses in the context of structure–activity relationships. [Vimalanathan, B. et al. 2023] All biological experiments were performed under standardized laboratory conditions using sterile procedures to minimize contamination and ensure reproducibility. Experimental design incorporated appropriate untreated controls, concentration-dependent exposure regimens, and temporal assessment to investigate both immediate and progressive biological responses. Particular emphasis was placed on maintaining consistent dispersion of graphene oxide throughout all experiments because aggregation can substantially alter nanoparticle–cell interactions and consequently influence biological outcomes. [Umar, M.F. et al. 2020]

The biological evaluation comprised two principal components:

1. **Assessment of antimicrobial activity** against representative Gram-positive and Gram-negative bacterial pathogens.
2. **Assessment of anticancer activity** using human lung adenocarcinoma and breast carcinoma cell lines representing distinct molecular subtypes.

Together, these investigations were intended to determine whether the intrinsic physicochemical characteristics of graphene oxide confer broad-spectrum biological activity across both microbial and mammalian systems.

## 2.2 Antimicrobial Evaluation of Graphene Oxide

### 2.2.1 Scientific Rationale

The antimicrobial activity of graphene oxide was investigated to determine its potential as a non-antibiotic antimicrobial nanomaterial. Unlike conventional antibiotics that inhibit specific intracellular enzymes or metabolic pathways, graphene oxide exerts antibacterial activity primarily through direct physicochemical interactions at the bacterial surface. Consequently, experimental evaluation was designed to maximize contact between uniformly dispersed GO nanosheets and bacterial cells while minimizing interference from solvent systems or experimental artifacts. [Ng, I.M.J. et al. 2022] Selection of bacterial species was based on their clinical importance and their fundamentally different cell-envelope architectures. Inclusion of both Gram-positive and Gram-negative organisms enabled evaluation of how bacterial ultrastructure influences susceptibility to graphene oxide.

Graphene oxide synthesized through controlled oxidation was characterized by complementary analytical techniques including Fourier-transform infrared spectroscopy (FTIR), ultraviolet–visible spectroscopy (UV–Vis), proton nuclear magnetic resonance spectroscopy (^1H NMR), electrospray ionization mass spectrometry (ESI-MS), powder X-ray diffraction (PXRD), thermogravimetric analysis (TGA), scanning electron microscopy (SEM), and high-resolution transmission electron microscopy (HR-TEM), thereby confirming its structural integrity, oxidation state, chemical heterogeneity, and nanoscale morphology. Biological evaluation subsequently assessed the functional implications of these physicochemical properties. Antibacterial activity was investigated using the agar well diffusion method against representative Gram-positive and Gram-negative bacterial pathogens. Anticancer efficacy was determined by colorimetric MTT assays following concentration- and time-dependent exposure of A549, MCF-7, and MDA-MB-231 cells to graphene oxide. Cellular viability, half-maximal inhibitory concentration ($IC_{50}$), and treatment-induced morphological alterations were systematically evaluated using phase-contrast microscopy under standardized cell culture conditions.

### 2.2.2 Preparation of Graphene Oxide Suspension

Graphene oxide synthesized during the present investigation was initially obtained as a dry powdered material. Prior to biological testing, the powder was dispersed in dimethyl sulfoxide (DMSO) to obtain a homogeneous suspension suitable for antimicrobial evaluation. DMSO was selected because of its excellent capacity to disperse graphene-based nanomaterials while maintaining colloidal stability and minimizing aggregation.

Preparation of a stable suspension represents one of the most critical methodological steps in graphene oxide research. Owing to the large surface area and strong intermolecular van der Waals interactions between adjacent nanosheets, inadequately dispersed GO readily forms aggregates. Such aggregation substantially reduces the accessible surface area available for bacterial interaction and may lead to considerable variability in antimicrobial performance. [Giacomo Biagiotti et al. 2021]

The suspension was therefore prepared under carefully controlled conditions to ensure uniform dispersion throughout the experimental period. DMSO concentration was maintained below levels known to exhibit intrinsic antibacterial activity, thereby ensuring that any observed inhibition resulted exclusively from graphene oxide rather than solvent-mediated toxicity. This approach is consistent with established antimicrobial testing protocols for graphene-based nanomaterials.

Uniform dispersion additionally facilitates reproducible exposure by maximizing the availability of individual nanosheets capable of interacting directly with bacterial membranes.

### 2.2.3 Selection of Bacterial Strains

Four clinically important bacterial species representing both major bacterial groups were selected for antimicrobial evaluation. [Olczak, K. et al. 2023]

**Gram-positive bacteria**

- *Staphylococcus aureus*
- *Enterococcus faecalis*

These organisms possess a thick peptidoglycan cell wall but lack an outer membrane, making them ideal models for investigating direct membrane interactions with graphene oxide.

**Gram-negative bacteria**

- *Escherichia coli*
- *Pseudomonas aeruginosa*

These organisms possess an additional outer lipopolysaccharide membrane that serves as an effective permeability barrier. Inclusion of these bacteria enabled assessment of whether outer membrane architecture influences graphene oxide-mediated antimicrobial activity.

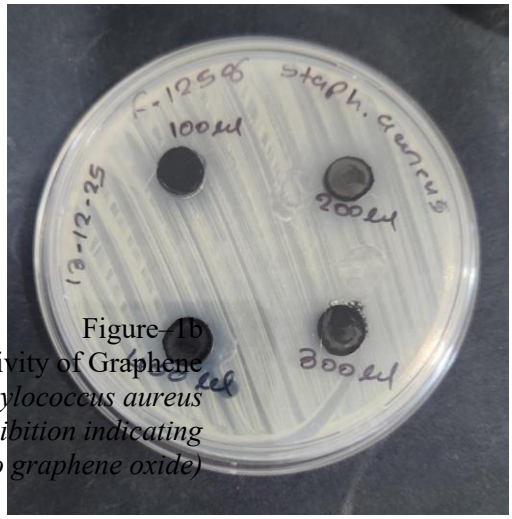
Particular attention was given to *Pseudomonas aeruginosa*, which is recognized for its multidrug resistance, efficient efflux pump systems, low membrane permeability, and exceptional biofilm-forming capability. Its inclusion provides a stringent model for evaluating the antimicrobial potential of graphene oxide against highly resistant pathogens.

### 2.2.4 Agar Well Diffusion Assay

Antibacterial activity was evaluated using the agar well diffusion method, one of the most widely accepted qualitative screening techniques for assessing antimicrobial efficacy of nanomaterials. [Jastrzębska, A.M. et. al. 2012, Ma, Y. et. al. 2014, Singh, Z., 2016] Fresh bacterial cultures were uniformly inoculated onto sterile agar plates to produce confluent bacterial lawns. Circular wells were then created within the agar medium using a sterile cork borer, after which predetermined volumes of the graphene oxide suspension were carefully introduced into each well. During incubation, graphene oxide diffused radially from the wells into the surrounding agar matrix. If bacterial growth was inhibited, clear zones surrounding the wells became visible. These zones of inhibition provided qualitative evidence of antibacterial activity. [Ajay Jose et al. 2023] Although agar diffusion assays do not directly determine minimum inhibitory concentrations (MIC), they provide valuable comparative information regarding bacterial susceptibility and permit rapid assessment of broad-spectrum antimicrobial activity. Untreated controls together with solvent controls were included to verify that bacterial inhibition resulted specifically from graphene oxide exposure.




Figure– 1a
Antimicrobial Activity of Graphene Oxide Against *Enterococcus faecalis* *(Agar well diffusion assay showing inhibitory response at varying concentrations)*




Figure–1b
Antimicrobial Activity of Graphene Oxide Against *Staphylococcus aureus* *(Clear zones of inhibition indicating susceptibility to graphene oxide)*

**Figure 1. Antimicrobial activity of graphene oxide against Gram-positive bacterial strains (*Staphylococcus aureus* and *Enterococcus faecalis*) showing clear zones of inhibition, indicating higher susceptibility due to absence of an outer membrane.**




Figure–2a
Antimicrobial Activity of Graphene Oxide Against *Escherichia coli* (Agar well diffusion assay showing dose-dependent inhibition)

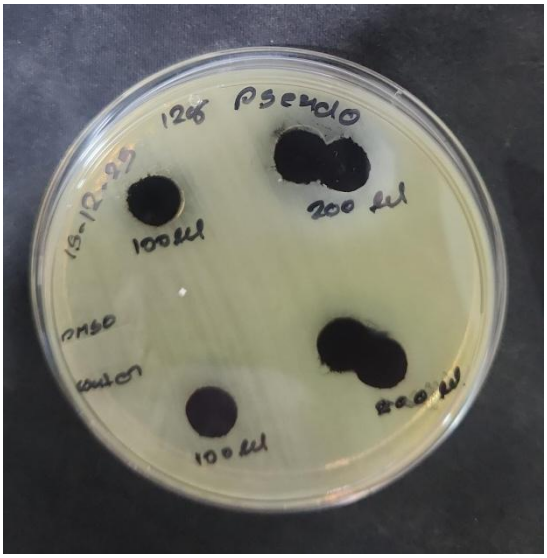



Figure – 2b
Antimicrobial Activity of Graphene Oxide Against *Pseudomonas aeruginosa* (Dose-dependent antibacterial effect assessed by agar diffusion method)

**Figure 2. Antimicrobial activity of graphene oxide against Gram-negative bacterial strains (*Escherichia coli* and *Pseudomonas aeruginosa*) demonstrating comparatively reduced but significant antibacterial response due to the presence of an outer lipopolysaccharide barrier.**

### 2.2.5 Interpretation of Antimicrobial Activity

Following incubation, antimicrobial activity was assessed by examining the presence, clarity, and relative diameter of inhibition zones surrounding each treatment well.

The size of the inhibition zone reflects the combined influence of several parameters, including

- diffusion characteristics,
- nanoparticle dispersion,
- bacterial growth rate,
- susceptibility of individual species,
- interaction between graphene oxide nanosheets and bacterial cell envelopes. [Ashraf Anila et al. 2024]
- Rather than relying solely on inhibition diameter, interpretation considered bacterial ultrastructure together with the physicochemical behaviour of graphene oxide to establish mechanistic explanations for observed differences between bacterial species. [Al-Thani, R. F. et al. 2014]

## 2.3 In Vitro Evaluation of Anticancer Activity

### 2.3.1 Experimental Overview

The anticancer potential of graphene oxide was investigated using human epithelial cancer cell lines representing both lung and breast malignancies.

The experimental design incorporated

- concentration-dependent exposure,
- temporal assessment,
- quantitative viability analysis,
- qualitative morphology assessment,

thereby allowing comprehensive characterization of graphene oxide-induced cytotoxicity. [Sangili Yandi Gurunathan et al. 2015]

### 2.3.2 Cell Culture Methodology

#### Materials

In this study two different breast cancer cell lines MCF-7 (estrogen receptor-positive, luminal A subtype) and MDA MB 231 (triple-negative breast cancer phenotype) were used for *in vitro* experiments. Both cell lines were procured from the National Centre for Cell Science (NCCS), Pune, India. MCF-7 cells were cultured in Minimum Essential Medium (MEM) and MDA MB 231 cells were cultured in Dulbecco's Modified Eagle Medium High Glucose (DMEM HG). Both the cell culture media were obtained from Gibco. These cell cultures were supplemented with 10% heat-inactivated fetal bovine serum (FBS) and 1% penicillin-streptomycin antimicrobial cocktail, both obtained from Gibco. The 3-(4,5-dimethylthiazol-2-yl)-2,5-diphenyltetrazolium bromide (MTT) reagent and dimethyl sulfoxide (DMSO) were procured from Sisco Research Laboratories Pvt. Ltd. (SRL), India. All biochemical reagents utilized were of analytical grade suitable for cell culture applications, and all experimental procedures were performed using sterile, tissue culture-treated plasticware. Both cell lines were cultured under controlled aseptic conditions within a humidified incubator maintained at 37°C in an atmosphere containing 5% carbon dioxide. [Eltahir S. et al. 2022, Gil Gonçalves et al. 2014, Lijun Liu et al. 2021]

#### Methods

**1. Cytotoxicity assay**

The colorimetric MTT assay was used to assess the cytotoxic potential of the prepared sample - Graphene Oxide Nanoparticles, against both breast cancer cell lines MCF-7 and MDA MB 231. The cells were cultured in their respective media, supplemented with 10% FBS and maintained under standard conditions (37°C, 5% $CO_2$, humidified atmosphere). Once cells attained the required confluency, the cells were harvested and seeded into a 96-well plate at a

cellular density of approximately 10,000 cells per well. The seeded cells were incubated for 24 hours to allow cellular attachment and attainment of the required cellular morphology. Following this incubation, cells were exposed to a concentration-dependent gradient of GrO NPs samples, spanning a range of 0.5 to 100 µg/mL in MDA MB 231 cells and 0.5 to 200 µg/mL in MCF-7 cells. [Choudhury, S. P. et al. 2025, Solanki, R. et al. 2024]

To assess the cytotoxic progression of the samples, two different treatment time intervals were chosen – 24 hours and 48 hours, for comparative analysis. At the conclusion of each treatment period, each well media was replaced with 50 µL of MTT solution (1 mg/mL in PBS). The cells were then incubated with MTT solution for 3 to 4 hours. During the incubation the viable cells metabolically reduce the yellow tetrazolium salt to form purple formazan crystals. These formazan crystals were then dissolved with 150 µL DMSO added in each well. Followed by observing the optical density of each well at 570 nm using a multimode microplate reader.[2] Wells containing culture medium supplemented with 10% FBS in the absence of test samples served as the negative control (untreated cells), enabling calculation of relative cell viability percentages. Cell viability was expressed as a percentage relative to the negative control, and calculated using the mathematic formula mentioned below:

**Percentage of cell viability (%) = (sample absorbance / control absorbance) × 100**

**1. Morphology examination of the treated breast cancer cells**

The morphological changes of MDA-MB-231 and MCF-7 breast cancer cells following exposure to graphene oxide (GrO) nanoparticles was observed using a phase-contrast inverted microscope. Cells were seeded in 35 mm tissue culture dishes at an optimal density of approximately $1.5 \times 10^5$/dish for MCF-7 and MDA-MB-231 cells. After allowing 24 h for proper attachment and attainment of characteristic morphology, the cells were treated with different concentrations of GrO NPs, categorized as low, medium high dosage concentration i.e. 10, 50 and 100 µg/mL respectively for MDA MB 231 cells and 50, 100 and 200 µg/mL respectively for MCF-7 cells. Untreated cells served as the control group. The cultures were then incubated under standard conditions (37 °C, 5% $CO_2$, and 95% humidity). Morphological changes were examined and images were captured at 0, 24, and 48 hours post-treatment using a phase-contrast microscope equipped with a digital imaging system. Changes such as cell shrinkage, rounding, detachment, and membrane irregularities were monitored to evaluate dose and time-dependent cytotoxic effects of GrO NPs. [Milena Keremidarska-Markova et al. 2018]

**Materials**

A549 human lung carcinoma cells were obtained from the National Centre for Cell Science (NCCS), Pune, India. The cells were maintained in Dulbecco's Modified Eagle Medium: Nutrient Mixture F-12 (DMEM/F12) supplemented with 10% fetal bovine serum (FBS) and 1% penicillin-streptomycin cocktail, from Gibco. The MTT reagent (3-(4,5-dimethylthiazol-2-yl) -2,5-diphenyltetrazolium bromide) and dimethyl sulfoxide (DMSO) were procured from Sisco Research Laboratories Pvt. Ltd. (SRL) - India. All reagents used were of cell culture grade, and sterile cell culture plasticware was utilized for all experiments. Cells were cultured under aseptic conditions in a humidified incubator at 37°C with 5% $CO_2$. [Chelliah, C. K. et al. 2025, Hatshan, M. et al. 2023, Gest, C. et al. 2013]

**Methods**

**1. Assessment of cell viability**

In the present study, the effects of prepared Graphene Oxide samples on lung adenocarcinoma cells A549, were studied by carrying out MTT colorimetric assay. The cells were cultured in DMEM F12 media, supplemented with 10% FBS, and maintained in humidified incubator at 37°C with 5% $CO_2$. Once the cells reached an optimum confluency, seeding of cells was done in a 96-well plate for the MTT experiment. Around 10,000 cells per well were seeded and kept for 24 hours in $CO_2$ incubator for attachment and attainment of healthy cellular morphology. Further, the cells were treated with a range of concentration of the GrO Samples (1-200 µg/mL). Two different time points of 24 hours and 48 hours was selected to study the cytotoxity effect of the samples. After completion of said time, the cell culture media in the wells was replaced with 50 µl of MTT solution prepared in PBS (1 mg/mL). The cells were incubated for 3-4 hours with MTT solution to form formazan crystals which were further dissolved using DMSO. The absorbance was then observed using a multimode plate reader. The cells having only media and no treatment sample were taken as negative control for calculations and assessment of cell viability percentage. [Front Inan-Rubio, J. et al. 2022, Yang, W. et al. 2019, Kumar, S. et al. 2020, Park, T. Y. et al. 2025, Li, R. Guiney et al. 2018]

**2. Morphology examination of the treated lung cancer cells, A549**

The morphological changes of A549 lung cancer cells following exposure to graphene oxide (GrO) nanoparticles was observed using a phase-contrast inverted microscope. Cells were seeded in 35 mm tissue culture dishes at an optimal density of approximately $1.5 \times 10^5$/dish for A549 cells. After allowing 24 h for proper attachment and attainment of characteristic morphology, the cells were treated with different concentrations of GrO-NPs, categorized as low, medium high dosage concentration i.e. 50, 100 and 200 µg/mL. Untreated cells served as the control group. The cultures were then incubated under standard conditions (37 °C, 5% $CO_2$,

and 95% humidity). Morphological changes were examined and images were captured at 0, 24, and 48 hours post-treatment using a phase-contrast microscope equipped with a digital imaging system. [Ou, L. et al. 2017, Martel-Estrada, S.-A. et al. 2025, Ghosh, S. et al. 2025, Krętowski, R. et al. 2025, Taheri Azam, A. et al. 2023] Changes such as cell shrinkage, rounding, detachment, and membrane irregularities were monitored to evaluate dose and time-dependent cytotoxic effects of GrO-NPs.

The selected cell lines were cultured under strictly controlled aseptic conditions within a humidified carbon dioxide incubator maintained at 37°C, 5% $CO_2$, and approximately 95% relative humidity. Appropriate culture media supplemented with fetal bovine serum and antibiotic–antimycotic solutions were employed according to the biological requirements of each cell line. Sterile tissue culture-treated plasticware was used throughout the investigation to minimize contamination and maintain experimental consistency. The culture conditions, media selection, and incubation parameters followed the protocols described in the uploaded experimental documents.

Maintenance of physiological temperature and controlled carbon dioxide concentration is essential for preserving intracellular pH through the bicarbonate buffering system of mammalian culture media. Even minor deviations in environmental conditions may alter cellular metabolism, proliferation rates, and sensitivity to nanoparticle exposure, thereby influencing experimental outcomes.

**2.3.3 Scientific Basis of the MTT Cytotoxicity Assay**

Quantitative evaluation of graphene oxide-induced cytotoxicity was performed using the 3-(4,5-dimethylthiazol-2-yl)-2,5-diphenyltetrazolium bromide (MTT) assay, one of the most extensively validated colorimetric techniques for assessing cellular metabolic activity.

Unlike direct cell counting methods, the MTT assay measures metabolic competence, providing an indirect but highly reliable indicator of viable cell number.

The assay is based upon the ability of metabolically active cells to reduce the yellow tetrazolium compound MTT into insoluble purple formazan crystals.

This biochemical reduction occurs primarily within mitochondria through the activity of NAD(P)H-dependent oxidoreductases, including mitochondrial succinate dehydrogenase and other intracellular dehydrogenase enzymes. [Gurunathan S. et al. 2015]

Viable cells possessing intact mitochondrial function continuously reduce tetrazolium rings through intracellular electron transfer reactions:

**Yellow MTT → Reduction by viable cellular dehydrogenases → Purple insoluble formazan crystals**

Cells undergoing apoptosis or necrosis progressively lose mitochondrial enzyme activity. Consequently, their capacity to reduce MTT declines, producing fewer formazan crystals and lower absorbance values following solubilization.

After incubation with MTT solution, the culture medium was replaced with dimethyl sulfoxide (DMSO) to dissolve the insoluble intracellular formazan crystals. The resulting-coloured solution was quantified spectrophotometrically at 570 nm, where absorbance is directly proportional to the number of metabolically active cells. This workflow follows the methodology detailed in the uploaded protocols.

**2.3.4 Optimization of Cell Seeding Density**

Appropriate cellular density represents a critical determinant of reproducible cytotoxicity assessment. For quantitative MTT analysis, approximately 10,000 cells per well were seeded into sterile 96-well tissue culture plates and incubated for 24 hours before graphene oxide treatment to allow firm attachment and recovery from harvesting. This density provides sufficient metabolic activity for reliable spectrophotometric detection while avoiding over-confluence during the treatment period.

For qualitative morphology assessment, approximately $1.5 \times 10^5$ cells were seeded into 35 mm tissue culture dishes, ensuring adequate cell coverage for microscopic visualization without excessive overlap. Following a 24-hour attachment period, cells were exposed to graphene oxide and monitored over time using phase-contrast microscopy.

The selected seeding densities ensure consistent cell–cell interactions, minimize nutrient limitation, and provide sufficient spatial resolution to identify treatment-induced morphological changes such as cell shrinkage, rounding, membrane blebbing, and detachment.

**2.3.5 Graphene Oxide Treatment Regimen and Concentration Selection**

The biological response of mammalian cells to nanomaterials is strongly influenced by nanoparticle concentration, exposure duration, physicochemical characteristics, and the intrinsic molecular phenotype of the target cells. Consequently, graphene oxide (GO) was evaluated using concentration-dependent exposure protocols designed to investigate both sub-cytotoxic and cytotoxic responses across multiple treatment windows.

The concentration ranges employed in this study were selected based on published literature concerning graphene oxide-mediated cytotoxicity together with preliminary optimization experiments, ensuring that the tested concentrations encompassed both biologically tolerated and biologically active exposure levels. This strategy enabled the generation of complete dose-response curves and accurate determination of the half-maximal inhibitory concentration ($IC_{50}$).

For the A549 human lung adenocarcinoma cell line, graphene oxide was evaluated over a concentration range of 1–200 μg/mL. This broad concentration interval was selected to investigate the progressive effects of graphene oxide from minimal cellular stress to substantial antiproliferative activity. The breast cancer cell lines were evaluated using concentration ranges optimized according to their known biological behaviour: 0.5–100 μg/mL for the MDA-MB-231 triple-negative breast cancer cells and 0.5–200 μg/mL for the MCF-7 luminal A breast cancer cells. These ranges were chosen to accommodate the expected differences in cellular sensitivity between the two molecular subtypes and to permit accurate comparison of treatment responses.

Two exposure periods, 24 hours and 48 hours, were selected for all cell lines. The 24-hour interval was intended to evaluate the early cellular response to graphene oxide, whereas the 48-hour interval allowed assessment of sustained nanoparticle exposure and progressive cytotoxicity. Evaluation at multiple time points is essential because many nanoparticle-induced biological effects develop gradually through cumulative oxidative stress, mitochondrial dysfunction, and disruption of cellular metabolism rather than through immediate acute toxicity.

Maintaining identical exposure conditions across all experiments ensured that differences in biological response reflected intrinsic cellular characteristics rather than variations in experimental methodology.

**2.3.6 Morphological Assessment by Phase-Contrast Microscopy**

Quantitative viability assays provide important information regarding metabolic activity; however, they do not directly reveal the structural alterations that accompany nanoparticle-induced cytotoxicity. Consequently, qualitative morphological evaluation was performed to complement the MTT assay and provide visual evidence of treatment-induced cellular injury.

Following graphene oxide exposure, cellular morphology was examined using an inverted phase-contrast light microscope equipped with a digital imaging system. Phase-contrast microscopy was selected because it enables visualization of living cells without fixation or staining, thereby preserving native cellular morphology throughout the observation period. The experimental protocol, including the use of 35 mm culture dishes, seeding density (~$1.5 \times 10^5$ cells/dish), and observation at 0, 24, and 48 hours, follows the procedures described in the uploaded studies.

Digital images were acquired at predetermined intervals of 0, 24, and 48 hours following treatment. The initial (0-hour) images served as baseline references, confirming healthy cellular

morphology before nanoparticle exposure. Subsequent observations allowed direct visualization of the temporal progression of graphene oxide-induced structural alterations.

Morphological evaluation focused on several characteristic indicators of cytotoxicity, including:

- reduction in cellular confluency,
- loss of normal epithelial morphology,
- cell rounding,
- cytoplasmic shrinkage,
- membrane blebbing,
- disruption of cell–cell junctions,
- membrane irregularities,
- reduced substrate adherence,
- cellular detachment,
- formation of floating apoptotic cells and debris.

These features collectively provide qualitative evidence of cellular stress and complement the quantitative reductions in metabolic activity measured by the MTT assay.

Unlike biochemical assays that evaluate a single endpoint, microscopic examination allows simultaneous assessment of multiple aspects of cellular behaviour, including changes in cell shape, adhesion, proliferation, and structural integrity. The combination of quantitative and qualitative methodologies therefore provides a more comprehensive evaluation of graphene oxide-induced cytotoxicity.

**2.3.7 Determination of Cell Viability**

Following completion of each treatment period, culture medium containing graphene oxide was carefully removed and replaced with freshly prepared MTT solution. During incubation, viable cells metabolically reduced the tetrazolium substrate to insoluble intracellular formazan crystals through mitochondrial oxidoreductase activity. The resulting crystals were subsequently dissolved using dimethyl sulfoxide (DMSO), producing a homogeneous purple solution suitable for spectrophotometric analysis.

Optical density was measured at 570 nm using a multimode microplate reader. Absorbance values obtained from untreated control wells represented 100% cellular viability, while treated wells were expressed relative to these controls according to the equation:

**Percentage of cell viability (%) = (sample absorbance / control absorbance) × 100**

This normalization minimizes experimental variation arising from differences in initial cell number, reagent preparation, or instrument performance, thereby enabling direct comparison

among independent experimental groups. The equation and measurement conditions are consistent with the protocols provided in the uploaded documents.

### 2.3.8 Determination of $IC_{50}$ Values

To quantify the antiproliferative efficacy of graphene oxide, the half-maximal inhibitory concentration ($IC_{50}$) was determined for each cancer cell line at both treatment intervals. [Anwar Fit Rianto et al. 2022]

The $IC_{50}$ represents the concentration of graphene oxide required to reduce cellular viability by 50% relative to untreated controls and is widely recognized as a standard parameter for comparing cytotoxic potency among different therapeutic agents and biological models.

Dose-response curves were generated by plotting the percentage of viable cells against graphene oxide concentration. Nonlinear regression analysis was subsequently applied to calculate $IC_{50}$ values. Determination of $IC_{50}$ values at both 24 and 48 hours enabled evaluation of temporal changes in graphene oxide potency and facilitated direct comparison among A549, MCF-7, and MDA-MB-231 cells.

Because the three cell lines represent distinct molecular phenotypes, comparative $IC_{50}$ analysis provides valuable insight into phenotype-dependent susceptibility to graphene oxide-mediated cytotoxicity.

## 2.4 Experimental Controls and Quality Assurance

Rigorous experimental controls were incorporated throughout the biological evaluation to ensure the validity and reproducibility of the findings.

Untreated cells cultured under identical environmental conditions served as the negative control, providing the reference for normal cellular growth, metabolic activity, and morphology. These control cultures established baseline absorbance values for calculation of relative cell viability and allowed treatment-induced alterations to be distinguished from normal physiological variation.

For antimicrobial studies, solvent controls containing DMSO without graphene oxide were included to confirm that any observed bacterial growth inhibition resulted from graphene oxide rather than solvent-mediated effects. Similarly, in the cytotoxicity studies, all treatment groups were exposed to identical culture conditions, media composition, incubation periods, and handling procedures, thereby minimizing potential experimental bias.

Sterile laboratory techniques were maintained throughout all experimental procedures. Cell culture manipulations were performed using aseptic practices within a controlled tissue culture environment to prevent microbial contamination. Culture media, reagents, and plasticware were selected specifically for mammalian cell culture applications, and incubation parameters

were continuously maintained at physiological conditions. Uniform graphene oxide dispersions were prepared immediately before experimentation to minimize nanoparticle aggregation. Because aggregation alters effective surface area and sedimentation behaviour, consistent dispersion is essential for reproducible nanoparticle exposure and accurate interpretation of biological responses.

**2.5 Statistical Analysis**

All biological experiments were performed with appropriate experimental replication to ensure statistical reliability and reproducibility.

Quantitative data obtained from MTT assays were expressed as mean ± standard deviation (SD). Statistical analysis was performed to compare treatment groups with untreated controls, enabling identification of significant differences in cellular viability resulting from graphene oxide exposure. Graphical representation of dose-response relationships facilitated visualization of concentration-dependent and time-dependent trends in cytotoxicity. Statistical significance was interpreted using conventional probability thresholds:

- $P \leq 0.05$ (*)
- $P \leq 0.01$ (**)
- $P \leq 0.001$ (***)
- $P \leq 0.0001$ (****)

These significance levels provide a standardized framework for evaluating the reliability of observed biological responses and facilitate comparison with previously published studies investigating graphene oxide-mediated cytotoxicity. The figures in your uploaded experimental datasets are presented using these same statistical thresholds.

**2.6 Methodological Considerations and Reproducibility**

The biological activity of graphene oxide is highly sensitive to variations in synthesis conditions, lateral sheet dimensions, oxidation degree, defect density, and dispersion stability. Consequently, interpretation of antimicrobial and anticancer activity requires careful consideration of the physicochemical characteristics established during material characterization.

In the present investigation, biological evaluation was performed only after comprehensive physicochemical characterization had confirmed the structural integrity, oxygen-containing surface functionalities, electronic heterogeneity, thermal stability, and nanosheet morphology of the synthesized graphene oxide. This sequential approach minimizes ambiguity in interpreting biological outcomes and permits direct correlation between material properties and biological performance. As discussed in the rationale for biological evaluation, correlating

morphology, surface chemistry, and electronic structure with antimicrobial and anticancer responses is essential for establishing meaningful structure–activity relationships rather than providing purely descriptive observations.

Furthermore, standardized cell culture conditions, optimized seeding densities, controlled incubation periods, uniform nanoparticle dispersion, and complementary quantitative and qualitative analyses collectively enhance the reproducibility of the experimental findings. By integrating physicochemical characterization with biological assessment, the present methodology provides a robust framework for investigating the biomedical potential of graphene oxide and facilitates comparison with future studies employing similar nanomaterial systems.

## 3. Results and Discussion

### 3.1 Antimicrobial Activity of Graphene Oxide

#### 3.1.1 Overview of Antibacterial Performance

The increasing prevalence of multidrug-resistant bacterial pathogens has intensified interest in alternative antimicrobial materials capable of overcoming the limitations of conventional antibiotics. Unlike classical antimicrobial agents that inhibit discrete biochemical pathways, graphene oxide (GO) exhibits antibacterial activity through direct physicochemical interactions at the nano–bio interface. Consequently, its antimicrobial efficacy depends primarily upon structural morphology, surface chemistry, oxidation state, dispersion stability, and electronic properties rather than conventional receptor-mediated pharmacology.

The antimicrobial evaluation performed in the present study demonstrated that the synthesized graphene oxide possessed broad-spectrum antibacterial activity against both Gram-positive and Gram-negative bacterial species. Growth inhibition was observed against all tested organisms, confirming that the biological activity of graphene oxide extends across bacteria possessing markedly different cell-envelope architectures. However, the magnitude of bacterial inhibition varied considerably among the tested microorganisms, indicating that bacterial susceptibility is strongly influenced by differences in cell-wall composition and membrane organization.

Representative agar well diffusion assays demonstrated distinct zones of inhibition surrounding graphene oxide-treated wells, confirming successful suppression of bacterial growth. Although all bacterial species exhibited measurable susceptibility, Gram-positive bacteria produced comparatively larger inhibition zones than Gram-negative organisms, suggesting more efficient interaction between graphene oxide nanosheets and Gram-positive cell envelopes. This pattern is consistent with the observations summarized in your antimicrobial evaluation document.

Importantly, these findings should not be interpreted as evidence that graphene oxide acts as a conventional antibiotic. Rather, they demonstrate that GO functions as a multi-mechanistic antimicrobial nanomaterial, whose biological activity originates directly from its intrinsic physicochemical properties established during synthesis and characterization.

### 3.1.2 Correlation Between Physicochemical Characteristics and Antibacterial Activity

One of the principal objectives of this investigation was to determine whether the antimicrobial activity of graphene oxide could be directly correlated with its physicochemical characteristics. Comprehensive material characterization performed prior to biological evaluation demonstrated that the synthesized GO possessed large-area flexible nanosheets with pronounced wrinkling, abundant oxygen-containing functional groups, residual graphitic domains, and expanded interlayer spacing. These structural features collectively provide the mechanistic basis for antibacterial activity by facilitating intimate contact with bacterial cell envelopes, promoting stable dispersion in aqueous media, and enabling redox-mediated interactions.

Scanning electron microscopy and high-resolution transmission electron microscopy revealed extensive sheet wrinkling and irregular edges. These morphological characteristics increase the effective surface area available for microbial interaction and permit graphene oxide sheets to conform closely to the complex topography of bacterial cell surfaces. Unlike spherical nanoparticles, whose interactions are restricted to discrete contact points, the two-dimensional architecture of GO enables prolonged membrane contact over a substantially larger interfacial area. The abundant hydroxyl, epoxy, carbonyl, and carboxyl groups confirmed by physicochemical analyses further contribute to antibacterial performance by enhancing hydrophilicity, colloidal stability, and electrostatic interactions with bacterial surfaces. Stable dispersion prevents aggregation of GO sheets, ensuring maximal exposure of reactive surface area throughout the antimicrobial assay. Simultaneously, oxygen-containing functional groups facilitate hydrogen bonding and electrostatic attraction with bacterial envelope components, increasing the probability of membrane perturbation.

Residual $sp^2$-hybridized graphitic domains interspersed within oxidized regions create localized electronic heterogeneity that supports electron-transfer reactions and reactive oxygen species (ROS) generation. Thus, the observed antibacterial activity should be viewed as the biological consequence of a synergistic interplay between morphology, surface chemistry, electronic structure, and dispersion behaviour rather than the effect of any single material property.

### 3.1.3 Differential Susceptibility of Gram-Positive and Gram-Negative Bacteria

A notable finding of the antimicrobial evaluation was the differential response of Gram-positive and Gram-negative bacteria to graphene oxide exposure. This observation provides valuable insight into the influence of bacterial ultrastructure on nanomaterial-mediated antibacterial activity.

The Gram-positive organisms, *Staphylococcus aureus* and *Enterococcus faecalis*, exhibited greater susceptibility to graphene oxide than the Gram-negative organisms *Escherichia coli* and *Pseudomonas aeruginosa*. This trend is consistent with numerous published investigations and reflects fundamental differences in bacterial cell-envelope architecture rather than variations in intrinsic toxicity of graphene oxide.

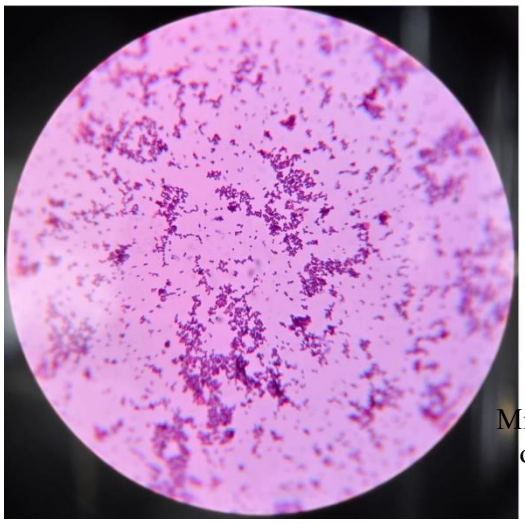
Gram-positive bacteria possess a relatively simple cell envelope comprising a cytoplasmic membrane surrounded by a thick but highly porous peptidoglycan meshwork enriched with teichoic and lipoteichoic acids. Although the peptidoglycan layer provides mechanical strength, its porous architecture permits direct interaction between graphene oxide nanosheets and the underlying cytoplasmic membrane. Furthermore, the negatively charged GO surface interacts electrostatically with positively charged components of the Gram-positive cell wall, promoting intimate membrane contact and facilitating subsequent physicochemical damage.

The absence of an outer membrane therefore exposes Gram-positive bacteria directly to the mechanical and oxidative effects of graphene oxide. Once close contact has been established, sharp sheet edges, reactive oxygen species, and membrane lipid extraction mechanisms act synergistically to compromise bacterial viability. By contrast, Gram-negative bacteria possess a considerably more complex envelope composed of an inner cytoplasmic membrane, a thin peptidoglycan layer, and an outer membrane enriched with lipopolysaccharide (LPS). The LPS layer functions as an effective permeability barrier that restricts penetration of many antimicrobial agents and reduces direct access of graphene oxide to the cytoplasmic membrane. Consequently, mechanical disruption by GO nanosheets is less efficient than in Gram-positive organisms.

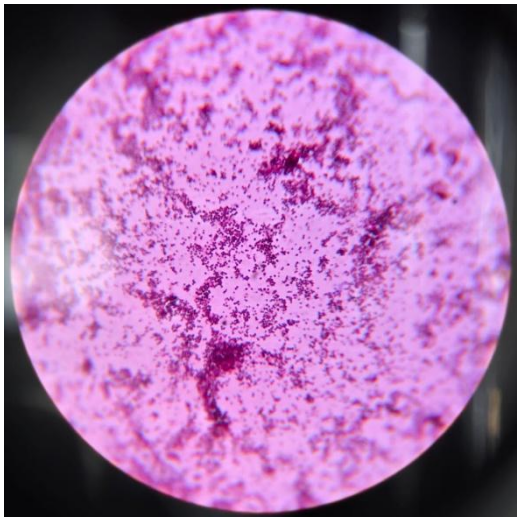
Among the Gram-negative bacteria examined, *Pseudomonas aeruginosa* displayed the lowest susceptibility. This observation is biologically plausible considering the exceptional defensive capabilities of this organism. In addition to its low-permeability outer membrane, *P. aeruginosa* expresses multiple multidrug efflux pumps, possesses highly adaptable metabolic pathways, and readily forms biofilms composed of extracellular polymeric substances. Biofilm matrices act as diffusion barriers that physically limit nanoparticle penetration while simultaneously altering the local physicochemical environment. These overlapping defence mechanisms collectively reduce the effectiveness of graphene oxide-mediated membrane interactions and

explain the comparatively smaller inhibition zones typically observed for *P. aeruginosa*. Similar conclusions are discussed in the antimicrobial analysis contained within your uploaded documents.

Importantly, the persistence of measurable antibacterial activity against all tested organisms demonstrates that graphene oxide retains broad-spectrum efficacy despite these structural barriers, highlighting its potential as a non-antibiotic antimicrobial material.

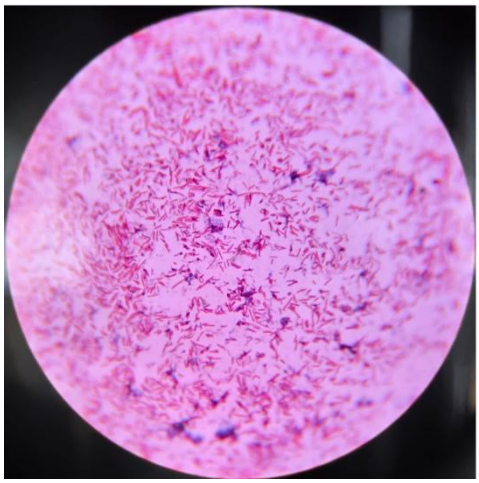


Figure– 3a
Microscopic Picture of *Enterococcus faecalis*

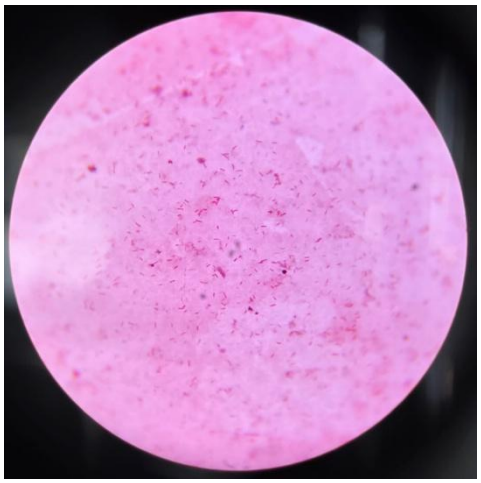


Figure– 3b
Microscopic Picture of *Staphylococcus aureus*

**Figure 3. Antimicrobial Assay and Microscopic Characterization of E. faecalis and S. aureus*(Gram Positive)**



Figure– 4a
Microscopic Picture of *Escherichia coli*



Figure– 4b
Microscopic Picture of *Escherichia coli*

**Figure 4. Antimicrobial Assay and Microscopic Characterization of E. coli and Pseudomonas* (Gram Negative)**

### 3.1.4 Concentration-Dependent Antibacterial Activity

The antimicrobial response observed in this investigation exhibited a clear concentration-dependent pattern, indicating that graphene oxide-mediated bacterial inhibition arises from progressive physicochemical interactions rather than indiscriminate toxicity.

At lower concentrations, only a limited number of graphene oxide nanosheets interact with bacterial cells, resulting in localized membrane perturbation and relatively modest growth inhibition. As graphene oxide concentration increases, the frequency and duration of nanoparticle–bacterium interactions increase substantially, enhancing opportunities for membrane disruption, oxidative damage, and cellular isolation.

Higher concentrations also increase the probability of multiple nanosheets simultaneously interacting with individual bacterial cells. Such cumulative interactions amplify mechanical stress and facilitate more extensive disruption of membrane integrity. Simultaneously, greater surface area availability increases electron-transfer reactions at the nano–bio interface, promoting higher levels of reactive oxygen species generation and oxidative damage.

This concentration-dependent behaviour suggests that graphene oxide acts through regulated physicochemical mechanisms rather than nonspecific chemical toxicity. Such behaviour is advantageous from a biomedical perspective because it indicates the possibility of defining therapeutic concentration windows that maximize antibacterial efficacy while minimizing unintended effects on surrounding tissues.

Furthermore, the reproducibility of concentration-dependent inhibition demonstrates that the graphene oxide suspension remained adequately dispersed throughout the experimental period. Uniform dispersion ensures consistent nanosheet availability and eliminates variability associated with sedimentation or aggregation, thereby improving the reliability of antimicrobial assessment.

### 3.1.5 Graphene Oxide as a Multi-Mechanistic Antibacterial Nanomaterial

Perhaps the most distinctive feature of graphene oxide is that its antibacterial activity cannot be attributed to a single dominant mechanism. Instead, bacterial killing results from the simultaneous operation of multiple complementary physicochemical processes that reinforce one another.

This multi-mechanistic behaviour fundamentally distinguishes graphene oxide from conventional antibiotics. Whereas most antibiotics inhibit a specific enzyme or biochemical pathway, GO disrupts several essential aspects of bacterial physiology concurrently. Such multifaceted activity not only enhances antibacterial efficacy but may also reduce the likelihood of rapid resistance development because microorganisms would need to adapt simultaneously to several independent mechanisms.

Current evidence, including the findings of the present study, supports four principal antibacterial mechanisms:

1. **Physical membrane disruption** through direct interaction of atomically sharp graphene oxide edges with bacterial envelopes.
2. **Oxidative stress induction** resulting from electron-transfer reactions that generate reactive oxygen species capable of damaging lipids, proteins, and nucleic acids.
3. **Extraction of membrane phospholipids**, destabilizing the lipid bilayer and compromising membrane integrity.
4. **Entrapment and isolation of bacterial cells** by flexible graphene oxide sheets, limiting nutrient diffusion, impairing gas exchange, and inhibiting cellular proliferation.

These mechanisms are not mutually exclusive; rather, they occur concurrently and synergistically. Initial membrane adhesion facilitates mechanical disruption, which increases membrane permeability and enhances oxidative injury. Membrane destabilization subsequently promotes phospholipid extraction, while the flexible two-dimensional morphology of GO allows partial or complete wrapping of bacterial cells, further restricting survival.

Collectively, these observations demonstrate that the antibacterial activity of graphene oxide is an intrinsic consequence of its physicochemical design. The large-area wrinkled nanosheets, abundant oxygen-containing functional groups, defect-rich carbon lattice, and electronic heterogeneity established during material characterization directly translate into broad-spectrum antimicrobial activity through coordinated nano–bio interactions.

### 3.2 Molecular Mechanisms Underlying the Antibacterial Activity of Graphene Oxide

Unlike conventional antibiotics, which generally inhibit one specific biochemical process such as cell-wall synthesis, protein synthesis, nucleic acid replication, or folate metabolism, graphene oxide (GO) exhibits antibacterial activity through a network of complementary physicochemical interactions that occur simultaneously at the nano–bio interface. The biological response therefore cannot be attributed to a single dominant pathway but instead reflects the cumulative effects of multiple mechanisms acting in concert.

This multi-mechanistic behaviour is one of the most significant advantages of graphene oxide as a prospective antimicrobial material. Because bacterial killing results from concurrent mechanical, oxidative, physicochemical, and metabolic disturbances, microorganisms would theoretically require simultaneous adaptation to several independent stresses to develop complete resistance. Such multifactorial interactions distinguish graphene oxide from conventional antibiotics and position it as a promising non-antibiotic antimicrobial platform.

The four principal mechanisms currently recognized include:

1. Physical membrane disruption ("nano-knife effect")
2. Oxidative stress mediated by reactive oxygen species (ROS)
3. Extraction of membrane phospholipids
4. Cellular wrapping and isolation

Although discussed individually below, these mechanisms operate simultaneously and reinforce one another during bacterial exposure.

### 3.2.1 Physical Membrane Disruption: The Nano-Knife Effect

Among the proposed antibacterial mechanisms, direct mechanical disruption of bacterial membranes is regarded as one of the earliest events following contact between graphene oxide and microbial cells. Graphene oxide possesses an exceptionally unusual geometry compared with conventional nanoparticles. Instead of spherical or rod-shaped structures, GO consists of atomically thin two-dimensional nanosheets whose thickness is generally limited to only a few atomic layers while extending laterally over hundreds of nanometres or several micrometres. This extremely high aspect ratio creates sheet edges possessing nanoscale sharpness.

Upon encountering bacterial cells, these sharp edges behave analogously to microscopic blades.

Rather than immediately penetrating cells, graphene oxide initially adsorbs onto the bacterial surface through electrostatic attraction, hydrogen bonding, hydrophobic interactions, and van der Waals forces. Once stable contact has been established, nanosheets gradually align parallel to the bacterial envelope before localized edge regions begin exerting mechanical stress on the phospholipid membrane.

The magnitude of this stress depends upon several physicochemical characteristics including

- lateral sheet dimensions,
- edge sharpness,
- nanosheet flexibility,
- oxidation degree,
- dispersion stability,
- bacterial membrane composition.

The wrinkled morphology observed during SEM characterization substantially enhances this interaction by increasing the effective contact area between GO and bacterial membranes. Large flexible sheets are capable of conforming closely to the curved bacterial surface, thereby maximizing edge contact while simultaneously increasing the probability of membrane penetration. These morphological features were established during the physicochemical characterization and provide the structural basis for the observed antimicrobial activity.

As membrane deformation progresses, phospholipid organization becomes increasingly disrupted. Localized membrane tension develops, eventually producing nanoscale defects through which intracellular ions and metabolites begin leaking into the surrounding environment.

Loss of membrane integrity rapidly disturbs bacterial osmotic regulation.

The bacterial cytoplasmic membrane maintains essential electrochemical gradients required for

- ATP synthesis,
- nutrient transport,
- respiratory metabolism,
- maintenance of intracellular pH,
- protein secretion.

Mechanical disruption therefore compromises numerous physiological processes simultaneously. Unlike antibiotics targeting a single enzyme, physical membrane destruction immediately affects virtually every essential cellular function. Experimental microscopy studies reported throughout the graphene nanotoxicology literature consistently demonstrate collapsed bacterial morphology following GO exposure, with distorted cell walls, membrane rupture, and leakage of intracellular material. Such observations strongly support the hypothesis that membrane damage represents one of the earliest initiating events in graphene oxide-mediated bacterial killing.

### 3.2.2 Reactive Oxygen Species (ROS)-Mediated Oxidative Stress

Mechanical membrane disruption alone does not fully explain the remarkable antibacterial activity of graphene oxide. Equally important is its ability to generate oxidative stress through the production of reactive oxygen species (ROS). The physicochemical characterization of graphene oxide demonstrated the coexistence of residual $sp^2$-hybridized carbon domains together with oxidized regions enriched in hydroxyl, epoxy, carbonyl, and carboxyl groups. This heterogeneous electronic structure creates localized electron-rich and electron-deficient regions capable of participating in biological redox reactions. As discussed in the rationale for biological evaluation, this electronic heterogeneity provides a mechanistic basis for ROS generation and oxidative cytotoxicity.

When graphene oxide contacts bacterial cells, electron transfer occurs between bacterial membrane components and redox-active regions of the GO nanosheet.

These reactions generate several reactive oxygen species including

- superoxide anion ($O_2^{\bullet -}$),

- hydrogen peroxide ($H_2O_2$),
- hydroxyl radicals (•OH),
- singlet oxygen ($^1O_2$).

Although produced in relatively small quantities individually, their cumulative effect produces extensive oxidative injury throughout the bacterial cell.

One of the earliest consequences is lipid peroxidation.

Bacterial membranes contain phospholipid molecules rich in unsaturated fatty acids.

Reactive oxygen species readily attack these lipids, initiating chain reactions that progressively destroy membrane architecture.

Lipid peroxidation results in

- increased membrane permeability,
- reduced membrane fluidity,
- disruption of membrane-associated enzymes,
- leakage of intracellular components.

ROS simultaneously oxidize bacterial proteins.

Many essential enzymes contain sulfur-containing amino acids or metal cofactors particularly susceptible to oxidative modification.

Oxidation alters protein conformation, reduces catalytic activity, disrupts respiratory metabolism, and impairs biosynthetic pathways.

Nucleic acids also represent major ROS targets.

Oxidative DNA damage includes

- strand breaks,
- base oxidation,
- formation of a basic site,
- replication errors.

Although bacteria possess antioxidant defence systems—including catalase, superoxide dismutase, and peroxidases—persistent ROS generation eventually overwhelms these protective mechanisms. Once antioxidant capacity is exceeded, oxidative injury accumulates exponentially until irreversible cellular dysfunction occurs. Importantly, oxidative stress acts synergistically with mechanical membrane disruption. Damage produced by sharp GO edges increases membrane permeability, allowing ROS easier access to intracellular targets. Conversely, oxidative weakening of membrane lipids further enhances susceptibility to mechanical rupture. Together these mechanisms amplify one another rather than functioning independently.

### 3.2.3 Extraction of Membrane Phospholipids

A third antibacterial mechanism that has received considerable attention involves the direct extraction of phospholipid molecules from bacterial membranes. Unlike membrane cutting or oxidative degradation, phospholipid extraction represents a physicochemical process driven primarily by strong interactions between graphene oxide and membrane lipids. The basal plane of graphene oxide retains residual graphitic domains capable of interacting hydrophobically with lipid acyl chains. Simultaneously, oxygen-containing functional groups establish hydrogen bonds with polar phospholipid headgroups. These combined interactions create sufficient thermodynamic driving force to remove individual phospholipid molecules from the bacterial membrane. Molecular dynamics simulations suggest that lipid molecules gradually migrate from the membrane surface onto graphene oxide nanosheets. Repeated extraction progressively destabilizes membrane organization. Loss of phospholipids has profound biological consequences. The bacterial membrane is not merely a physical barrier.

It serves as the principal site for

- oxidative phosphorylation,
- ATP production,
- transport proteins,
- nutrient uptake,
- ion homeostasis,
- environmental sensing.

Progressive phospholipid depletion therefore compromises membrane integrity long before complete membrane rupture occurs.

The membrane gradually loses structural cohesion, resulting in increased permeability and diminished capacity to maintain essential electrochemical gradients. This mechanism is particularly significant because it demonstrates that graphene oxide actively removes structural components from bacterial cells rather than simply damaging them externally.

The efficiency of phospholipid extraction is influenced by several material characteristics. Greater lateral sheet dimensions increase available adsorption surface. Higher dispersion stability maximizes contact frequency. Appropriate oxidation levels preserve sufficient graphitic domains for hydrophobic interaction while maintaining adequate aqueous dispersibility. Phospholipid extraction provides another example of how subtle variations in graphene oxide physicochemical properties directly influence biological activity.

### 3.2.4 Cellular Entrapment and Isolation

Perhaps the most distinctive antibacterial mechanism exhibited by graphene oxide is its ability to physically isolate bacterial cells from their surrounding environment. Unlike conventional antimicrobial agents that diffuse freely through tissues, graphene oxide possesses highly flexible two-dimensional nanosheets capable of bending, folding, and wrapping around microorganisms. This behaviour originates from the remarkable mechanical flexibility of atomically thin GO sheets. Following adsorption onto bacterial surfaces, nanosheets may progressively curl around individual bacteria or bacterial aggregates. Large lateral sheets are especially effective because they can envelop multiple microorganisms simultaneously. This process has frequently been described as bacterial wrapping or cellular entrapment. Once wrapped, bacteria experience several physiological consequences. Nutrient diffusion becomes restricted.

Gas exchange decreases.

Removal of metabolic waste products becomes inefficient.

Opportunities for cell division become limited.

Collectively these changes create a microenvironment incompatible with sustained bacterial proliferation.

Entrapment also prolongs direct contact between graphene oxide and bacterial membranes.

Rather than brief transient interactions, wrapped bacteria remain continuously exposed to membrane stress and oxidative injury.

Consequently, mechanical disruption, ROS generation, and phospholipid extraction continue operating over extended periods.

This prolonged exposure substantially increases antibacterial efficacy.

The wrapping mechanism may be particularly relevant during early biofilm formation.

Biofilm development depends upon close bacterial communication, extracellular polymer production, and coordinated community organization.

Graphene oxide sheets physically interfere with these processes by separating bacterial cells and disrupting spatial organization required for mature biofilm formation.

Such anti-biofilm behaviour is especially valuable when considering highly resistant organisms such as *Pseudomonas aeruginosa*, whose pathogenicity is closely linked to robust biofilm production.

### 3.2.5 Integrated Model of Graphene Oxide-Mediated Bacterial Killing

Although each antibacterial mechanism has been described individually, the biological response observed following graphene oxide exposure results from their simultaneous operation.

The antibacterial process may be conceptualized as a sequential yet overlapping cascade.

Initially, well-dispersed graphene oxide nanosheets establish intimate contact with bacterial surfaces through electrostatic attraction and hydrogen bonding.

This contact permits sharp sheet edges to mechanically deform the membrane while localized electron transfer initiates ROS production.

Membrane weakening facilitates phospholipid extraction, further destabilizing membrane architecture.

Meanwhile, flexible nanosheets progressively wrap around bacterial cells, prolonging exposure and restricting access to nutrients.

Ultimately, bacterial metabolism collapses.

Loss of membrane integrity, oxidative damage, impaired respiration, disrupted ATP synthesis, and nutrient deprivation collectively exceed the physiological capacity for recovery.

Cell death therefore represents the cumulative consequence of multiple interconnected physicochemical mechanisms rather than any isolated molecular event.

This integrated model explains why graphene oxide demonstrates antibacterial activity against both Gram-positive and Gram-negative bacteria despite their markedly different cell-envelope structures. It also reinforces the central hypothesis of the present investigation: the antimicrobial activity of graphene oxide is an intrinsic consequence of its structural morphology, surface chemistry, electronic heterogeneity, and colloidal behaviour, all of which were established during physicochemical characterization prior to biological evaluation.

### 3.3 Anticancer Activity of Graphene Oxide

#### 3.3.1 Overview of Cytotoxic Activity

Graphene oxide has emerged as a promising nanomaterial for cancer therapy because its biological activity extends beyond its role as a passive drug carrier. Unlike many nanocarriers that merely facilitate delivery of chemotherapeutic agents, GO possesses intrinsic cytotoxic properties arising from its unique physicochemical characteristics, including its two-dimensional morphology, high specific surface area, oxygen-rich surface chemistry, defect-rich carbon lattice, and heterogeneous electronic structure. These features enable GO to interact directly with cellular membranes, intracellular organelles, and redox systems, resulting in concentration-dependent and time-dependent inhibition of tumour cell proliferation.

The present investigation evaluated the anticancer activity of graphene oxide against three human cancer cell lines representing distinct tumour types and molecular phenotypes:

- **A549** human lung adenocarcinoma cells,
- **MCF-7** luminal A breast carcinoma cells,

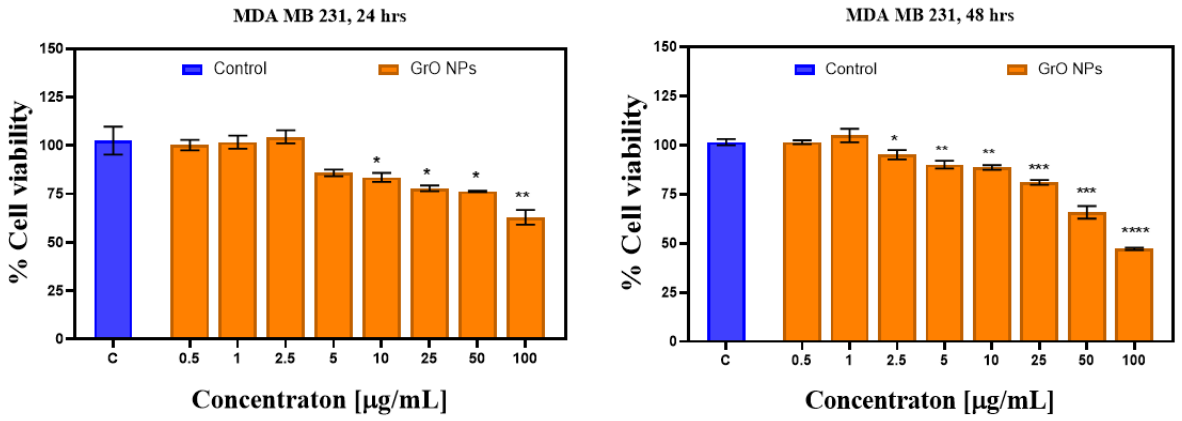
- **MDA-MB-231** triple-negative breast carcinoma cells.

These cell lines were intentionally selected because they differ markedly in receptor expression, metabolic characteristics, cell-cycle regulation, invasive behaviour, and genetic background. Such diversity provides an opportunity to determine whether graphene oxide exerts indiscriminate cytotoxicity or whether its activity is influenced by tumour phenotype.

Overall, graphene oxide demonstrated significant antiproliferative activity against all three cancer models. However, the magnitude of cytotoxicity differed substantially among the cell lines, indicating that the biological response to GO is not uniform but is strongly influenced by intrinsic cellular characteristics. Across all experiments, increasing graphene oxide concentration and prolonged exposure consistently resulted in progressive reductions in cell viability, supporting a dose-dependent and time-dependent mechanism of action.

### 3.3.2 Experimental Results and Discussion of MDA MB 231, MCF 7 AND A549

**(a)**




**(b)**

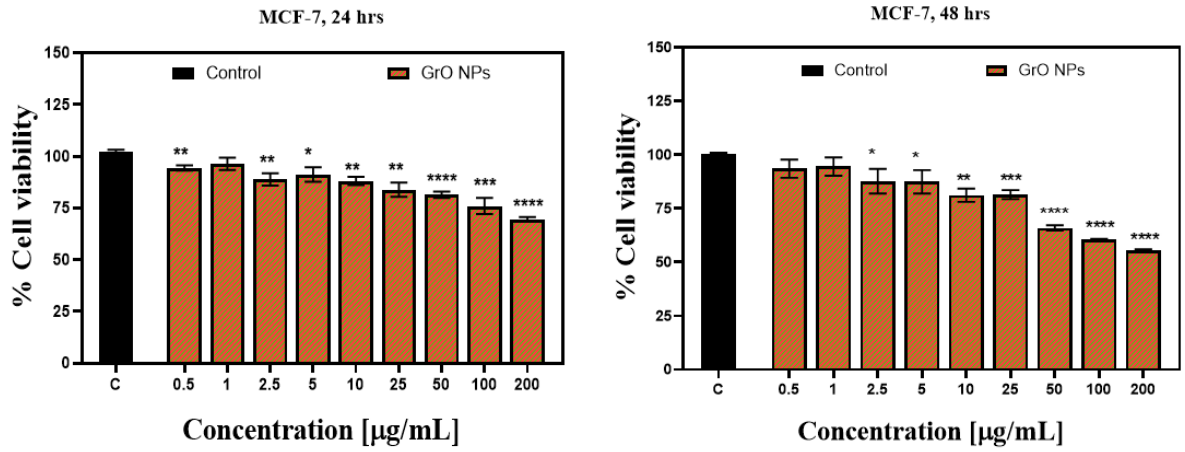



**Figure 5. (a) Evaluation of cell viability of MDA MB 231 cells in presence of GrO NPs. The cells were treated with a range of GrO NPs concentration and the viability was**

**evaluated using MTT assay. (b) Evaluation of cell viability of MCF-7 cells after treatment with varying concentrations of GrO NPs, also assessed using MTT assay. (* is $P \leq 0.05$, ** is $P \leq 0.01$, *** is $P \leq 0.001$, **** is $P \leq 0.0001$).**

### 3.3.2.1. Cytotoxic Effects of Graphene Oxide on Breast Cancer Cell Lines

In the present study, the cytotoxic potential of graphene oxide nanoparticles was systematically evaluated against two different human breast cancer cell lines: MCF-7 (estrogen receptor-positive, luminal A subtype) and MDA-MB-231 (triple-negative breast cancer phenotype).

The half-maximal inhibitory concentration ($IC_{50}$) values of GrO for time periods of 24 hours and 48 hours against MDA-MB-231 and MCF-7 cells were calculated for comparative analysis. In MDA MB 231 cells as shown in Table 1(a), the $IC_{50}$ value for 24 hours was 219.44 µg/mL and for 48 hours it was 105.40 µg/mL, indicating the cytotoxic effect of GrO was more pronounced with increasing incubation time. Conversely, MCF-7 cells exhibited significantly reduced sensitivity, with $IC_{50}$ values of 1578.34 µg/mL at 24 hours and 306.7 µg/mL at 48 hours, Table 1(b). An approximately 7.9-fold higher $IC_{50}$ at 24 hours and a 3-fold higher $IC_{50}$ at 48 hours were observed in MCF-7 cells relative to MDA-MB-231 cells. Therefore, it can be concluded that MDA-MB-231 cells demonstrated greater sensitivity to graphene oxide nanoparticles compared to MCF-7 cells across both temporal time points examined.

Even at the highest tested dosage, distinct cell viability was observed in both cell lines. At the highest treatment dosage (100 µg/mL), MDA-MB-231 cells maintained 63% viability at 24 hours and 47% viability at 48 hours. Comparatively, in MCF-7, the observed cell viability percentage for 24 hours and 48 hours was 75.95% and 60.72% respectively (Figure 1(a) and (b). Hence, MCF-7 cells demonstrated greater resistance to the treatment.

**Table 1(a).**

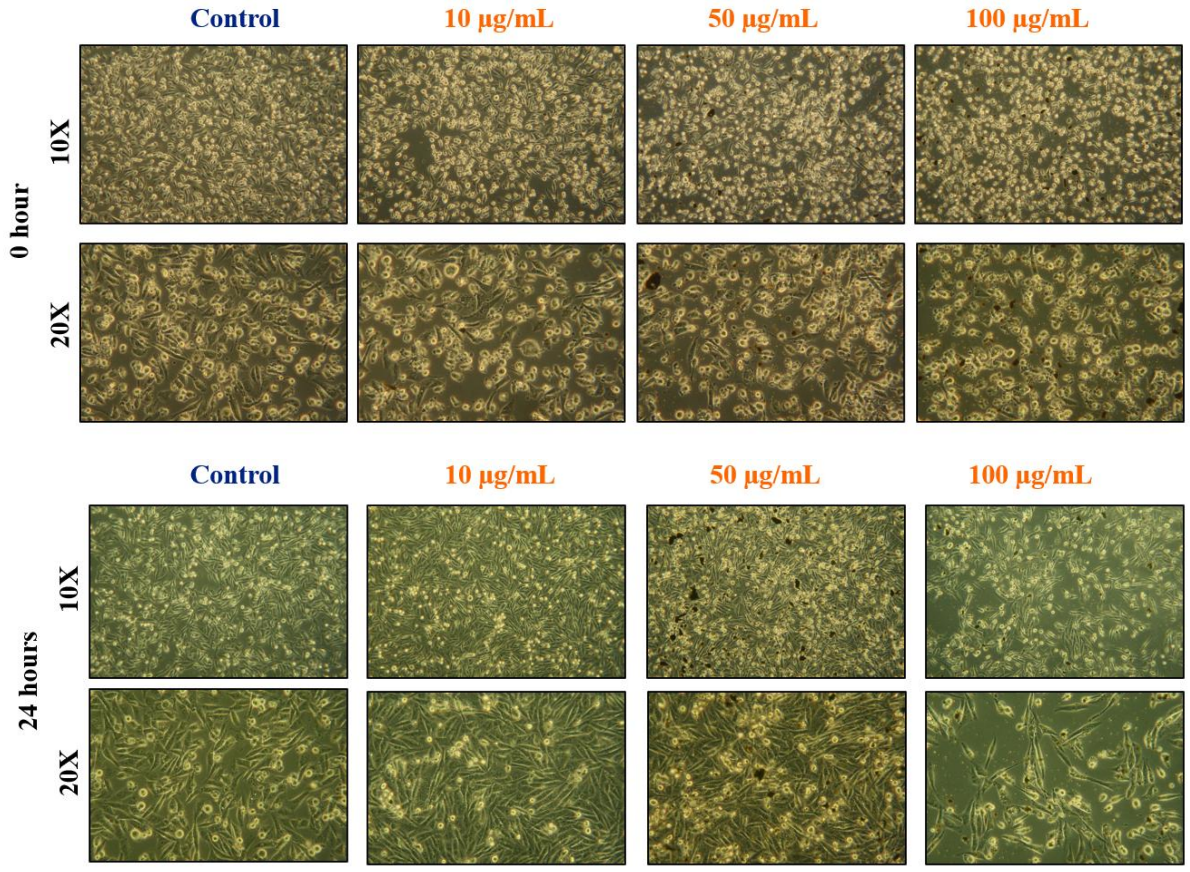
| S.No. | Time Point (MDA MB 231 ) | $IC_{50}$ Values (µg/mL) |
|---|---|---|
| 1. | 24 hours | 219.44 ± 8.80 |
| 2. | 48 hours | 105.40 ± 10.56 |

**Table 1(b).**

| S.No. | Time Period (MCF-7 Cells) | $IC_{50}$ values (µg/mL) |
|---|---|---|
| 1. | 24 hours | 1578.34 ± 290.53 |
| 2. | 48 hours | 306.7 ± 40.08 |

Both cell lines demonstrated increased cytotoxic effects with longer incubation times. However, the magnitude of this time-dependent effect varied significantly between the two phenotypes. These findings show that graphene oxide nanoparticles have anticancer potency and selectively impact breast cancer cells, with triple-negative MDA-MB-231 cells showing significantly higher sensitivity than luminal MCF-7 cells across all parameters and time points tested.

**3.3.2.1.1. Morphology assessment of Breast cancer cells treated with GrO NPs**



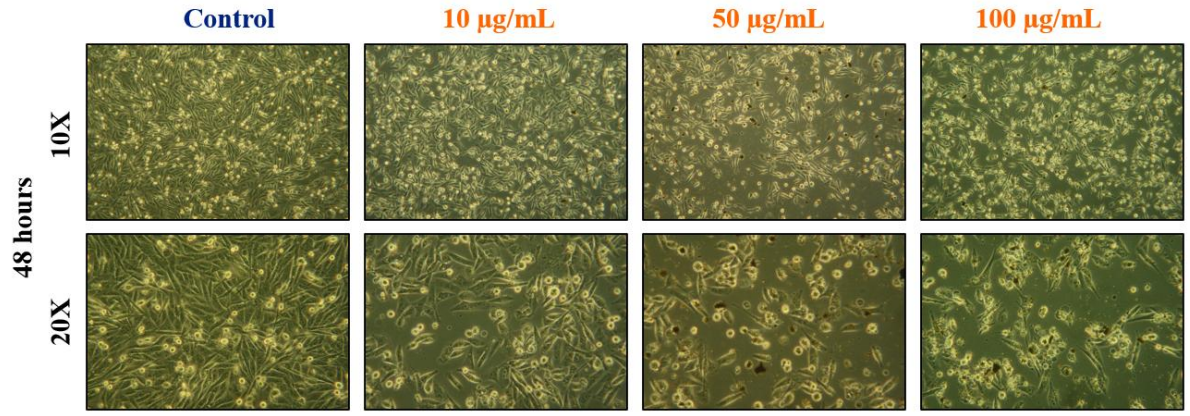



**Figure 6. Morphology assessment of MDA-MB-231 cells across three different cocentrations of 10, 50 and 100 µg/mL was done at magnifications 10X and 20X.**

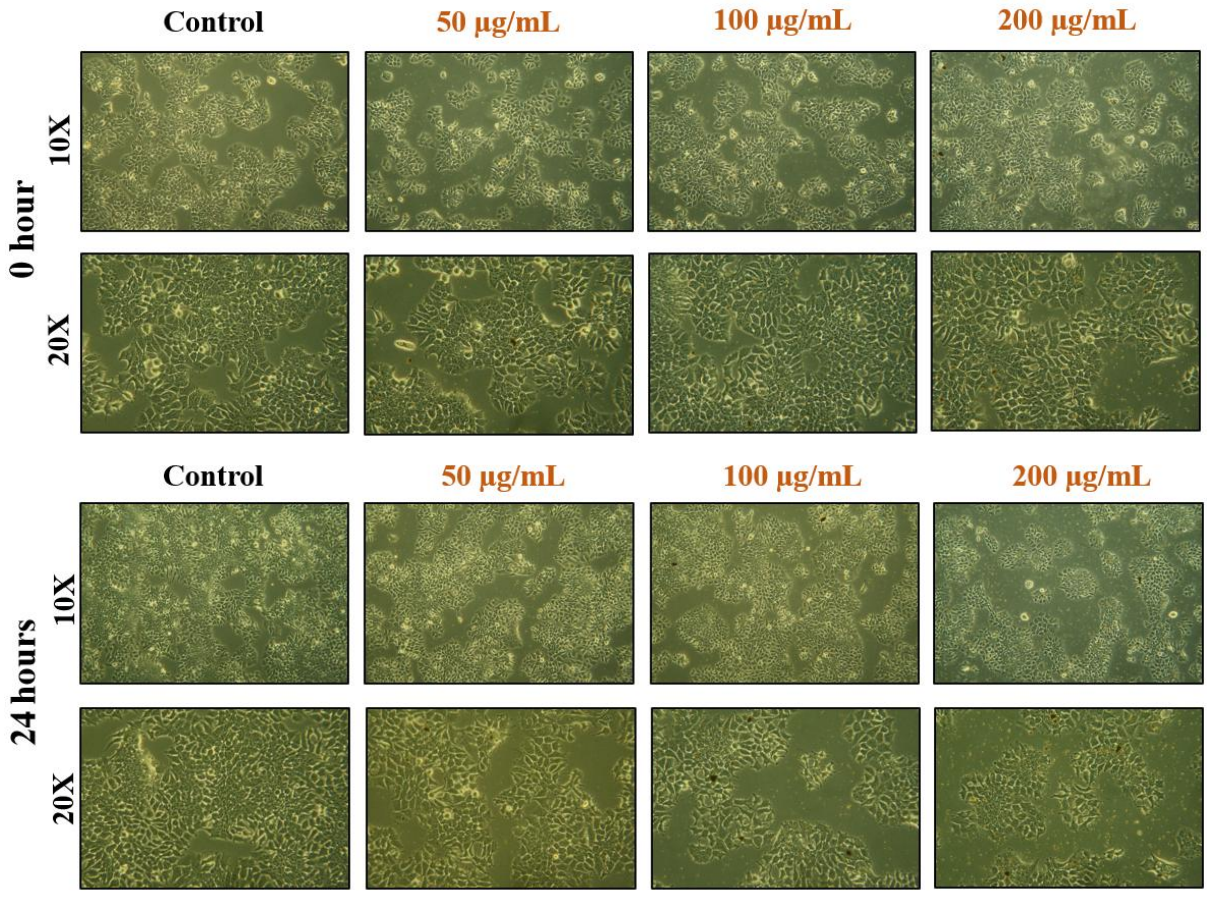
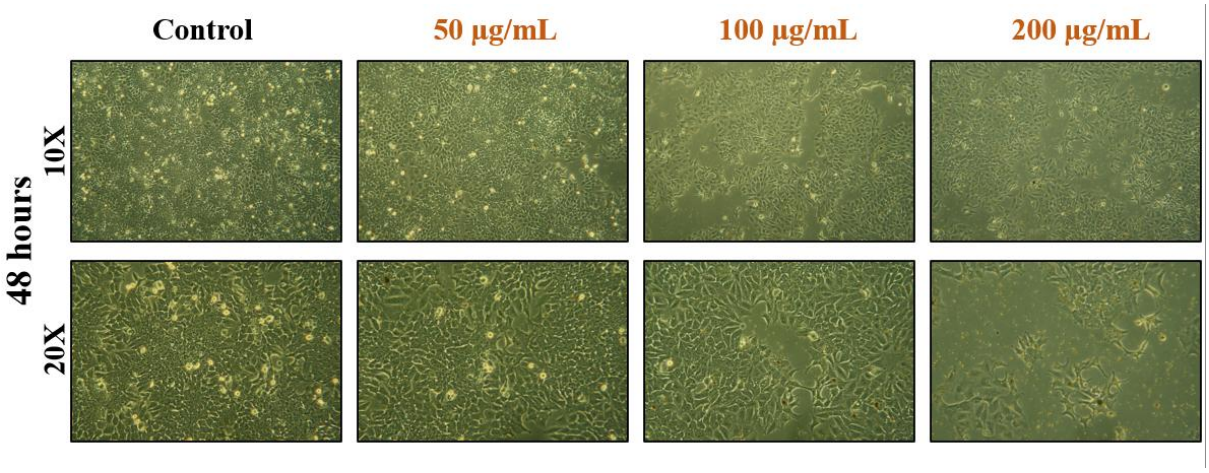


**Figure 7. Morphology assessment of MCF-7 cells across three different concentrations of 50, 100 and 200 µg/mL was done at magnifications 10X and 20X.**

At 0 h, both MDA-MB-231 and MCF-7 cells were observed under phase contrast microscope and images were taken. Both cell lines showed their typical healthy morphology, with intact plasma membranes, well-defined edges, and tight cell-to-cell junctions forming a uniform monolayer. After 24 h of treatment with lower concentrations of GrO NPs (10 µg/mL for MDA-MB-231 and 50 µg/mL for MCF-7, figure 2 and figure 3 respectively), most cells maintained a healthy appearance which was comparable with the control cells without any treatment. When the concentration was increased to the higher dosage of 100 µg/mL for MDA MB 231 and 200 µg/mL for MCF-7, clear morphological changes were observed in both cell lines. Cells appeared shrunken with a few rounded morphologies, with visible membrane blebbing, and many started detaching from the surface and floating in the medium. By 48 h, these effects became more evident, particularly in MDA-MB-231 cells, where a large number of cells lost their typical structure and displayed apoptotic-like features such as cell shrinkage and fragmentation. Microscopic images captured at 0, 24, and 48 h clearly highlight the




progressive, dose-dependent morphological alterations caused by graphene oxide exposure in both breast cancer cell lines.

**3.3.2.1.1.1.Discussion of MDA-MB-231 and MCF-7**

**1. Cytotoxicity response**

The present study demonstrates distinguished cytotoxic responses to prepared Graphene nanoparticles in two molecularly and clinically different breast cancer cell line *in vitro* models. Triple-negative breast cancer MDA-MB-231 cells exhibited relatively enhanced sensitivity to GrO, compared to MCF-7 luminal A cell line. Breast cancer is often characterized by its

intrinsic biological heterogeneity, hence the prepared GrO has differential responsiveness in two different cell lines showing significant implications for the therapeutic potential of graphene-based nanoparticles in breast cancer treatment.

The pronounced sensitivity to triple negative breast MDA-MB-231 cells, aligns with the emerging indications suggesting that basal-like carcinomas express heightened vulnerability to oxidative stress-mediated cytotoxic pathways compared to luminal subtypes. These results may be attributable to the fundamental differences in p53 status and metabolic characteristics between the cell lines examined in the present study.

It is well known that MCF-7 cells express wild-type p53 and have intact checkpoint control mechanisms. Mechanistically these cells show p21-mediated cell cycle arrest and coordinated apoptotic responses for any DNA damage or severe cellular stress. Conversely, MDA-MB-231 cells have mutant p53, which exhibit impaired cell cycle checkpoint function and altered apoptotic thresholds, which could explain their increased susceptibility to acute cytotoxic stress. As shown in the results, MCF-7 resisting the effect of GrO even at higher concentrations likely demonstrates the activation of survival pathways driven by p53. Recent studies of Graphene oxide based anticancer reagents have shown to induce cell cycle disruption by S-phase arrest along with increased TP53 expression. In contrast, the sensitivity of MDA MB 231 cells can be attributed to weak or absent p53- dependent checkpoint, leading to accumulation of unchecked damage in cells causing rapid apoptosis or necrosis.

**1.1. Maintenance of normal morphology at low doses**

At 0 h, both MDA-MB-231 and MCF-7 cells exhibited typical epithelial cellular morphology with intact plasma membranes, clear cell-to-cell junctions, and attached confluent monolayers, confirming a healthy phenotype before treatment. Exposure to lower GrO NPs concentrations (10 µg/mL for MDA-MB-231 and 50 µg/mL for MCF-7) for 24 h did not show much disruption of cell morphology, and treated cells remained comparable to untreated control group suggesting that sub-cytotoxic doses are well tolerated in the short term. Similar concentration windows with low toxicity at early time points have been reported for GrO in MCF-7 cells, where only higher surface doses induced significant morphological and viability changes.[3] The preservation of monolayer integrity as observed at low doses is consistent with the notion that graphene-based materials show a threshold behaviour, where below a critical concentration cells can compensate for oxidative and membrane stress through homeostatic mechanisms. Such a profile is particularly relevant for nanomedicine, as it suggests a potential therapeutic window in which GrO NPs can be exploited for targeted applications without widespread nonspecific damage to all cells.[4]

### 1.2. Dose-dependent cytotoxic morphology of MDA-MB-231 and MCF-7

At higher GrO NP concentrations (100 µg/mL for MDA-MB-231 and 200 µg/mL for MCF-7), the phase contrasted images showed cells progressively losing their typical morphology, becoming shrunken and rounded with membrane blebbing and detachment, especially evident after 48 h. These alterations are classical hallmarks of cytotoxic damage in cancerous cells and are routinely described in breast cancer cells treated with Graphene Oxide based NPs, including cell shrinkage, loss of adherence, membrane disruptions, and decreased cell density. Studies on graphene oxide have shown that increasing concentration and exposure time significantly reduce viability and colony-forming ability in breast cancer lines, confirming a dose- and time-dependent anti-proliferative effect.

The severe and earlier morphological destruction in MDA-MB-231 compared to MCF-7 in the present dataset aligns with previous reports showing a higher sensitivity of triple-negative or more invasive phenotypes to graphene-based nanomaterials. In particular, MDA-MB-231 cells have been reported to exhibit stronger growth inhibition, increased LDH release, and elevated ROS levels supporting the current pattern of sensitivity of MDA-MB-231 cells towards the prepared GrO NPs.

#### 3.3.2.1.1.1.1. Cytotoxic Effects of Graphene Oxide on A549 Lung Cancer Cells

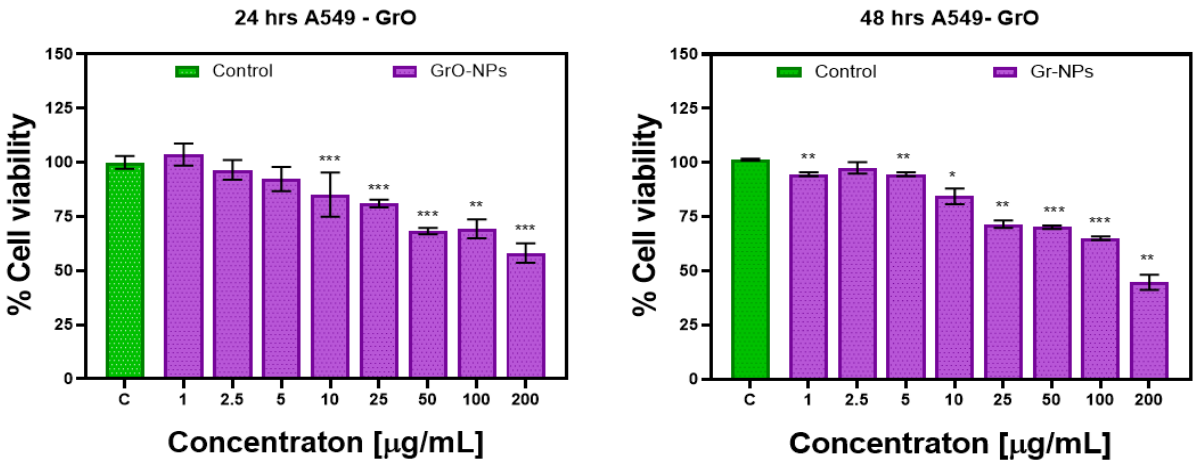



**Figure 8. (a) Evaluation of cell viability of A549 cells in presence of GrO-NPs. The cells were treated with a range of GrO-NPs test concentrations and the viability was evaluated using MTT assay. (* is P ≤ 0.05, ** is P ≤ 0.01, *** is P ≤ 0.001, **** is P ≤ 0.0001).**

The antiproliferative activity of graphene oxide (GrO) was evaluated against human lung adenocarcinoma A549 cells using the MTT colorimetric assay. A549 cells were treated with varying concentrations of GrO ranging from 1 to 200 µg/mL for 24 and 48 hours to establish

dose-response and time-dependent cytotoxicity profiles. The concentration range was selected based on the relevant therapeutic doses to thoroughly analyse the cytotoxic potential of graphene oxide against lung cancer cells.

Following 24 hours of treatment, GrO exhibited concentration-dependent cytotoxic effects on A549 cells. At lower concentrations (1-25 µg/mL), the sample demonstrated minimal to moderate cytotoxicity. However, at elevated concentrations, the cytotoxic effects became more pronounced. Specifically, at 100 µg/mL, cell viability was reduced to 69.35%, representing a 31% decrease in metabolically active cells compared to untreated controls. At the highest tested concentration of 200 µg/mL, cell viability further declined to 58.13%, indicating a 42% reduction in viable cells. After the 48-hour treatment time point the results were more pronounced. At the concentration of 100 µg/mL, cell viability was reduced to 68% and at 200 µg/mL a significantly low cell viability of 44.71 % was observed. This represents a significant temporal progression of cytotoxicity, with an additional 14% decrease in viability compared to the 24-hour timepoint at the same concentration.

**Table 2.**

| S.No. | Time Period (A549 Cells) | $IC_{50}$ values (µg/mL) |
|---|---|---|
| 1. | 24 hours | 356.63 ± 107.07 |
| 2. | 48 hours | 198.133 ± 35.82 |

These *in vitro* results observed in our study demonstrate that GrO-NPs exhibits substantial cytotoxicity against A549 lung cancer cells. Table 1, depicts the calculated $IC_{50}$ values based on the cell viability results observed in MTT assay. The dose- and the time-dependent increase in cytotoxicity suggest that the prepared samples of GrO-NPs may exert anti-proliferative effects through the sustained disruption of cellular metabolism and the induction of cell death mechanisms in cancer cells. These findings provide evidence for the potential application of graphene oxide as a therapeutic agent in lung cancer treatment strategies.

**3.3.2.1.1.1.1.1.Morphology assessment of Lung Cancer cells treated with GrO-NPs**

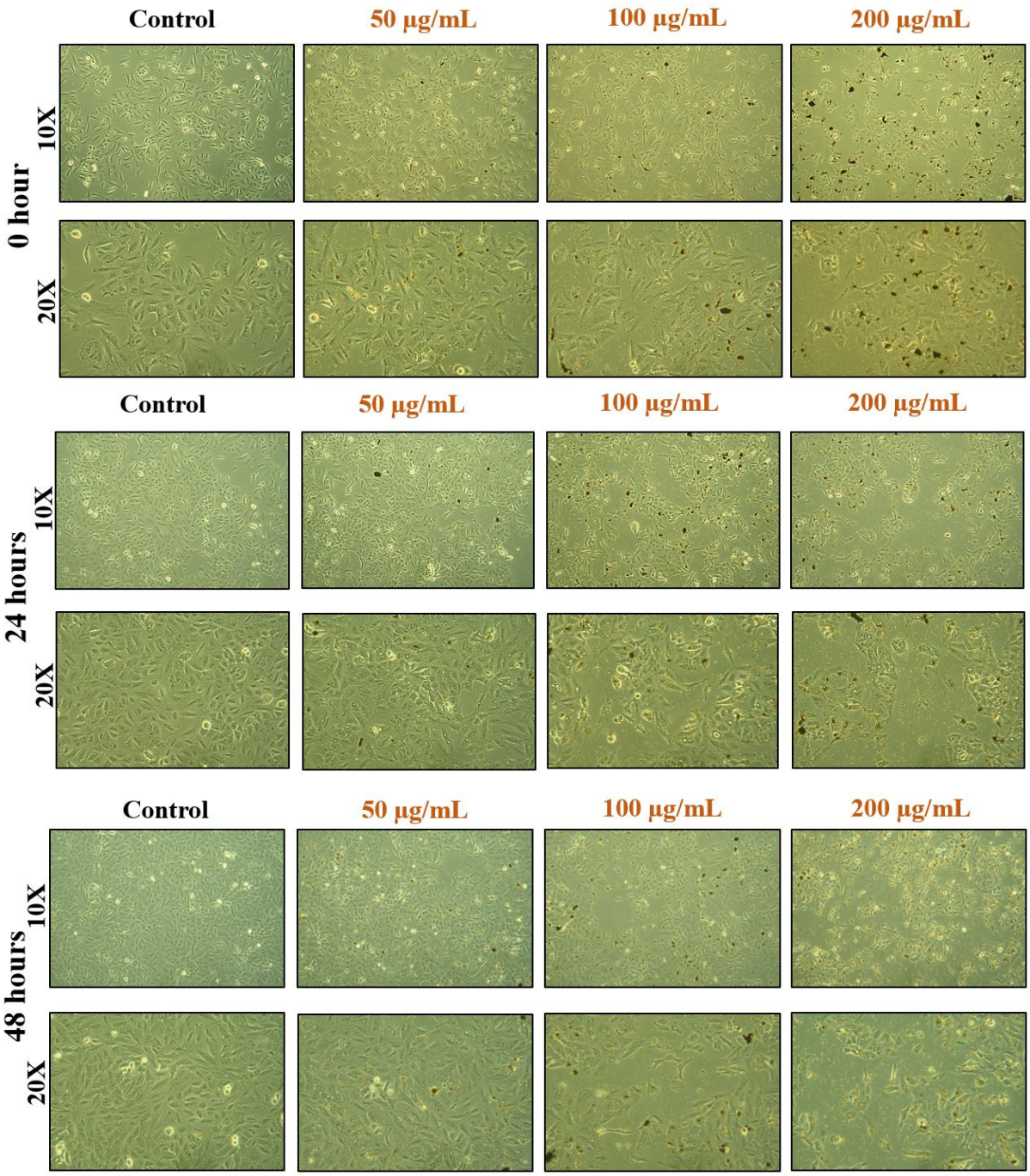



**Figure 9. Morphology assessment of A549 cells across three different concentrations of 50, 100 and 200 µg/mL was done at magnifications 10X and 20X.**

The morphological changes in A549 human lung adenocarcinoma cells were evaluated following treatment with graphene oxide nanoparticles (GrO-NPs) at concentrations of 50, 100, and 200 µg/mL, observed over a period of 48 hours. Post completion of treatment time points at 0-, 24-, and 48- hours phase-contrast light microscopy images were acquired using digital imaging system attached to the microscope. Representative micrographs are presented in Figure 2.

At the 0-hour treated time point, it was observed that untreated and treated cells exhibited comparable morphology, having healthy, epithelial phenotype with intact cell-cell contacts, smooth and well-shaped plasma membranes and uniform surface adherence. This observation suggests that no changes were observed in the cellular morphology in the initial exposure time. By the end of 24 hours, post-treatment, dose-dependent changes became evident. Cell exposed at lower test concentration (50 µg/mL), displayed relatively preserved morphology as control cells, with only mild changes. While cells treated with 100 µg/mL test concentration exhibited more pronounced alterations in cellular morphology, including cell rounding, and less cellular confluency with appearance of intercellular gaps indicative of disrupted cell-cell junctions. At the highest treated test concentration of 200 µg/mL, cells showed evident morphological disruptions, characterized by extensive cell rounding, cell shrinkage, and partial detachment from surface, suggesting early cytotoxic stress and the onset of apoptotic or necrotic processes. At 48 hours, the morphological disruption was more severe, showing dose dependent and time dependent effects of the GrO-NPs treatment. In the 50 µg/mL treated group, cells displayed moderate changes, including reduced cell density and disrupted irregular cell membranes. In the 100 µg/mL treated group, showed substantial loss of characteristic epithelial monolayer, with increase in rounded cells, cytoplasmic shrinkage, and reduced overall cell density. The most pronounced effects were observed in the 200 µg/mL treated group, where extensive cell death was evident, severe cell shrinkage, formation of apoptotic bodies, and significantly reduce number of cells. The near-complete disruption of cellular morphology at this time point and concentration implies the potent cytotoxic potential of GrO-NPs.

This section should include:

- Cell viability graphs (24 h and 48 h)
- $IC_{50}$ tables
- Representative phase-contrast microscopy images
- Statistical analysis
- Morphology figures
- Dose-response curves
- Figure legends

The experimental datasets should be inserted exactly as generated during the in vitro investigations. These include MTT-derived viability curves, $IC_{50}$ calculations, and phase-contrast images acquired at 0, 24, and 48 hours for A549, MCF-7, and MDA-MB-231 cells.

#### 3.3.2.1.1.1.1.1.1. Discussion of A549 cells

**1. Cytotoxity response of GrO-NPs on A549 cells**

The present study explores the effects of the prepared nano-formulations of Graphene Oxide on human lung adenocarcinoma cells. As the results demonstrated, after 24 hours, the cell viability was 69% and 58% at concentrations of 100 and 200 µg/mL, respectively. Further cell viability declined to 44% at 200 µg/mL after 48 hours. This demonstrates that GrO induces significant toxic effects at concentrations exceeding 50-100 µg/mL which aligns with the reported studies based on GrO formulations and its effect against certain cancers.[1, 2]

The observed cytotoxicity in the present study may also be attributed to the physicochemical properties of GrO, including its large surface area, and high oxidative potential.[3] These properties facilitate prominent interactions with cellular membranes and organelles.[4] These interactions consequently result in compromising membrane integrity and inducing oxidative stress[5], leading to impaired cell metabolism as reflected in the MTT assay results.

GrO is known to be involved in the generation of reactive oxygen species (ROS) through the activation of mitochondrial NADH dehydrogenase. This ROS accumulation leads to mitochondrial dysfunction, characterized by a loss of membrane potential, disruption of the electron transport chain, and mechanistically leading to the subsequent activation of intrinsic apoptotic pathways mediated by caspase-3 activation and cytochrome c release.[6]

Additionally, the possible molecular mechanisms underlying these effects involve several interconnected cellular pathways. Comparative studies demonstrate that GrO-based formulations involve activation of multiple programmed cell death pathways, including apoptosis, autophagy, and necroptosis.[7] The cell death depends on many factor including the dosage, interaction of GrO with cells and exposure duration. Based on the available data in similar studies, GrO likely induces both apoptotic and necrotic cell death pathways in the present study.[8]

### 1.1. Morphology assessment of A549 cells treated with GrO-NPs at different test concentrations

The morphological findings are consistent with the well-documented cytotoxic mechanisms attributed to graphene oxide nanoparticles in mammalian cancer cells. The characteristic morphology alterations exhibited by the treatment of GrO NPs on A549 cells showed dose and time dependent progression.[9,10] Mild shrinkage at low concertation and early time point to significant cell death and membrane disruption at higher concentration and later time points, suggests that GrO-NPs exert cytotoxicity through cumulative cellular stress mechanisms rather than immediate toxicity. Several reported mechanisms likely are responsible for these effects.

Graphene oxide is known to induce oxidative stress by generating reactive oxygen species (ROS)[11], this reportedly damages lipid membranes, proteins, and DNA, simultaneously triggering apoptosis or necrotic pathways.[12,13]

The A549 cells exposed to graphene oxide nanoparticle showed morphological alterations indicating substantial cellular stress and loss of normal structural integrity. Compared with untreated control cells, the lung cancer cells appeared rounded, shrunken, with reduced adherence, increased membrane irregularity and lower overall cell density. These changes are consistent with nanoparticle-induced cytotoxicity and suggest disruption of membrane stability, cytoskeletal organization, and cell viability. Overall, the observed morphological response supports the conclusion that graphene oxide exerts a dose- and/or time-dependent inhibitory effect on A549 cell survival and proliferation.

### 3.3.3 Dose-Dependent Cytotoxic Response

The MTT assay demonstrated that graphene oxide inhibited the proliferation of all investigated cancer cell lines in a concentration-dependent manner. At lower concentrations, only modest reductions in metabolic activity were observed, indicating that sub-cytotoxic doses were relatively well tolerated during the early stages of exposure. As the graphene oxide concentration increased, however, cellular viability progressively declined, reflecting increasing metabolic dysfunction and loss of viable cells.

This concentration-dependent behaviour is characteristic of nanomaterial-mediated cytotoxicity. At low concentrations, only a limited fraction of the cellular population is exposed to sufficient nanosheet–cell interactions to induce irreversible injury. The remaining cells maintain mitochondrial function through endogenous antioxidant systems and cellular repair mechanisms. As nanoparticle concentration increases, both the frequency and intensity of interactions between graphene oxide and the cell surface increase markedly. Larger numbers of nanosheets adhere to the plasma membrane, increasing opportunities for membrane perturbation, oxidative stress, and intracellular uptake.

The large two-dimensional geometry of graphene oxide further amplifies this response. Unlike spherical nanoparticles that contact the membrane at relatively small surface areas, GO sheets establish extensive interfacial contact with the plasma membrane. This prolonged contact facilitates sustained physicochemical interactions, increasing the probability of membrane disruption and intracellular signalling disturbances.

The concentration-dependent decrease in cell viability therefore reflects cumulative biological stress rather than acute chemical toxicity. Progressive impairment of mitochondrial

metabolism, disruption of membrane integrity, oxidative damage, and interference with cellular homeostasis collectively contribute to the observed reduction in MTT reduction capacity.

### 3.3.4 Time-Dependent Cytotoxic Progression

In addition to concentration-dependent effects, graphene oxide exhibited pronounced time-dependent cytotoxicity across all investigated cell lines. Cells exposed for 48 hours consistently demonstrated lower viability than cells treated for 24 hours, indicating that graphene oxide-induced cellular injury accumulates with prolonged exposure.

This temporal progression provides important mechanistic insight into the mode of action of graphene oxide. Unlike highly reactive chemical toxins that produce immediate cell death, GO exerts cytotoxicity through gradual physicochemical interactions that evolve over time. Initial membrane contact is followed by progressive oxidative stress, mitochondrial dysfunction, cytoskeletal disruption, and activation of programmed cell death pathways.

Prolonged exposure also increases the likelihood of nanoparticle internalization through endocytic mechanisms. Once internalized, graphene oxide interacts with intracellular organelles including mitochondria, lysosomes, and the endoplasmic reticulum, thereby amplifying cellular stress responses. Sustained oxidative damage progressively overwhelms antioxidant defence systems, resulting in irreversible impairment of metabolic activity and loss of cell viability.

The greater cytotoxicity observed at 48 hours therefore reflects cumulative intracellular injury rather than delayed experimental variability. This observation supports the hypothesis that graphene oxide acts through progressive biological disruption rather than immediate nonspecific toxicity.

### 3.3.5 Comparative Cytotoxicity Among A549, MCF-7, and MDA-MB-231 Cells

Although graphene oxide reduced viability in all three cancer models, substantial differences were observed in the magnitude of cytotoxicity among the investigated cell lines.

The MDA-MB-231 triple-negative breast cancer cells demonstrated the greatest sensitivity to graphene oxide treatment. $IC_{50}$ values decreased from approximately 219.44 μg/mL at 24 hours to 105.40 μg/mL at 48 hours, indicating that prolonged exposure nearly doubled the cytotoxic potency of graphene oxide against this aggressive breast cancer subtype.

By contrast, the MCF-7 luminal A breast cancer cells exhibited considerably greater resistance. The calculated $IC_{50}$ values were approximately 1578.34 μg/mL after 24 hours and 306.70 μg/mL after 48 hours, values that were substantially higher than those observed for MDA-MB-231 cells. These findings indicate that MCF-7 cells possess a markedly higher capacity to tolerate graphene oxide-induced stress, particularly during the early phase of treatment.

The A549 lung adenocarcinoma cells displayed an intermediate response. Cell viability decreased progressively with increasing graphene oxide concentration and exposure time. At higher concentrations (100–200 μg/mL), viability declined substantially, and the calculated $IC_{50}$ values indicated meaningful antiproliferative activity, although the degree of sensitivity remained between that observed for MDA-MB-231 and MCF-7 cells. These findings demonstrate that graphene oxide does not exert uniform cytotoxicity across all tumour types. Instead, the biological response is strongly influenced by tumour phenotype and molecular characteristics, emphasizing the importance of considering cancer heterogeneity when evaluating nanomaterial-based therapeutics.

**3.3.6 Phenotype-Dependent Susceptibility of Breast Cancer Cells**

One of the most significant observations in the present investigation was the marked difference in graphene oxide sensitivity between the two breast cancer models.

Although both MCF-7 and MDA-MB-231 originate from human breast carcinomas, they represent fundamentally different molecular subtypes with distinct biological behaviour.

MCF-7 cells are classified as luminal A breast cancer, characterized by expression of estrogen receptors, relatively low proliferative rates, preserved epithelial morphology, and functional cell-cycle checkpoints. These cells retain wild-type TP53, enabling activation of p21-dependent cell-cycle arrest following oxidative stress or DNA damage. Temporary arrest provides an opportunity for DNA repair and restoration of cellular homeostasis before proliferation resumes. MCF-7 cells demonstrate relatively strong resistance to graphene oxide-induced oxidative injury. Their intact checkpoint mechanisms permit repair of sublethal damage and delay progression toward apoptosis.

In contrast, MDA-MB-231 cells represent triple-negative breast cancer, one of the most clinically aggressive breast cancer subtypes. These cells lack expression of estrogen receptor, progesterone receptor, and HER2, and they harbour mutant TP53, resulting in impaired checkpoint regulation and defective coordination of DNA damage responses. The uploaded breast cancer study discusses this mechanistic distinction as a likely explanation for the greater sensitivity of MDA-MB-231 cells to GO treatment.

Because mutant p53 is unable to efficiently coordinate cell-cycle arrest and DNA repair, oxidative injury accumulates rapidly following graphene oxide exposure. Rather than repairing damage, MDA-MB-231 cells progress toward apoptosis or necrotic cell death after comparatively lower levels of intracellular stress.

This molecular difference provides a biologically plausible explanation for the substantially lower $IC_{50}$ values observed in MDA-MB-231 cells compared with MCF-7 cells. The results

therefore suggest that graphene oxide may exhibit preferential activity against highly aggressive triple-negative breast cancer phenotypes, an observation with potential translational significance given the limited targeted treatment options currently available for TNBC.

### 3.4 Molecular Mechanisms Underlying the Anticancer Activity of Graphene Oxide

The concentration-dependent reduction in cell viability observed across A549, MCF-7, and MDA-MB-231 cells indicates that graphene oxide (GO) exerts its anticancer effects through a progressive disruption of multiple cellular processes rather than through immediate nonspecific toxicity. Unlike conventional chemotherapeutic agents that often target a single molecular pathway, GO interacts with cancer cells through a complex sequence of physicochemical and biochemical events beginning at the cell surface and extending to intracellular organelles. The ultimate biological response represents the cumulative outcome of membrane perturbation, oxidative stress, mitochondrial dysfunction, metabolic collapse, cytoskeletal disruption, and activation of programmed cell death pathways.

The mechanistic basis of GO-mediated cytotoxicity is intrinsically linked to its physicochemical characteristics established during material characterization. The atomically thin morphology provides an exceptionally large contact area for interaction with the plasma membrane, while abundant oxygen-containing functional groups promote stable dispersion and electrostatic interactions with cellular surfaces. Simultaneously, the coexistence of oxidized domains and residual $sp^2$-hybridized carbon networks create localized redox-active regions capable of initiating intracellular oxidative stress. Consequently, the biological activity observed in the present investigation is not an incidental property of graphene oxide but rather the direct expression of its structural and chemical architecture at the nano–bio interface.

#### 3.4.1 Initial Interaction Between Graphene Oxide and the Cancer Cell Membrane

The plasma membrane represents the first biological barrier encountered by graphene oxide following exposure to cultured cancer cells. Successful interaction at this interface determines the subsequent intracellular fate of the nanomaterial and strongly influences the magnitude of the biological response.

Unlike spherical nanoparticles that establish relatively limited contact with cellular membranes, graphene oxide possesses a flexible two-dimensional geometry that permits extensive adhesion across the membrane surface. Electrostatic interactions between negatively charged oxygen-containing functional groups and positively charged membrane proteins, together with hydrogen bonding, van der Waals forces, and hydrophobic interactions involving residual graphitic domains, collectively stabilize GO adsorption onto the plasma membrane.

The large lateral dimensions of graphene oxide enable simultaneous interaction with multiple membrane receptors and phospholipid domains. This broad contact area may alter membrane fluidity, disrupt lipid organization, and influence receptor clustering, thereby modifying intracellular signalling even before particle internalization occurs.

At lower graphene oxide concentrations, these interactions are generally well tolerated because endogenous membrane repair mechanisms preserve structural integrity. As nanoparticle concentration increases, however, membrane perturbation becomes progressively more pronounced. Increased surface coverage by graphene oxide reduces membrane flexibility, disturbs cytoskeletal attachment points, and promotes localized mechanical stress. These early events initiate the cascade of cellular responses that ultimately culminates in reduced metabolic activity and cell death.

The extensive wrinkling and edge irregularities identified during graphene oxide characterization are particularly relevant at this stage because they increase effective contact area and facilitate intimate interaction with the irregular topography of the cancer cell surface. Similar structure–function relationships were highlighted in the biological rationale developed from the physicochemical characterization of the synthesized GO.

### 3.4.2 Cellular Uptake and Intracellular Localization

Following membrane adhesion, graphene oxide may enter cancer cells through several endocytic pathways. The precise mechanism of uptake depends upon nanosheet dimensions, oxidation degree, surface charge, and the biological characteristics of the target cell.

The predominant internalization routes include clathrin-mediated endocytosis, caveolae-mediated endocytosis, micropinocytosis, and, in some circumstances, direct membrane penetration by nanosheet edges. Internalized graphene oxide is subsequently trafficked through early endosomes toward lysosomal compartments, although partial escape into the cytoplasm has also been reported.

Once inside the cell, graphene oxide is capable of interacting with several intracellular organelles. Mitochondria appear particularly susceptible because of their central role in energy production and redox regulation. The close association of GO with mitochondrial membranes promotes oxidative stress and disturbs mitochondrial homeostasis, leading to impaired ATP synthesis and activation of intrinsic apoptotic pathways.

The intracellular persistence of graphene oxide also prolongs cellular exposure beyond the initial treatment period. This prolonged intracellular residence provides a mechanistic explanation for the greater cytotoxicity observed after 48 hours compared with 24 hours in all investigated cell lines. Rather than acting as an acute toxin, GO continues to perturb

intracellular processes over time, producing cumulative biological damage that progressively reduces cellular viability.

### 3.4.3 Oxidative Stress as the Central Mechanism of Cytotoxicity

Among the numerous mechanisms proposed for graphene oxide-mediated anticancer activity, oxidative stress is widely regarded as the central event linking nanoparticle exposure to cellular injury. Cancer cells differ fundamentally from normal cells in their redox biology. Owing to accelerated metabolism, mitochondrial dysfunction, oncogenic signalling, and rapid proliferation, malignant cells continuously generate elevated basal levels of reactive oxygen species (ROS). Although antioxidant systems are simultaneously upregulated to maintain redox homeostasis, many tumour cells exist close to their maximum oxidative tolerance. Consequently, relatively modest additional ROS production may shift intracellular redox balance beyond the threshold compatible with survival.

Graphene oxide is particularly effective at exploiting this vulnerability. Residual graphitic domains embedded within oxidized regions facilitate electron-transfer reactions that promote the generation of superoxide anions, hydrogen peroxide, and hydroxyl radicals. These reactive intermediates attack multiple intracellular targets simultaneously.

Lipid membranes undergo extensive peroxidation, compromising membrane integrity and altering membrane-associated signalling. Oxidative modification of proteins disrupts enzyme activity, cytoskeletal organization, and intracellular transport. DNA experiences oxidative damage in the form of strand breaks, base modifications, and replication errors, activating stress-responsive signalling pathways.

Unlike physiological oxidative signalling, which is transient and tightly regulated, graphene oxide induces sustained ROS generation. Persistent oxidative stress progressively overwhelms endogenous antioxidant systems, including glutathione, catalase, and superoxide dismutase, thereby amplifying cellular injury over time.

This cumulative oxidative mechanism provides a biologically plausible explanation for the progressive decline in viability observed during the MTT assay and supports the concentration-dependent and time-dependent nature of graphene oxide cytotoxicity reported in the uploaded A549 and breast cancer studies.

### 3.4.4 Mitochondrial Dysfunction and Metabolic Collapse

The reduction in MTT absorbance observed following graphene oxide treatment reflects more than a simple decrease in cell number. Because the MTT assay measures mitochondrial dehydrogenase activity, declining absorbance indicates progressive impairment of mitochondrial metabolic function.

Mitochondria occupy a central position in graphene oxide-mediated cytotoxicity. Reactive oxygen species generated following GO exposure damage mitochondrial membranes, resulting in depolarization of the mitochondrial membrane potential. Loss of membrane potential disrupts the electron transport chain, reducing oxidative phosphorylation and ATP synthesis.

As ATP availability declines, numerous energy-dependent cellular processes become compromised, including protein synthesis, cytoskeletal maintenance, membrane transport, and DNA repair. Cells gradually transition from adaptive metabolic stress toward irreversible metabolic collapse.

Damage to the outer mitochondrial membrane further promotes release of cytochrome c into the cytoplasm, initiating assembly of the apoptosome complex and subsequent activation of caspase-9 and downstream executioner caspases such as caspase-3 and caspase-7. Although the specific apoptotic proteins were not directly measured in the present investigation, the observed reduction in metabolic activity together with the characteristic morphological alterations strongly support activation of mitochondrial-dependent apoptotic pathways.

The time-dependent decline in cell viability observed across all three cell lines is therefore consistent with progressive mitochondrial dysfunction rather than immediate membrane lysis.

**3.4.5 Morphological Evidence of Graphene Oxide-Induced Cytotoxicity**

Quantitative reductions in cell viability were accompanied by distinct morphological alterations that provide direct visual evidence of graphene oxide-mediated cellular injury. Phase-contrast microscopy demonstrated progressive structural deterioration of A549, MDA-MB-231, and MCF-7 cells with increasing graphene oxide concentration and treatment duration. Representative images acquired at 0, 24, and 48 hours illustrate this progression in the uploaded studies.

At the initial 0-hour time point, untreated and treatment groups exhibited comparable healthy morphology. Cells formed well-organized monolayers with intact plasma membranes, clear intercellular junctions, and characteristic epithelial architecture, indicating that graphene oxide had not yet induced detectable structural alterations.

Following 24 hours of exposure, cells treated with lower concentrations generally retained normal morphology, although subtle reductions in confluency and slight changes in cell shape were occasionally evident. In contrast, intermediate and higher graphene oxide concentrations produced pronounced structural abnormalities, including cellular rounding, cytoplasmic shrinkage, reduced substrate adhesion, widening of intercellular spaces, and disruption of the characteristic epithelial monolayer.

After 48 hours, morphological deterioration became substantially more severe. Large numbers of cells exhibited membrane blebbing, marked shrinkage, fragmentation, and detachment from the culture surface. The reduction in cell density observed microscopically closely paralleled the decrease in metabolic activity measured by the MTT assay, demonstrating excellent agreement between qualitative and quantitative indicators of cytotoxicity.

Among the three investigated cell lines, MDA-MB-231 cells displayed the earliest and most extensive morphological disruption, whereas MCF-7 cells retained comparatively greater structural integrity at equivalent graphene oxide concentrations. A549 cells exhibited an intermediate phenotype characterized by progressive cell rounding, membrane irregularities, and reduced adherence with increasing treatment intensity. These observations are consistent with the differences in $IC_{50}$ values and support the conclusion that tumour phenotype significantly influences susceptibility to graphene oxide-mediated cytotoxicity.

The morphological progression observed in this investigation—transitioning from healthy adherent epithelial cells to rounded, shrunken, blebbed, and detached cells—is characteristic of apoptosis accompanied by advanced cytotoxic stress. Although additional molecular assays would be required to distinguish apoptosis from secondary necrosis conclusively, the combined MTT and microscopy findings strongly indicate activation of programmed cell death pathways following graphene oxide exposure.

### 3.5 Molecular Basis for Differential Sensitivity of A549, MDA-MB-231, and MCF-7 Cells to Graphene Oxide

One of the most scientifically significant observations in the present investigation is that graphene oxide did not produce identical cytotoxic responses across all cancer cell lines. Although all three models exhibited concentration-dependent and time-dependent reductions in viability, the magnitude of these responses varied considerably according to tumour phenotype. This finding demonstrates that graphene oxide-mediated cytotoxicity is not indiscriminate but is strongly influenced by the intrinsic molecular characteristics of the target cells.

Among the investigated models, MDA-MB-231 cells exhibited the greatest susceptibility, followed by A549 cells, whereas MCF-7 cells displayed the highest resistance to graphene oxide treatment. The calculated $IC_{50}$ values clearly illustrate this pattern. MDA-MB-231 cells showed a marked decrease in $IC_{50}$ from 219.44 μg/mL at 24 hours to 105.40 μg/mL at 48 hours, indicating a substantial increase in cytotoxicity with prolonged exposure. In contrast, MCF-7 cells required significantly higher concentrations to achieve equivalent inhibition, with $IC_{50}$ values of 1578.34 μg/mL at 24 hours and 306.70 μg/mL at 48 hours. A549 cells demonstrated

an intermediate response, with progressive reductions in viability and increasingly pronounced morphological alterations as treatment concentration and duration increased.

These differences cannot be explained solely by graphene oxide concentration. Rather, they reflect fundamental variations in tumour biology, including differences in genomic stability, oxidative stress tolerance, metabolic phenotype, membrane composition, and cell-cycle regulation.

### 3.5.1 Influence of p53 Status on Cellular Response to Graphene Oxide

Among the molecular determinants governing sensitivity to graphene oxide, the tumour suppressor protein p53 occupies a central position. p53 functions as the principal regulator of the cellular response to DNA damage, oxidative stress, and metabolic disturbance. Under physiological conditions, activation of p53 promotes transcription of genes involved in cell-cycle arrest, DNA repair, antioxidant defence, senescence, or apoptosis depending upon the severity of intracellular injury.

The MCF-7 breast cancer cell line retains wild-type TP53, allowing effective activation of p53-dependent checkpoint pathways following graphene oxide exposure. Oxidative stress generated by GO stimulates p53 stabilization, which subsequently induces expression of p21 (CDKN1A), a cyclin-dependent kinase inhibitor responsible for G1/S cell-cycle arrest.

Temporary arrest of the cell cycle provides MCF-7 cells with an opportunity to repair oxidative DNA damage before re-entering the proliferative cycle. Simultaneously, p53 regulates expression of numerous antioxidant enzymes that reduce intracellular ROS accumulation, thereby limiting oxidative injury.

Consequently, MCF-7 cells possess several protective mechanisms that delay progression toward irreversible cell death.

This molecular behaviour provides a biologically plausible explanation for the relatively high $IC_{50}$ values observed in the present investigation. The uploaded breast cancer discussion similarly attributes the greater resistance of MCF-7 cells to intact p53-dependent checkpoint control and p21-mediated survival responses.

In contrast, MDA-MB-231 cells harbour mutant TP53, resulting in profound impairment of normal checkpoint regulation.

Mutation of TP53 compromises several essential protective mechanisms.

These include:

- defective G1/S checkpoint activation,
- impaired DNA repair,
- reduced antioxidant regulation,

- altered apoptotic signalling,
- increased genomic instability.

Following graphene oxide exposure, oxidative DNA damage accumulates rapidly because mutant p53 cannot effectively coordinate repair processes. Instead of entering temporary cell-cycle arrest, MDA-MB-231 cells continue proliferating despite increasing molecular damage. This accumulation of unrepaired injury eventually exceeds the threshold compatible with cellular survival, resulting in rapid activation of apoptotic or secondary necrotic pathways.

The marked reduction in $IC_{50}$ values observed after 48 hours therefore reflects progressive accumulation of oxidative and metabolic damage in the absence of effective checkpoint regulation. This molecular explanation is entirely consistent with the significantly greater sensitivity observed experimentally.

### 3.5.2 Oxidative Stress Threshold Theory

The concept of an oxidative stress threshold provides another useful framework for interpreting the differential responses of the investigated cell lines.

Cancer cells generally maintain higher basal ROS levels than normal cells because of:

- accelerated glycolysis,
- mitochondrial dysfunction,
- oncogene activation,
- chronic inflammatory signalling,
- rapid proliferation.

Although increased antioxidant activity partially compensates for this elevated oxidative burden, malignant cells frequently operate near the upper limit of their oxidative tolerance.

Graphene oxide exploits this biological vulnerability.

Following cellular uptake, GO further increases intracellular ROS production through electron-transfer reactions occurring at oxidized and graphitic domains.

The resulting oxidative burden may remain below the tolerance threshold in resistant cells but exceed that threshold in susceptible phenotypes.

MCF-7 cells appear capable of maintaining redox homeostasis for longer periods owing to efficient antioxidant responses and intact p53 signalling.

Conversely, MDA-MB-231 cells possess diminished capacity to neutralize sustained oxidative stress, leading to rapid mitochondrial injury and loss of metabolic function.

A549 cells exhibit an intermediate phenotype.

Although these cells experience substantial oxidative injury following graphene oxide exposure, their response suggests partial preservation of adaptive antioxidant mechanisms, resulting in cytotoxicity that is intermediate between the two breast cancer models.

The oxidative stress threshold model therefore explains not only the observed $IC_{50}$ differences but also the progressively greater cytotoxicity observed after prolonged graphene oxide exposure.

### 3.5.3 Morphological Progression of Cytotoxic Injury

Phase-contrast microscopy provided direct visual confirmation of the biochemical events measured by the MTT assay.

At the beginning of treatment (0 hours), all three cell lines exhibited characteristic healthy morphology.

Cells displayed:

- intact plasma membranes,
- uniform cytoplasmic appearance,
- well-defined cellular boundaries,
- extensive substrate adherence,
- continuous epithelial monolayers.

Following 24 hours of graphene oxide exposure, subtle concentration-dependent alterations became evident.

Low concentrations produced only minor changes.

Intermediate and higher concentrations resulted in:

- reduced confluency,
- loss of intercellular junctions,
- cell rounding,
- cytoplasmic contraction,
- decreased adherence.

These observations indicate early disruption of cytoskeletal organization and membrane stability.

At 48 hours, morphological deterioration became substantially more pronounced.

Many cells demonstrated:

- membrane blebbing,
- extensive shrinkage,
- fragmented cytoplasm,
- floating detached cells,

- reduced cellular density,
- near-complete loss of epithelial architecture.

Among all investigated cell lines, MDA-MB-231 demonstrated the earliest onset and greatest severity of these structural alterations, whereas MCF-7 retained relatively greater morphological integrity under equivalent treatment conditions. A549 cells displayed progressive rounding, membrane irregularity, and detachment, consistent with an intermediate level of susceptibility. These qualitative findings closely parallel the quantitative viability data obtained from the MTT assay, reinforcing the conclusion that graphene oxide induces dose- and time-dependent cytotoxicity across all three models.

Importantly, the sequence of morphological changes observed in this study closely resembles the classical progression of apoptosis.

Initially, cells lose their characteristic flattened morphology.

Subsequently,

- cytoplasmic shrinkage occurs,
- membrane blebs develop,
- cellular adhesion decreases,
- apoptotic bodies begin forming,
- eventual detachment follows.

Although apoptosis-specific biochemical assays (for example, Annexin V staining, caspase activity assays, or TUNEL analysis) were not performed, the observed morphology strongly supports activation of programmed cell death pathways following graphene oxide exposure.

**3.5.4 Integrated Mechanistic Model of Graphene Oxide-Mediated Cytotoxicity**

The collective findings of this investigation support a sequential model of graphene oxide-induced anticancer activity that links material physicochemistry to cellular outcome.

The process begins with stable dispersion of graphene oxide in the biological medium, enabling extensive interaction between nanosheets and the plasma membrane. The large surface area and oxygen-containing functional groups facilitate membrane adhesion through electrostatic attraction, hydrogen bonding, and hydrophobic interactions.

Following adhesion, graphene oxide is internalized through endocytic pathways and accumulates within intracellular compartments. Electron-transfer reactions associated with residual graphitic domains and oxidized regions initiate excessive production of reactive oxygen species, producing sustained oxidative stress.

Persistent ROS generation damages membrane lipids, proteins, and DNA while simultaneously disrupting mitochondrial membrane potential. Loss of mitochondrial function reduces ATP

synthesis, impairs cellular metabolism, and promotes release of cytochrome *c*, leading to activation of the intrinsic apoptotic pathway.

The efficiency of this process is strongly influenced by tumour phenotype. Cells with functional checkpoint mechanisms, such as MCF-7, temporarily arrest proliferation and repair sublethal damage, thereby exhibiting greater resistance. In contrast, cells with defective checkpoint regulation, exemplified by MDA-MB-231, accumulate oxidative injury rapidly and progress toward apoptosis or secondary necrosis. A549 cells display an intermediate response reflecting their distinct molecular characteristics.

Thus, the biological activity of graphene oxide arises not from a single cytotoxic event but from a cascade of interconnected physicochemical and molecular processes. This integrated mechanism explains the observed concentration dependence, time dependence, and phenotype dependence of graphene oxide-mediated cytotoxicity.

**3.6 Translational Significance of the Present Findings**

The combined antimicrobial and anticancer investigations demonstrate that the biological activity of graphene oxide is intrinsically linked to its physicochemical characteristics rather than to conventional pharmacological mechanisms. From a translational perspective, this distinction is particularly important because it broadens the potential applications of GO beyond those of traditional antimicrobial agents or chemotherapeutic drugs.

The pronounced antibacterial activity observed against both Gram-positive and Gram-negative bacteria suggests that graphene oxide may serve as an effective component of infection-resistant biomaterials. Its ability to damage bacterial membranes through multiple complementary mechanisms reduces dependence on conventional antibiotics and may help address challenges associated with antimicrobial resistance.

Similarly, the selective cytotoxicity demonstrated against highly aggressive MDA-MB-231 triple-negative breast cancer cells highlights the potential of graphene oxide for targeting malignancies that lack effective molecularly targeted therapies. The greater susceptibility of triple-negative cells relative to luminal MCF-7 cells suggests that tumour-specific molecular characteristics influence therapeutic response and may ultimately enable more personalized applications of graphene oxide-based nanomedicine.

Beyond its intrinsic biological activity, graphene oxide also possesses exceptional potential as a multifunctional therapeutic platform. Its high surface area and abundant oxygen-containing functional groups permit conjugation of anticancer drugs, nucleic acids, peptides, antibodies, and imaging agents. Consequently, future graphene oxide-based systems could combine

targeted drug delivery, controlled release, molecular imaging, and intrinsic cytotoxic activity within a single nanoscale platform.

These findings therefore support continued investigation of graphene oxide not only as a biologically active nanomaterial but also as a versatile foundation for next-generation antimicrobial coatings, implantable biomaterials, tissue engineering scaffolds, and multifunctional cancer nanotherapeutics. [Gil G., et. al. 2014, Liu et al., 2021]

## 4. Conclusion and Future Perspectives

### 4.1 Conclusion

The present investigation provides a comprehensive evaluation of the antimicrobial and anticancer properties of graphene oxide, demonstrating that its biological activity is fundamentally governed by its physicochemical characteristics rather than by conventional pharmacological mechanisms. Through systematic integration of material characterization with biological evaluation, the study establishes a clear structure–activity relationship linking nanoscale architecture, surface chemistry, electronic heterogeneity, and dispersion behaviour to antimicrobial efficacy and selective cytotoxicity against cancer cells.

Comprehensive physicochemical characterization confirmed the successful synthesis of graphene oxide possessing large-area two-dimensional nanosheets with pronounced wrinkling, abundant oxygen-containing functional groups, residual $sp^2$-hybridized carbon domains, expanded interlayer spacing, and controlled structural integrity. These characteristics collectively transformed graphene oxide into a chemically active and biologically interactive nanoplatform capable of forming stable dispersions under physiological conditions and interacting efficiently with cellular membranes. The rationale for biological evaluation developed from these physicochemical observations provided the conceptual basis for interpreting the antimicrobial and anticancer findings obtained during the present study.

The antimicrobial investigations demonstrated that graphene oxide possesses reproducible broad-spectrum antibacterial activity against both Gram-positive and Gram-negative organisms. The greater susceptibility of *Staphylococcus aureus* and *Enterococcus faecalis* compared with *Escherichia coli* and *Pseudomonas aeruginosa* highlights the decisive influence of bacterial cell-envelope architecture on nanomaterial-mediated antibacterial activity. The absence of an outer membrane in Gram-positive bacteria permits more direct interaction between graphene oxide nanosheets and the cytoplasmic membrane, whereas the lipopolysaccharide-rich outer membrane of Gram-negative organisms provides an additional permeability barrier that reduces direct nanosheet access. The comparatively lower susceptibility of *Pseudomonas aeruginosa* further reflects the combined influence of low

membrane permeability, multidrug efflux systems, metabolic adaptability, and biofilm-forming capability. These findings reinforce the concept that the antimicrobial performance of graphene oxide arises through reciprocal interactions between nanomaterial physicochemistry and bacterial ultrastructure rather than through a single universal mechanism.

Mechanistically, the antibacterial activity observed in this study can be attributed to the synergistic action of four complementary pathways: (i) physical membrane disruption by atomically sharp graphene oxide edges, (ii) oxidative damage mediated by reactive oxygen species, (iii) extraction of membrane phospholipids leading to destabilization of lipid bilayers, and (iv) physical wrapping and isolation of bacterial cells by flexible two-dimensional nanosheets. Rather than acting independently, these mechanisms reinforce one another, producing cumulative membrane injury, metabolic dysfunction, and irreversible loss of bacterial viability. Such multifactorial behaviour distinguishes graphene oxide from conventional antibiotics and suggests that it may offer a reduced propensity for the rapid emergence of resistance, although this hypothesis requires further investigation in long-term experimental models.

The anticancer investigations likewise demonstrated that graphene oxide exhibits substantial concentration-dependent and time-dependent antiproliferative activity against all investigated cancer cell lines. However, the magnitude of cytotoxicity varied considerably according to tumour phenotype. The triple-negative breast cancer cell line MDA-MB-231 displayed the greatest sensitivity, with $IC_{50}$ values decreasing from 219.44 μg/mL after 24 hours to 105.40 μg/mL after 48 hours, whereas the luminal A MCF-7 cell line exhibited markedly greater resistance, with corresponding $IC_{50}$ values of 1578.34 μg/mL and 306.70 μg/mL. A549 human lung adenocarcinoma cells demonstrated an intermediate response characterized by progressive reductions in viability and pronounced morphological alterations following prolonged graphene oxide exposure.

The observed phenotype-dependent cytotoxicity emphasizes the importance of tumour molecular biology in determining the response to graphene oxide. The comparatively greater resistance of MCF-7 cells is consistent with preservation of wild-type p53 signalling and p21-mediated cell-cycle arrest, which permit temporary growth inhibition and repair of oxidative damage. Conversely, the enhanced sensitivity of MDA-MB-231 cells is compatible with mutant p53 status, impaired checkpoint regulation, and reduced capacity to repair cumulative oxidative injury, resulting in accelerated progression toward apoptosis or secondary necrosis. The intermediate response observed in A549 cells further demonstrates that graphene oxide-

mediated cytotoxicity is modulated by tumour-specific molecular characteristics rather than by tissue origin alone.

Phase-contrast microscopy provided important qualitative confirmation of the biochemical findings obtained from the MTT assay. Progressive morphological deterioration—including cell rounding, cytoplasmic shrinkage, membrane blebbing, loss of adherence, reduced confluency, and cellular detachment—closely paralleled reductions in metabolic activity, supporting the conclusion that graphene oxide induces sustained cellular stress leading to programmed cell death. Together, the MTT assay and microscopic observations indicate that graphene oxide exerts its cytotoxic effects through progressive membrane perturbation, oxidative stress, mitochondrial dysfunction, metabolic collapse, and activation of intrinsic apoptotic pathways.

Collectively, the findings of the present investigation establish that the biological activity of graphene oxide is not an incidental consequence of carbon nanomaterials but is an intrinsic manifestation of its structural and chemical organization. The large lateral dimensions, defect-rich carbon lattice, oxygen-containing functional groups, and heterogeneous electronic structure function cooperatively to produce multifunctional biological responses across both microbial and mammalian systems. By integrating physicochemical characterization with biological evaluation, this study provides a comprehensive framework for understanding how material properties govern biological performance and thereby contributes to the broader field of structure–activity relationships in nanomedicine.

**4.2 Key Findings**

Graphene oxide demonstrated broad-spectrum antibacterial activity against all bacterial species examined, although susceptibility varied according to bacterial cell envelope architecture. Gram-positive bacteria exhibited greater inhibition than Gram-negative organisms, consistent with the absence of an outer lipopolysaccharide membrane that otherwise restricts direct contact between graphene oxide nanosheets and the bacterial cytoplasmic membrane. Among Gram-negative bacteria, *Pseudomonas aeruginosa* displayed the greatest resistance, attributable to its highly impermeable outer membrane, multidrug efflux systems, and biofilm-forming capability.

Graphene oxide also exhibited pronounced concentration- and time-dependent antiproliferative activity against all three cancer cell lines. Triple-negative MDA-MB-231 breast cancer cells displayed the greatest sensitivity, with $IC_{50}$ values decreasing from approximately 219.44 µg/mL after 24 hours to 105.40 µg/mL following 48 hours of treatment. In comparison, luminal A MCF-7 cells demonstrated substantially greater resistance, with $IC_{50}$ values of approximately

1578.34 μg/mL at 24 hours and 306.70 μg/mL at 48 hours. A549 lung adenocarcinoma cells exhibited intermediate susceptibility, demonstrating progressive reductions in cell viability with increasing concentration and exposure duration. Morphological examination further confirmed characteristic features of cytotoxic injury, including cellular shrinkage, membrane blebbing, rounding, reduced cellular adherence, and extensive detachment from culture surfaces following prolonged graphene oxide exposure.

**4.3 Mechanistic Insights**

The biological activity of graphene oxide originates from the synergistic interaction of its structural and chemical attributes. Its atomically thin, defect-rich nanosheets facilitate intimate physical contact with cellular membranes, while abundant hydroxyl, epoxy, carbonyl, and carboxyl functionalities promote electrostatic interactions and stable dispersion under physiological conditions. Antibacterial activity is mediated through multiple complementary mechanisms, including physical membrane disruption by sharp sheet edges, oxidative damage induced by reactive oxygen species, extraction of membrane phospholipids, and physical isolation of bacterial cells by graphene oxide sheets. Anticancer activity involves mitochondrial dysfunction, intracellular oxidative stress, disruption of cellular redox homeostasis, impairment of metabolic activity, activation of intrinsic apoptotic pathways, and progressive loss of membrane integrity. Differential sensitivity among cancer cell lines appears closely associated with molecular heterogeneity, particularly differences in p53 status, cell-cycle regulation, metabolic adaptation, and oxidative stress tolerance.

**4.4 Translational Significance**

The translational implications of the present findings extend well beyond the experimental systems investigated. The demonstrated antimicrobial activity of graphene oxide supports its development as a functional component of next-generation infection-control technologies. Incorporation of GO into wound dressings, surgical meshes, implant coatings, catheter surfaces, dental materials, biosensors, and antimicrobial packaging may provide localized protection against bacterial colonization while reducing dependence on conventional antibiotics. The multi-mechanistic mode of antibacterial action is particularly attractive for applications where prolonged exposure to microorganisms creates a high risk of resistance development. The findings establish graphene oxide as a multifunctional nanomaterial possessing substantial promise for biomedical applications extending beyond conventional antimicrobial and anticancer therapies. Its broad-spectrum antibacterial efficacy, combined with selective cytotoxicity toward malignant cells, supports continued investigation into graphene oxide-based wound dressings, antimicrobial implant coatings, drug-delivery systems,

biosensors, tissue engineering scaffolds, and multifunctional cancer therapeutics. Future studies should prioritize systematic structure–activity mapping, targeted functionalization strategies, pharmacokinetic characterization, and comprehensive in vivo safety profiling to facilitate clinical translation while minimizing off-target toxicity.

The intrinsic anticancer activity of graphene oxide offers considerable promise for the development of multifunctional nanotherapeutic platforms. Because graphene oxide possesses abundant oxygen-containing functional groups and an exceptionally large specific surface area, it can simultaneously serve as a drug carrier, molecular imaging platform, photothermal agent, and biologically active therapeutic material. Conjugation of graphene oxide with chemotherapeutic drugs, antibodies, peptides, nucleic acids, or tumour-targeting ligands could potentially enhance therapeutic selectivity while reducing systemic toxicity. The enhanced sensitivity observed in triple-negative breast cancer cells is particularly encouraging given the limited targeted treatment options currently available for this aggressive breast cancer subtype. [Ajay J. et. al. 2023] The dual antimicrobial and anticancer activities demonstrated in the present investigation also suggest opportunities for multifunctional biomedical devices. For example, graphene oxide-coated implants could simultaneously resist bacterial colonization while reducing the risk of tumour recurrence following surgical excision of malignant tissues. Similarly, graphene oxide-containing tissue engineering scaffolds may combine regenerative capacity with antimicrobial protection and localized anticancer activity in selected clinical settings.

**4.5 Limitations of the Present Study**

Despite the promising findings obtained in the present investigation, several limitations should be acknowledged.

First, the biological evaluation was performed exclusively under in vitro conditions. Although cultured bacterial and mammalian cells provide valuable mechanistic insight, they cannot fully reproduce the complexity of living organisms, where immune responses, protein corona formation, vascular transport, extracellular matrix interactions, and organ-specific biodistribution significantly influence nanomaterial behaviour.

Second, the mechanisms proposed in the present discussion are inferred primarily from physicochemical characterization, cell viability assays, and morphological observations. Direct confirmation of specific molecular pathways would require complementary investigations involving reactive oxygen species quantification, mitochondrial membrane potential analysis, flow cytometric apoptosis assays, caspase activation studies, Western blotting of signalling proteins, transcriptomic analysis, and high-resolution intracellular imaging.

Third, only a limited number of bacterial strains and cancer cell lines were examined. Although the selected models represent clinically important pathogens and tumour phenotypes, broader evaluation across additional microbial species, multidrug-resistant clinical isolates, patient-derived tumour models, and normal human cells would strengthen conclusions regarding biological selectivity and therapeutic applicability.

Finally, the physicochemical properties of graphene oxide—including lateral sheet size, oxidation degree, defect density, and surface functionalization—are known to influence biological responses substantially. Systematic variation of these parameters would facilitate more precise identification of the material characteristics responsible for optimal antimicrobial efficacy and selective anticancer activity.

**4.6 Future Perspectives**

Future research should focus on establishing quantitative structure–activity relationships that directly correlate individual physicochemical parameters with biological outcomes. Such investigations should include systematic variation of nanosheet dimensions, oxygen-to-carbon ratio, oxidation level, surface charge, colloidal stability, and defect density to identify the optimal physicochemical profile for biomedical applications.

Mechanistic investigations should be expanded through comprehensive molecular analyses involving oxidative stress biomarkers, mitochondrial bioenergetics, apoptosis signalling networks, autophagy pathways, DNA damage responses, transcriptomics, proteomics, and metabolomics. Integration of these approaches will provide a more complete understanding of graphene oxide-mediated cellular responses and facilitate rational optimization of nanomaterial design.

The development of surface-functionalized graphene oxide represents another important research direction. Covalent or non-covalent attachment of polymers, peptides, antibodies, aptamers, or tumour-specific ligands may enhance biocompatibility, improve target specificity, and reduce off-target toxicity while preserving the intrinsic biological activity of graphene oxide. Such multifunctional systems may ultimately combine targeted drug delivery, molecular imaging, photothermal therapy, gene delivery, and intrinsic cytotoxicity within a single nanoplatform.

Translation toward clinical application will require comprehensive in vivo evaluation using appropriate animal models. Future studies should examine pharmacokinetics, biodistribution, biodegradation, long-term toxicity, immunogenicity, reproductive safety, and environmental impact. Particular attention should be directed toward understanding the interactions of

graphene oxide with blood components, immune cells, and major organs following systemic administration.

Standardization of graphene oxide synthesis, purification, characterization, and biological testing protocols will be essential for improving reproducibility across laboratories and facilitating regulatory approval. Establishment of internationally accepted guidelines for graphene-based nanomaterials will greatly accelerate their progression from laboratory research to clinical practice.

## 5. Final Statement

In conclusion, this investigation demonstrates that graphene oxide represents a highly versatile two-dimensional nanomaterial whose antimicrobial and anticancer activities are direct consequences of its structural architecture and surface chemistry. Through the integration of physicochemical characterization with systematic biological evaluation, the present study establishes a coherent structure–activity framework that advances understanding of graphene oxide–mediated nano–bio interactions. These findings support continued exploration of graphene oxide as a multifunctional platform for antimicrobial technologies, infection-resistant biomaterials, and next-generation cancer nanomedicine, while emphasizing the necessity of rigorous mechanistic studies and comprehensive in vivo safety assessment before clinical translation.

**Funding Declaration:** There is no funding provided for this research

**Clinical trial number:** Not Applicable

**'Ethics, Consent to Participate, and Consent to Publish declarations:** Not Applicable

## 6. References:

1. Adéla Jiříčková, Ondřej Jank ovský, Zdeněk Sofer, and David Sedmidubský, 2022; 'Synthesis and Applications of Graphene Oxide', *Journal of MDPI*, *15*(3), pp. 920; https://doi.org/10.3390/ma15030920.
2. David López-Díaz, M. Dolores Merchan, M. Mercedes Velázquez, *and Armando Maestro*, 2020; 'Understanding the Role of Oxidative Debris on the Structure of Graphene Oxide Films at the Air−Water Interface: A Neutron Reflectivity Study', *Journal of ACS Applied Materials & Interfaces*,12 (22), 25453-25463, doi: https://doi.org/10.1021/acsami.0c05649.
3. Tais Monteiro Magne,Thamires de Oliveira Vieira,Luciana Magalhães Rebelo Alencr, Francisco Franciné Maia Junior, Sara Gemini-Piperni, Samuel V. Carneiro, Lillian M. U. D. Fechine, Rafael M. Freire, Kirill Golokhvast, Pierangelo Metrangolo,

Pierre B. A. Fechine, Ralph Santos-Oliveira, 2021; 'Graphene and its derivatives: understanding the main chemical and medicinal chemistry roles for biomedical applications,' *Journal of Nano struct* Chem 12, 693-727,doi: https://doi.org/10.1007/s40097-021-00444-3.

4. Zare, P.; Alee Mardani, M.; Seifalian, A.; Bagher, Z.; Seifalian, A.M., 2021; 'Graphene Oxide: Opportunities and Challenges in Biomedicine', Journal of Nanomaterials, 11(5): 1083, doi: https://doi.org/10.3390/nano11051083.
5. Geim, A. K., & Novoselov, K. S., 2007; 'The rise of graphene', *Journal of Nature Materials*, 6(3):183-191, doi: https://doi.org/10.1038/nmat1849.
6. Hummers, W. S., & Offeman, R. E., 1958; 'Preparation of graphitic oxide', *Journal of J. Am. Chem. Soc.*, 80(6):1339, doi: https://doi.org/10.1021/ja01539a017.
7. Gostaviceanu, A.; Gavrilas, S.; Copolovici, L.; Copolovici, D.M., 2024; 'Graphene-Oxide Peptide-Containing Materials for Biomedical Applications', *International Journal of Molecular Sciences*, 25(18):10174, doi: https://doi.org/10.3390/ijms251810174.
8. Oliveira, A.M.L.; Machado, M.; Silva, G.A.; Bitoque, D.B.; Tavares Ferreira, J.; Pinto, L.A.; Ferreira, Q., 2022; 'Graphene Oxide Thin Films with Drug Delivery Function', Journal *of Nanomaterials*, 12:1149, doi: https://doi.org/10.3390/nano12071149.
9. Grilli, Francesca, Gohari, Parisa Hajimohammadi, and Zou, Shan, 2022; 'Characteristics of Graphene Oxide for Gene Transfection and Controlled Release in Breast Cancer Cells', *International Journal of Molecular Sciences,* 23(12): 6802, doi: https://doi.org/10.3390/ijms23126802.
10. Kian Ping Loh, Qiaoliang Bao; Priscilla Kailian Ang, Jiaxiang Yang, 2010; 'The chemistry of graphene', *Journal of J. Mater. Chem.*, 20(12):2277-2289, doi: https://doi.org/10.1039/b920539j.
11. Armano, A.; Agnello, S., 2019; 'Two-Dimensional Carbon: A Review of Synthesis Methods, and Electronic, Optical, and Vibrational Properties of Single-Layer Graphene', J*ournal of Carbon Research* 5: 67, doi: https://doi.org/10.3390/c5040067
12. Daniela C. Marcano[†], Dmitry V. Kosynkin[†], Jacob M. Berlin, Alexander Sinitskii, Zhengzong Sun, Alexander Slesarev, Lawrence B. Alemany, Wei Lu, James M. Tour[*], 2010; 'Improved synthesis of graphene oxide', *Journal of ACS Nano*, 4(8), 4806-4814, doi: https://doi.org/10.1021/nn1006368.

13. Sali, S.; Mackey, H.R.; Abdala, A.A., 2019; 'Effect of Graphene Oxide Synthesis Method on Properties and Performance of Poly Sulfone-Graphene Oxide Mixed Matrix Membranes', *Journal of Nanomaterials*, *9:* 769, doi: https://doi.org/10.3390/nano9050769.
14. Tadyszak, K.; WY Chowaniec, J.K.; Litowczenko, J., 2018; 'Biomedical Applications of Graphene-Based Structures', *Journal of Nanomaterials*, *8:* 944, doi: https://doi.org/10.3390/nano8110944.
15. Vejpravová, J., 2021; 'Mixed $sp^2$–$sp^3$ Nanocarbon Materials: A Status Quo Review', *Journal of Nanomaterials*, *11*:2469, doi: https://doi.org/10.3390/nano11102469.
16. Mohammad Rezaei D, Golzar H, Rezai Rad M, Omidi M, Rashedi H, Yazdian F, Khojasteh A, Tayebi L., 2018; '*In vitro* effect of graphene structures as an osteo inductive factor in bone tissue engineering: A systematic review', *J Biomed Mater Res Part A*, 106A: 2284–2343, doi: https://doi.org/10.1002/jbm.a.36422.
17. Paredes, J. I., S. Villar-Rodil, P. Solís-Fernández, A. Martínez-Alonso, J. M. D. Tascón, 2009; 'Atomic force and scanning tunneling microscopy imaging of graphene sheets exfoliated from graphite oxide', *Journal of Langmuir*, 25(10): 5957-5968, doi: https://doi.org/10.1021/la804216z.
18. J. I. Paredes*, S. Villar-Rodil, A. Martínez-Alonso. J. M. D. Tascón, 2008; 'Graphene Oxide Dispersions in Organic Solvents', *Journal of Langmuir*, 24(19): 10560-10564, doi: https://doi.org/10.1021/la801744a.
19. San, H.; Paresoglou, M.; Minne boo, M.; van Hengel, I.A.J.; Yilmaz, A.; Gonzalez-Garcia, Y.; Fluit, A.C.; Hagedoorn, P.-L.; Fratila-Apachitei, L.E.; Apachitei, I.; et al., 2022; 'Fighting Antibiotic-Resistant Bacterial Infections by Surface Biofunctionalization of 3D-Printed Porous Titanium Implants with Reduced Graphene Oxide and Silver Nanoparticles', *Int. J. Mol. Sci.*, *23:* 9204, doi: https://doi.org/10.3390/ijms23169204.
20. Sasha Stankovich, Dmitriy A. Dikin, Richard D. Piner, Kevin A. Kohlhaas, Alfred Kleinhammes, Yuanyuan Jia, Yue Wu, Son Binh T. Nguyen, Rodney S. Ruoff, 2007; 'Synthesis of graphene-based nanosheets via chemical reduction of exfoliated graphite oxide', *Journal of Carbon*, 45(7):1558-1565, doi: https://doi.org/ 10.1016/j.carbon.2007.02.034.

21. Anton Lerf,Heyong He,Michael Forster,Jacek Klinowski,1998; 'Structure of graphite oxide revisited', *Journal of Physical Chemistry B*, 102(23):4477-4482, doi: https://doi.org/10.1021/jp9731821.
22. D'Amora, U.; Dacrory, S.; Hasanin, M.S.; Longo, A.; Soriente, A.; Kamel, S.; Raucci, M.G.; Ambrosio, L.; Scialla, S., 2023; 'Advances in the Physico-Chemical, Antimicrobial and Angiogenic Properties of Graphene-Oxide/Cellulose Nanocomposites for Wound Healing', *Journal of Pharmaceutics*, *15:* 338, doi: https://doi.org/10.3390/pharmaceutics15020338.
23. Anastasiadis, S.H.; Chrissopoulou, K.; Stratakis, E.; Kavatzikidou, P.; Kak Lamani, G.; Ranella, A., 2022; 'How the Physicochemical Properties of Manufactured Nanomaterials Affect Their Performance in Dispersion and Their Applications in Biomedicine: A Review', *Journal of Nanomaterials,* 12*:* 552, doi: https://doi.org/10.3390/nano12030552.
24. Gorohovs, M.; Dekhtyar, Y., 2025; 'Surface Functionalization of Nanoparticles for Enhanced Electrostatic Adsorption of Biomolecules', *Journal of Molecules*, 30(15): 3206, doi: https://doi.org/10.3390/molecules30153206.
25. Shabnam Sattari, Mohsen Adeli, Siamak Beyranvand, Mohammad Nemati; 2021; 'Functionalized Graphene Platforms for Anticancer Drug Delivery', *International Journal of Nanomedicine,* 16:5955-5980, doi: https://doi.org/10.2147/IJN.S249712.
26. Kim, C.; Lee, J.; Wang, W.; Fortner, J.,2020; 'Organic Functionalized Graphene Oxide Behaviour in Water', *Journal of Nanomaterials*, *10:* 1228, doi: https://doi.org/10.3390/nano10061228.
27. Luceño-Sánchez, J.A.; Maties, G.; Gonzalez-Arellano, C.; Diez-Pascual, A.M., 2018; 'Synthesis and Characterization of Graphene Oxide Derivatives via Functionalization Reaction with Hexamethylene Diisocyanate', *Journal of Nanomaterials*, *8:* 870, doi: https://doi.org/10.3390/nano8110870.
28. Ximena Jaramillo-Fierro 1, * and Guisella Cuenca 2, 2024; 'Theoretical and Experimental Analysis of Hydroxyl and Epoxy Group Effects on Graphene Oxide Properties', *Journal of Nanomaterials,* 14:714, doi: https://doi.org/10.3390/nano14080714.
29. Gurunathan, S.; Kang, M.-H.; Jeyaraj, M.; Kim, J.-H., 2019; 'Differential Immunomodulatory Effect of Graphene Oxide and Vanillin-Functionalized Graphene

Oxide Nanoparticles in Human Acute Monocytic Leukaemia Cell Line (THP-1)', *Int. J. Mol. Sci.*, 20*:* 247, doi: https://doi.org/10.3390/ijms20020247.

30. Shiva Shahriari 1 Murali Sastry2 Santosh Panjikar3,4 RK Singh Raman1, 2021; 'Graphene and Graphene Oxide as a Support for Biomolecules in the Development of Biosensors', *Journal of Nanotechnology, Science and Applications,* 14:197-200, doi: https://doi.org/10.2147/NSA.S334487.
31. Choi, Y.-J.; Gurunathan, S.; Kim, J.-H., 2018; 'Graphene Oxide–Silver Nanocomposite Enhances Cytotoxic and Apoptotic Potential of Salinomycin in Human Ovarian Cancer Stem Cells (OvCSCs): A Novel Approach for Cancer Therapy', *Int. J. Mol. Sci.*, *19*: 710, doi: https://doi.org/10.3390/ijms19030710.
32. Shaobin Liu[†],Tingying Helen Zeng[‡],Mario Hofmann[§],Ehdi Burcombe[§],Jun Wei,Rongrong Jiang[†],Jing Kong[‡§],Yuan Chen[†],2011; 'Antibacterial activity of graphite, graphite oxide, graphene oxide, and reduced graphene oxide: Membrane and oxidative stress', *Journal of ACS Nano*, 5(9):6971-6980, doi: https://doi.org/10.1021/nn202451x.
33. Ng, I.M.J.; Shamsi, S., 2022; 'Graphene Oxide (GO): A Promising Nanomaterial against Infectious Diseases Caused by Multidrug-Resistant Bacteria', *Int. J. Mol. Sci.*, *23*:9096, doi: https://doi.org/10.3390/ijms23169096.
34. François Perreault, Andreia Fonseca de Faria, Siamak Nejati, Menachem Elimelech[*], 2015; 'Antimicrobial properties of graphene oxide nanosheets: Why size matters', *Journal of ACS Nano*, 9(7):7226-7236, doi: https://doi.org/10.1021/acsnano.5b02067.
35. Vi, T.T.T.; Kumar, S.R.; Pang, J.-H.S.; Liu, Y.-K.; Chen, D.W.; Lue, S.J., 2020; 'Synergistic Antibacterial Activity of Silver-Loaded Graphene Oxide towards *Staphylococcus Aureus* and *Escherichia Coli*.', *Journal of Nanomaterials*, 10: 366, doi: https://doi.org/10.3390/nano10020366.
36. Mauricio D. Rojas-Andrade, Gustavo Chata, Dara Rouholiman , Junli Liu, Chad Saltikov Corresponding Author ,Shaowei Chen, 2017; 'Antibacterial mechanisms of graphene-based composite nanomaterials', *Journal of Nanoscale, 9 (3): 994–1006*, doi: https://doi.org/10.1039/c6nr08733g.
37. Umar, M.F.; Ahmad, F.; Saeed, H.; Usmani, S.A.; Owais, M.; Rafat Ullah, M., 2020; 'Bio-Mediated Synthesis of Reduced Graphene Oxide Nanoparticles from *Chenopodium album*: Their Antimicrobial and Anticancer Activities', *Journal of Nanomaterials*, 10: 1096, doi: https://doi.org/10.3390/nano10061096.

38. Yaragalla, S.; Bhavitha, K.B.; Athanassiou, A., 2021; 'A Review on Graphene Based Materials and Their Antimicrobial Properties', *Journal of Coatings*, 11: 1197, doi: https://doi.org/10.3390/coatings11101197.

39. Krasteva, Natalia, Keremidarska-Markova, Milena, Hristova-Panusheva, Kamelia, Andreeva, Tonya, Speranza, Giorgio, Wang, Dayong, Draganova-Filipova, Milena, Miloshev, George, Georgieva, Milena, 2019; 'Aminated Graphene Oxide as a Potential New Therapy for Colorectal Cancer', *Journal of Oxidative Medicine and Cellular Longevity*, 1(15):3738980, doi: https://doi.org/10.1155/2019/3738980.

40. Jarosz, Anna, Skoda, Marta, Dudek, Ilona, Szukiewicz, Dariusz,2016; 'Oxidative Stress and Mitochondrial Activation as the Main Mechanisms Underlying Graphene Toxicity against Human Cancer Cells', *Journal of Oxidative Medicine and Cellular Longevity*, 14:5851035, doi: https://doi.org/10.1155/2016/5851035 .

41. Krętowski, R.; Cechowska-Pasko, M., 2022; 'The Reduced Graphene Oxide (rGO) Induces Apoptosis, Autophagy and Cell Cycle Arrest in Breast Cancer Cells', *Int. J. Mol. Sci.*, 23: 9285, doi: https://doi.org/10.3390/ijms23169285.

42. Amedea B. Seabra[†], Amauri J. Paula[‡§], Renata de Lima[∥⊥], Oswaldo L. Alves[#], Nelson Durán[*‡▽], 2014; 'Nanotoxicity of Graphene and Graphene Oxide', *Journal of Chem. Res. Toxicol.* 27(2): 159–168, doi: https://doi.org/10.1021/tx400385x.

43. Jing Wu ,Rui Yang, Lei Zhang, Zhijuan Fan & Shuye Liu, 2015; 'Cytotoxicity effect of graphene oxide on human MDA-MB-231 cells', *Journal of Toxicology Mechanisms and Methods,* 25(4):312-319, https://doi.org/10.3109/15376516.2015.1031415.

44. Tanveer A Tabish, Md Zahidul I Pranjol, Hasan Hayat, Alma A M Rahat, Trefa M Abdullah, Jacqueline L Whatmore and Shaowei Zhang, 2017; '*In vitro* toxic effects of reduced graphene oxide nanosheets on lung cancer cells', *Journal of Nanotechnology*, 28 : 504001, doi: https://doi.org/ 10.1088/1361-6528/aa95a8.

45. Ruomin Liao[a] · Yi Zhang[b] · Wenwei Mao[c] , 2024; 'Functionalized graphene oxide NPs as a nanocarrier for drug delivery system in quercetin/ lurbinectedin as dual sensitive therapeutics for A549 lung cancer treatment', *Journal of Research article (Heliyon),* 10(11): e31212, doi: https://doi.org/10.1016/j.heliyon.2024.e31212.

46. Anna Jarosz, Marta Skoda, Ilona Dudek, Dariusz Szukiewicz, 2015; 'Oxidative Stress and Mitochondrial Activation as the Main Mechanisms Underlying Graphene Toxicity

against Human Cancer Cells', *Journal of* Oxidative Medicine and Cellular Longevity, 2016(5851035) : 14, doi: http://dx.doi.org/10.1155/2016/5851035.

47. Khan, M., Khan, M., Al-Marri, A. H., Al-Warthan, A., Alkhathlan, H. Z., Siddiqui, M. R. H., … Adil, S. F., 2016; 'Apoptosis inducing ability of silver decorated highly reduced graphene oxide nanocomposites in A549 lung cancer', *International Journal of Nanomedicine*, *11*: 873–883, doi: https://doi.org/10.2147/IJN.S100903.
48. Shih-Ming Tsai, Preeti Bangalore, Eric Y Chen, David Lu, Meng-Hsuen Chiu, Andrew Suh, Matthew Gehring, John P. Cangco, Santiago G. Garcia & Wei-Chun Chin, 2017; 'Graphene-induced apoptosis in lung epithelial cells through EGFR', *Journal of J Nano part Res,* 19: 262, doi: https://doi.org/10.1007/s11051-017-3957-9.
49. Sandeep Mittal, Veeresh Kumar, Nitesh Dhiman, Lalit Kumar Singh Chauhan, Renu Pasricha & Alok Kumar Pandey ,2016; 'Physico-chemical properties based differential toxicity of graphene oxide/reduced graphene oxide in human lung cells mediated through oxidative stress', *Journal of Sci Rep,* 6: 39548, doi: https://doi.org/10.1038/srep39548.
50. Neha Arya, an Aditya Arora, a K. S. Vasu, b A. K. Soodb and Dhirendra S. Katti*a, 2013; 'Combination of single walled carbon nanotubes/graphene oxide with paclitaxel: a reactive oxygen species mediated synergism for treatment of lung cancer†', *Journal of The Royal Society of Chemistry*, doi: http://pubs.rsc.org | doi:10.1039/C3NR33190C.
51. Fengxia Chen [a], Hongmei Zhang [b], Ling Jiang [a], Wei Wei [a], Chunchun Liu [a], Shundon g Cang [a], 2019; 'Enhancing the cytotoxic efficacy of combined effect of doxorubicin and Cyclosporin encapsulated photoluminescent graphene dotted mesoporous nanoparticles against lung cancer cell-specific drug targeting for the nursing care of cancer patients', *Journal of Photochemistry and Photobiology B: Biology,* 198:111578, doi: https://doi.org/10.1016/j.jphotobiol.2019.111578.
52. Aggarwal, V.; Tuli, H.S.; Varol, A.; Thakral, F.; Yerer, M.B.; Sak, K.; Varol, M.; Jain, A.; Khan, M.A.; Sethi, G., 2019; 'Role of Reactive Oxygen Species in Cancer Progression: Molecular Mechanisms and Recent Advancements', *Journal of Biomolecules*, *9 (11):* 735, doi: https://doi.org/10.3390/biom9110735.
53. Hany E. Marei, Asmaa Althani, Nahla Afifi, Anwarul Hasan, Thomas Caceci, Giacomo Pozzoli, Andrea Morrione, Antonio Giordano & Carlo Cenciarelli , 2021; 'p53 signaling in cancer progression and therapy', *Journal of Cancer Cell Int,* 21: 703, doi: https://doi.org/10.1186/s12935-021-02396-8.

54. Haolan Wang, Ming Guo, Hudie Wei & Yongheng Chen, 2023; 'Targeting p53 pathways: mechanisms, structures and advances in therapy', *Journal of Sig Trans duct Target Ther* ,8: 92, doi: https://doi.org/10.1038/s41392-023-01347-1.

55. Weiyu Feng, Jinbang Wang, Baodong Li, Yonggang Liu, Dongli Xu, Ke Cheng, Jing Zhuang, 2022; 'Graphene oxide leads to mitochondrial-dependent apoptosis by activating ROS-p53-mPTP pathway in intestinal cells', *The International Journal of Biochemistry & Cell Biology,* 146,doi: https://doi.org/10.1016/j.biocel.2022.106206.

56. Yi, L., Zhang, Y., Shi, X., Du, X., Wang, X., Yu, A., & Zhai, G., 2019; 'Recent progress of functionalised graphene oxide in cancer therapy', *Journal of Drug Targeting*, *27*(2):125–144, doi: https://doi.org/10.1080/1061186X.2018.1474359.

57. Liu CC, Zhao JJ, Zhang R, Li H, Chen B, Zhang LL, Yang H., 2017; 'Multi functionalization of graphene and graphene oxide for controlled release and targeted delivery of anticancer drugs, Am J Transl Res., 9(12):5197-5219. PMID: 29312477; PMCID: PMC5752875.

58. Alfredo Cruz-Gregorio, 2026; 'Mitochondrial Redox Vulnerabilities in Triple-Negative Breast Cancer: Integrative Perspectives and Emerging Therapeutic Strategies', *Journal of Metabolites, 16(1):60, doi: https://doi.org/10.3390/metabo16010060.*

59. Syed K Sohaebuddin, Paul T Thevenot, David Baker, John W Eaton & Liping Tang, 2010; 'Nanomaterial cytotoxicity is composition, size, and cell type dependent', *Journal of Particle and Fibre Toxicology*, 7:22, doi: https://doi.org/10.1186/1743-8977-7-22.

60. Singh, S., Singh, T.G.,2021; 'Emerging perspectives on mitochondrial dysfunctioning and inflammation in epileptogenesis', *Journal of Inflamm. Res.,* 70: 1027–1042, doi: https://doi.org/10.1007/s00011-021-01511-9.

61. Amedea B. Seabra[†], Amauri J. Paula[‡§], Renata de Lima[∥⊥], Oswaldo L. Alves[#], Nelson Durán[*‡▽] 2014; 'Nanotoxicity of Graphene and Graphene Oxide', *Journal of Chem. Res. Toxicol.*, 27( 2): 159–168, doi: https://doi.org/10.1021/tx400385x.

62. Kai Yang[†], Shuai Zhang[†], Guoxin Zhang[‡], Xiaoming Sun[‡], Shuit-Tong Lee[§], Zhuang Liu[*†,] ,2010; 'Graphene in Mice: Ultrahigh In Vivo Tumor Uptake and Efficient Photothermal Therapy', *Journal of Nano Lett.,* 10(9): 3318–3323, doi: https://doi.org/10.1021/nl100996u.

63. Vimalanathan, B.; Vijaya, J.J.; Mary, B.C.J.; Mary, R.N.; Km, M.; Jayavel, R.; Abu Mousa, R.A.; Bououdina, M., 2023; 'The Cytotoxic Effectiveness of Thiourea-Reduced Graphene Oxide on Human Lung Cancer Cells and Fungi', *Journal of Nanomaterials*, 13(1): 149, doi: https://doi.org/10.3390/nano13010149.

64. Giacomo Biagiotti, Annalisa Salvatore, Gianluca Toniolo, Lucrezia Caselli, Maura Di Vito, Margherita Cacaci, Luca Contiero, Tommaso Gori, Michele Maggini, Maurizio Sanguinetti, Debora Berti, Francesca Bugli, Barbara Richichi, Stefano Cicchi, 2021; 'Metal-Free Antibacterial Additives Based on Graphene Materials and Salicylic Acid: From the Bench to Fabric Applications', *Journal of ACS Appl. Mater. Interfaces,* 13 (22): 26288–26298. https://doi.org/10.1021/acsami.1c02330.

65. Olczak, K.; Jakubowski, W.; Szymański, W., 2023; 'Bactericidal Activity of Graphene Oxide Tests for Selected Microorganisms', *Journal of Materials*, *16*(11):4199, doi: https://doi.org/10.3390/ma16114199.

66. Jastrzębska, A.M., Kurtycz, P. & Olszyna, A.R., 2012; 'Recent advances in graphene family materials toxicity investigations', *J Nanopart Res,* 14: 1320, doi: https://doi.org/10.1007/s11051-012-1320-8.

67. Ma, Y., Shen, H., Tu, X., & Zhang, Z., 2014; 'Assessing *In Vivo* Toxicity of Graphene Materials: Current Methods and Future Outlook', *Journal of Nanomedicine*, *9*(10):1565–1580, doi: https://doi.org/10.2217/nnm.14.68.

68. Singh, Z., 2016; 'Applications and toxicity of graphene family nanomaterials and their composites', *Journal of Nanotechnology, Science and Applications*, *9*: 15–28, doi: https://doi.org/10.2147/NSA.S101818.

69. Ajay Jose, Marija Gizdavic-Nikolaidis and Simon Swift, 2023; 'Antimicrobial Coatings: Reviewing Options for Healthcare Applications', *Journal of Appl. Microbiol.*, *3*(1): 145-174, doi: https://doi.org/10.3390/applmicrobiol3010012.

70. Ashraf, Anila, Altaf, Muhammad, Abasi, Fozia, Shahbaz, Muhammad, Hussain, Tanveer, Ali, Md. Arshad, Seelan, Jaya Seelan Sathiya, Ali, Baber, Mahmoud, Maged Mostafa, Harakeh, Steve and Saleem, Muhammad Hamzah, 2024; 'Exploring the antimicrobial potential of biogenically synthesized graphene oxide nanoparticles against targeted bacterial and fungal pathogens', *Journal of Green Processing and Synthesis*, 13(1): 20230130, doi: https://doi.org/10.1515/gps-2023-0130.

71. Al-Thani, R. F., Patan, N. K. & Al-Maadeed, M. A., 2014; 'GRAPHENE OXIDE AS ANTIMICROBIAL AGAINST TWO GRAM-POSITIVE AND TWO GRAM-

NEGATIVE BACTERIA IN ADDITION TO ONE FUNGUS', *Online Journal of Biological Sciences*, 14(3), 230-239, doi: https://doi.org/10.3844/ojbsci.2014.230.239.

72. Sangili Yandi Gurunathan, Jae Woong Han, Eun Su Kim, Jung Hyun Park, Jin-hoi Kim, 2015; 'Reduction of graphene oxide by resveratrol: a novel and simple biological method for the synthesis of an effective anticancer nanotherapeutic molecule, *International Journal of Nanomedicine,* 10: 2951–2969, doi: http://dx.doi.org/10.2147/IJN.S79879.
73. Eltahir, S.; Al homsi, R.; Jagal, J.; Ahmed, I.S.; Haider, M., 2022; 'Graphene Oxide/Chitosan Injectable Composite Hydrogel for Controlled Release of Doxorubicin: An Approach for Enhanced Intratumoral Delivery', *Journal of Nanomaterials*, 12(23): 4261, doi: https://doi.org/10.3390/nano12234261.
74. Gil Gonçalves, Mercedes Vila, María-Teresa Portolés, María Vallet-Regi, José Gracio, Paula Alexandrina A. P. Marques, 2014; ' Nano-Graphene Oxide: A Potential Multifunctional Platform for Cancer Therapy', *Journal of* Advanced Healthcare Materials, 2(8): 1072-1090, doi: https://doi.org/10.1002/adhm.201300023.
75. Lijun Liu, Qingming Ma, Jie Cao, Yang Gao, Shangcong Han, Yan Liang, Tingting Zhang, Yang Song & Yong Sun, 2021; 'Recent progress of graphene oxide-based multifunctional nanomaterials for cancer treatment', *Journal of Cancer Nano,* 12:18, doi: https://doi.org/10.1186/s12645-021-00087-7.
76. Choudhury, S. P.; Jadav, M.; Jodha, B.; Patel, S.; Kulhari, H.; Pooja, D., 2025; 'Monoamine Neurotransmitter Functionalized Poly (Amidoamine) Dendrimers for Targeting of Cabazitaxel to Human Prostate Cancer Cells', Journal of Discover Nano, 20 (1):221, doi: https://doi.org/10.1186/s11671-025-04368-7.
77. Solanki, R.; Rajput, P. K.; Jodha, B.; Yadav, U. C. S.; Patel, S., 2024; 'Enhancing Apoptosis-Mediated Anticancer Activity of Evodiamine through Protein-Based Nanoparticles in Breast Cancer Cells', Journal of Sci Rep, 14 (1), doi: https://doi.org/10.1038/s41598-024-51970-3.
78. Milena Keremidarska-Markova, Kamelia Hristova-Panu sheva, Tonya Andreeva, Giorgio Speranza, Dayong Wang, Natalia Krasteva, 2018; 'Cytotoxicity Evaluation of Ammonia-Modified Graphene Oxide Particles in Lung Cancer Cells and Embryonic Stem Cells', 2018(1): 9571828, doi: https://doi.org/10.1155/2018/9571828.

79. Chelliah, C. K.; Rajiv Gandhi, G.; Maruthu pandy, M.; Chackaravarthi, G.; Ramachandran, G.; Liu, Y.-H.; Mohamad, O. A. A.; Li, S.; Li, W.-J.; Bhaviripudi, V. R.; Sathik Basha, S.; Shahapurkar, K.; Gebremaryam, G., 2025; 'Dual Role of ROS-Dependent Anti-Cancer Activity and Photocatalytic Degradation of Graphene Oxide against MCF-7 Breast Cancer Cells and Organic Dye', Journal of Sci Rep, 15 (1), https://doi.org/10.1038/s41598-025-24602-7.

80. Hatshan, M.; Saquib, Q.; Siddiqui, M.; Faisal, M.; Ahmad, J.; Al-Khedhairy, A.; Shaik, M.; Khan, M.; Wahab, R.; De Matteis, V.; Adil, S., 2023; 'Effectiveness of Nonfunctionalized Graphene Oxide Nanolayers as Nanomedicine against Colon, Cervical, and Breast Cancer Cells', Journal of IJMS, 24 (11): 9141, doi: https://doi.org/10.3390/ijms24119141 .

81. Gest, C.; Joimel, U.; Huang, L.; Pritchard, L.-L.; Petit, A.; Dulong, C.; Buquet, C.; Hu, C.-Q.; Mir Shahi, P.; Laurent, M.; Fauvel-Lafève, F.; Cazin, L.; Vannier, J.-P.; Lu, H.; Soria, J.; Li, H.; Varin, R.; Soria, C., 2013; 'Rac3 Induces a Molecular Pathway Triggering Breast Cancer Cell Aggressiveness: Differences in MDA-MB-231 and MCF-7 Breast Cancer Cell Lines', BMC Cancer, 13 (5):63, doi: https://doi.org/10.1186/1471-2407-13-63 .

82. Front Inan-Rubio, J.; González, V. J.; Vázquez, E.; Durán-Prado, M., 2022; 'Rapid and efficient testing of the toxicity of graphene-related materials in primary human lung cells', Journal of Scientific Reports, 12 (1); 7664, doi: https://doi.org/10.1038/s41598-022-11840-2.

83. Yang, W.; Deng, X.; Huang, W.; Qing, X.; Shao, Z., 2019; 'The physicochemical properties of graphene nanocomposites influence the anticancer effect', Journal of Oncology, 2019 (1): 7254534, doi: https://doi.org/10.1155/2019/7254534.

84. Kumar, S.; Parekh, S. H., 2020; 'Linking graphene-based material physicochemical properties with molecular adsorption, structure and cell fate', Journal of Communications Chemistry, 3 (1): 8, doi: https://doi.org/10.1038/s42004-019-0254-9.

85. Park, T. Y.; Kim, S. Y.; Park, C. S.; Kim, W. Y.; Jung, J. W.; Kim, J. Y.; Shin, J. W., 2025; 'Cell Toxicity and Autophagy in A549 Cells Treated with Surface-

Functionalized Graphene Derivatives', Journal of Applied Toxicology, 46: 821-832, doi: https://doi.org/10.1002/jat.4869.

86. Li, R.; Guiney, L. M.; Chang, C. H.; Mansukhani, N. D.; Ji, Z.; Wang, X.; Liao, Y.-P.; Jiang, W.; Sun, B.; Hersam, M. C., 2018; 'Surface oxidation of graphene oxide determines membrane damage, lipid peroxidation, and cytotoxicity in macrophages in a pulmonary toxicity model', Journal of ACS nano, 12 (2): 1390-1402, doi: https://doi.org/10.1021/acsnano.7b07737.

87. Ou, L.; Lin, S.; Song, B.; Liu, J.; Lai, R.; Shao, L., 2017; 'The mechanisms of graphene-based materials-induced programmed cell death: a review of apoptosis, autophagy, and programmed necrosis', International journal of nanomedicine, 12: 6633-6646, doi: https://doi.org/10.2147/IJN.S140526.

88. Martel-Estrada, S.-A.; Vargas-Requena, C.-L.; Sifuentes-Chavarría, J.-I.; Yepes-Mendoza, M.-Y.; Palacio-Castillo, D.-S.; Jimenez-Vega, F.; Olivas-Armendáriz, I.,2025; 'Cell Death Mechanisms Produced by Carbon-Based Nanoparticles', Journal of Nanotechnology, 2025 (1): 9961520, doi: https://doi.org/10.1155/jnt/9961520.

89. Ghosh, S.; Ui key, G.; Mishra, S.; Nelson, A.; Azmi, M. S., 2025; 'Evaluation of the Cytotoxic Effects of Graphene Oxide on Oral Squamous Carcinoma Cells', Journal of Pharmacy and Bio allied Sciences, 17 (Suppl 2): S1779-S1781, doi: https://doi.org/10.4103/jpbs.jpbs_378_25.

90. Krętowski, R.; Szynaka, B.; Borzym-Kluczyk, M.; Tyszka, N.; Jabłońska-Trypuć, A.; Gil, M.; Cechowska-Pasko, M., 2025; 'Effectiveness of Graphene Oxide (GO) in Activating the Mitochondrial Pathway of Oxidative Stress-Induced Apoptosis in Breast Cancer Cells', Journal of Cells, 14 (21): 1717, doi: https://doi.org/10.3390/cells14211717.

91. Taheri Azam, A.; Abad, G. G. Y.; Hajimazdarany, S.; Imani, M. H.; Ziaolhagh, S.; Zandieh, M. A.; Bayan Zadeh, S. D.; Mirzaei, S.; Hamblin, M. R.; Entezari, M., 2023; 'Graphene oxide nanoarchitectures in cancer biology: Nano-modulators of autophagy and apoptosis', Journal of Controlled Release, 354: 503-522, doi: https://doi.org/10.1016/j.jconrel.2023.01.028.

92. Gurunathan S, Han JW, Kim E, Park JH, Kim J., 2015; 'Reduction of graphene oxide by resveratrol: a novel and simple biological method for the synthesis of an effective anticancer nanotherapeutic molecule', *Int J Nanomedicine*, 10(1):2951-2969, doi: https://doi.org/10.2147/IJN.S79879.

93. Anwar Fitrianto1, Siau Man Mah2, Siau Hui Mah3, 2022; 'Statistical model for IC50 determination of acetylcholinesterase enzyme for Alzheimer's disease', *International Journal of Public Health Science,* 11(3):770-778 (ISSN 2252-8806), doi: http://doi.org/10.11591/ijphs.v11i3.21282.